



Title	Controlled and Alternating Cationic Copolymerization of o-Phthalaldehyde with Vinyl Monomers: Elucidation of the Exceptional Copolymerizability and Strategy for the Polymerization of Sterically Hindered Monomers
Author(s)	林, 恵佑
Citation	大阪大学, 2022, 博士論文
Version Type	VoR
URL	https://doi.org/10.18910/87845
rights	
Note	

The University of Osaka Institutional Knowledge Archive : OUKA

<https://ir.library.osaka-u.ac.jp/>

The University of Osaka

**Controlled and Alternating Cationic Copolymerization of
o-Phthalaldehyde with Vinyl Monomers: Elucidation of the
Exceptional Copolymerizability and Strategy for the Polymerization
of Sterically Hindered Monomers**

A Doctoral Thesis

By

Keisuke Hayashi

Submitted to
the Graduate School of Science,
Osaka University

February 2022

Acknowledgements

This thesis presents the research that the author performed at the Department of Macromolecular Science, Graduate School of Science, Osaka University under the direction of Professor Sadahito Aoshima from 2016 to 2022.

First of all, the author would like to express his deepest and sincere gratitude to Professor Sadahito Aoshima for his numerous and valuable advices, enthusiastic discussion, and always being supportive throughout the author's laboratory life. The author has been impressed by his insightful suggestions, great ideas, and enthusiasm on science. The author also would like to thank Associate Professor Arihiro Kanazawa for his enormous help, deep knowledge, and fruitful suggestions.

The author would like to express his deep appreciation to Professor Hiroyasu Yamaguchi and Professor Yoshinori Takashima for kindly reviewing this thesis and providing helpful suggestions.

The author is also deeply grateful to Associate Professor Nathaniel A. Lynd (The University of Texas at Austin) and the members of his group for providing fruitful advices during their visit to our group.

The author expresses his gratitude to Dr. Naoya Inazumi for ^1H NMR measurements, and Dr. Akihiro Ito for mass spectroscopy.

The author is deeply indebted to Professor Yoshio Okamoto (Nagoya Univesity; Harbin Engineering University), Professor Mitsuo Sawamoto (Kyoto University; Chubu University), Professor Yoshitsugu Hirokawa (The University of Shiga Prefecture), Professor Eiji Yashima (Nagoya University), Professor Masami Kamigaito (Nagoya University), Professor Shokyoku Kanaoka (University of Shiga Prefecture), Professor Kotaro Satoh (Tokyo Institute of Technology), Professor Makoto Ouchi (Kyoto University), Associate Professor Tsuyoshi Ando (Nara Institute of Science and Technology), and all "ORION" members for active discussion and great interaction.

The author thanks all the members in the Aoshima group. Specifically, the author is grateful to Dr. Sensho Kigoshi, Dr. Suzuka Matsumoto, Dr. Norifumi Yokoyama, Dr. Daichi Yokota, Dr. Motoki Higuchi, Dr. Hironobu Watanabe, Mr. Hiroshi Oda, Ms. Chihiro Suemitsu, Ms. Fumina Koga, Mr. Yoshiki Tatsuno, Mr. Tadashi Naito, Mr. Tsuyoshi Nishikawa, Ms. Yurika Miyamae, Mr. Shintaro Araoka, Ms. Haruka Nishimura, Mr. Daisuke Hotta, Mr. Kazutoshi Mishima, Ms. Haruna Kagasaki, Mr. Ryusei Kato, Mr. Kazuya Maruyama, Ms. Maki Mimura, Mr. Tomohito Asakawa, Ms. Rui Haraguchi, Ms. Kano Hyoui, Mr. Takuya Yamamoto, Ms. Tomo Yoshiki, Mr. Yuya Asada, Mr. Masamichi Inoue, Ms. Yui Kawamura, Mr. Yuya Kinoshita, Ms. Sae Taniguchi, Mr. Shun-ya Hasegawa, Mr. Jun-ichi Azuma, Mr. Mikiya Umemoto, Mr. Tomoki Nara, Mr. Ryosuke Hada, Mr. Masahiro Ueda, Ms. Yuka Takahashi, Ms. Kana Takebayashi, Mr. Naoki Matsuo, Mr. Yuji Mishima, Mr. Yuto Eguchi, Ms. Aya Katto, Mr. Akihisa Numao, and Ms. Yuyu Furuki for their kind assistance

and valuable discussion. The author is also obliged to Ms. Misato Nishiuchi, Ms. Mariko Okamoto, Ms. Naomi Imai, and Ms. Izumi Ichimura for their thoughtful assistance in laboratory life.

Finally, the author would like to express a great appreciation to his father Katsuhiko Hayashi, his mother Seiko Hayashi, and his grandfather Yuji Hayashi for their financial support and warm encouragement.

February 2022

林 惠 佑

Keisuke Hayashi

Department of Macromolecular Science

Graduate School of Science

Osaka University

Contents

Chapter 1	General Introduction.....	1
Part I Understanding the Nature of Cyclic Active Species Derived from <i>o</i>-Phthalaldehyde		
Chapter 2	Exceptional Copolymerizability of <i>o</i> -Phthalaldehyde in Cationic Copolymerization with Vinyl Monomers	15
Part II New Copolymerization Based on the Copolymerizability of <i>o</i>-Phthalaldehyde		
Chapter 3	Cationic Copolymerization of <i>o</i> -Phthalaldehyde and Vinyl Monomers with Various Substituents on the Vinyl Group or in the Pendant: Effects of the Structure and Reactivity of Vinyl Monomers on Copolymerization Behavior	35
Chapter 4	Living and Alternating Cationic Copolymerization of <i>o</i> -Phthalaldehyde and Various Bulky Enol Ethers: Expanding the Range of Polymerizable Monomers.....	55
Chapter 5	Summary.....	89
List of Publications	91

General Introduction

1. Background

1.1 Advantages and limitations of copolymerization

Copolymers have great potential to exhibit various properties and functions compared to homopolymers or mixtures of homopolymers since different structures can be incorporated into the side chains or the main chain of a copolymer. Copolymers are also expected to form higher-order structures such as microphase-separated structures (**Figure 1** upper). There have been many reports for copolymers with various primary structures, such as blocks¹⁻⁷, gradients⁸⁻¹⁰, and alternating sequences.¹¹⁻¹⁵ The specific properties and functions of such copolymers have also been demonstrated. To realize efficient copolymerization of monomers that have different structures at a position adjacent to polymerizable groups or different polymerizable groups, various factors, such as the reactivity of each monomer, the stability of each monomer-derived propagating species, and the stability of the structures obtained by the crossover reactions, must be considered (**Figure 1** lower). Although there have been many attempts to copolymerize different types of monomers, frequent crossover reactions often do not occur, particularly in ionic¹⁶⁻¹⁸ or coordination copolymerization.¹⁹

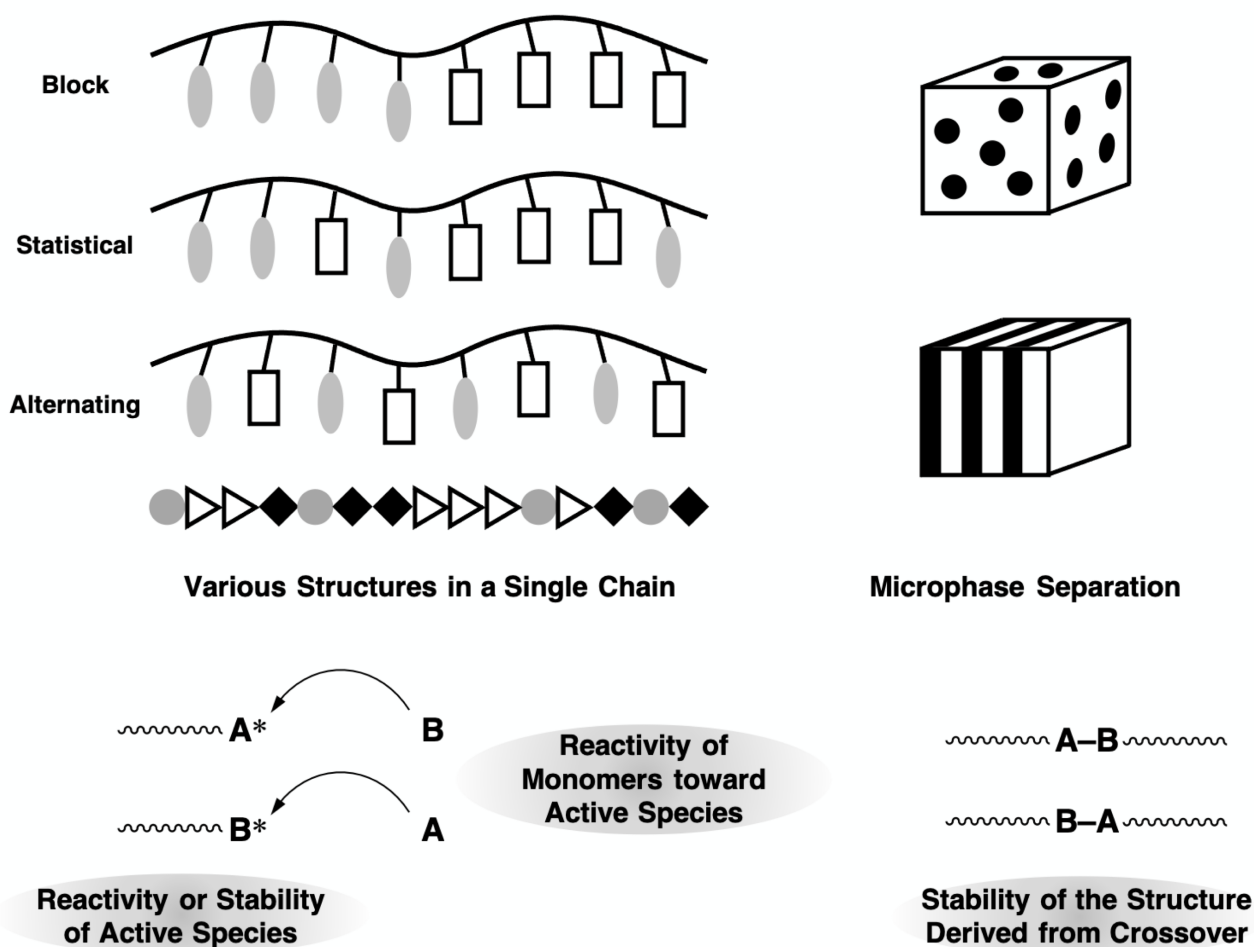


Figure 1. Advantages of copolymers and factors required to be considered for the copolymerization of monomers with different structures.

1.2 Polymerization of sterically hindered monomers

The polymerizability of monomers and the properties of the obtained polymers are significantly governed by the structures formed around a polymerizable group of monomers (**Figure 2**). Monomers with small substituents can easily polymerize to generate a high-molecular-weight polymer that has a flexible main chain. In contrast, monomers with large substituents or multisubstituted monomers are often difficult to polymerize due to a low ceiling temperature or steric repulsion between substituents. However, the main polymer chain obtained from such bulky monomers is expected to be rigid and exhibit specific properties compared to polymers obtained from monomers with small substituents.^{20–30} Copolymerization enables the incorporation of such bulky monomers into polymer chains; however, some monomers have been reported to be inert even for copolymerization.^{31,32} Thus, the design of polymerization systems in which highly bulky monomers are efficiently incorporated into polymer chains is one of the challenges in polymer synthetic chemistry. By precisely investigating and designing the propagation reactions, molecules that have not been previously regarded as monomers, such as tri- or tetra-substituted olefins, can be incorporated into polymer chains.

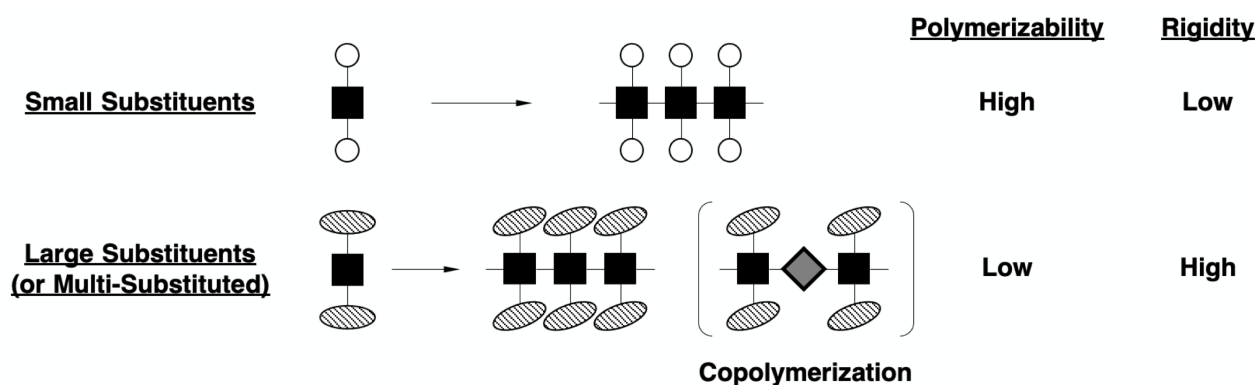
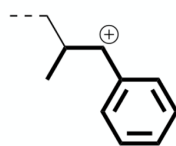


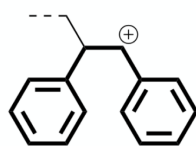
Figure 2. Polymerization of sterically hindered monomers.

1.3 Polymerization mediated by the cyclic propagating species

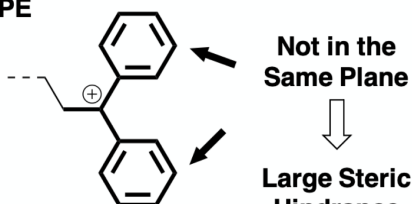
The structures formed around the propagating species greatly affect the polymerization behavior. There are some pairs of monomers that exhibit different polymerization behavior for acyclic and cyclic types of monomers, such as *cis*- β -methylstyrene^{33–35} and indene^{25,26}, *cis*-stilbene^{36,37} and acenaphthylene^{38,39}, or 1,1-diphenylethylene^{40,41} and dibenzofulvene.⁴² Acyclic monomers do not undergo cationic homopolymerization, whereas cyclic monomers exhibit high homopolymerizability. Two driving forces are most likely responsible for these special polymerizabilities. First, the steric hindrance of a monomer and the propagating species is small due to the cyclic structure, and second, the sp^2 orbital of the cyclic monomer-derived propagating carbocation is highly strained and subject to change into a sp^3 orbital via the addition of a monomer (**Figure 3**). This difference is also observed in the cationic polymerization of aromatic aldehydes. Benzaldehyde is known to be difficult to homopolymerize⁴³, whereas *o*-phthalaldehyde (OPA) exhibits high homopolymerizability since OPA generates a cyclic propagating carbocation by the intramolecular cyclization⁴⁴ (**Figure 4**). Recently, the generation of macrocyclic polymers by the cationic mechanism has also been reported.^{45,46} By using this unique cyclic propagating species for copolymerization, distinct polymerization behavior, such as copolymerization with very bulky monomers or the generation of unique sequence, can be observed.

Vinyl Monomers sp^2 (Not Strained) \Rightarrow Low Reactivity β MeSt

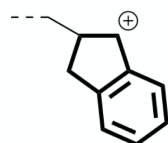
Stb



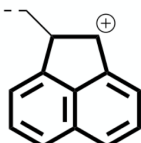
DPE

Not in the
Same PlaneLarge Steric
Hindrance sp^2 (Strained) \Rightarrow High Reactivity

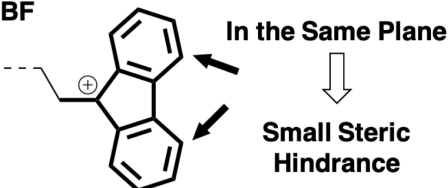
Indene



AcN



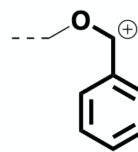
DBF



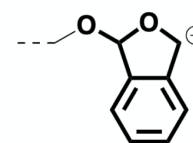
In the Same Plane

Small Steric
Hindrance**This Thesis:**
Aromatic Aldehydes

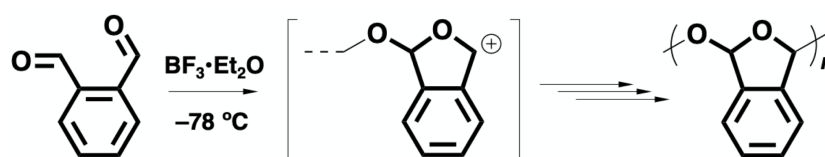
BzA

No
Homopolymerizability

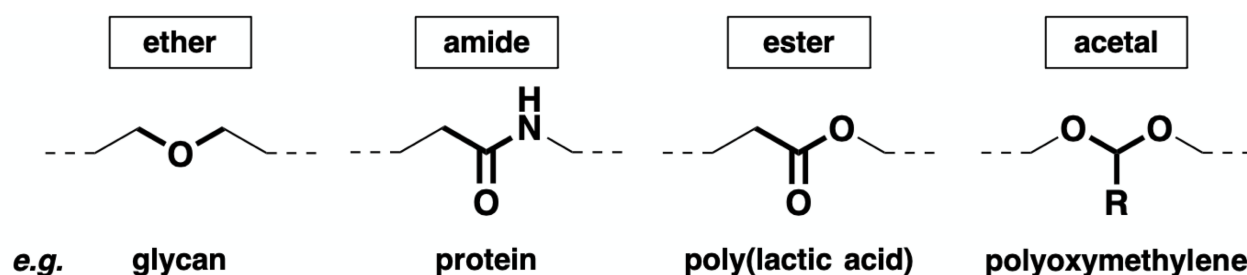
OPA



Homopolymerizability

Figure 3. The difference of propagating species derived from acyclic (upper) or cyclic (lower) monomers.**Figure 4.** Cationic polymerization of *o*-phthalaldehyde (OPA).**1.4 Degradable polymers**

Natural polymers such as proteins and glycans consist of cleavable moieties at specific positions and exhibit further functions upon degradation. To realize these precise functions in synthetic polymers, the design of degradable polymers has been widely studied. Degradable polymers are also expected to be applied for drug delivery systems and chemical recycling of synthetic polymers. In general, functional groups consisting of covalent bonds between a carbon atom and heteroatoms, such as ether,^{47,48} and acetal⁴⁹, are used as cleavable units (**Figure 5**). The cleavage of carbon–carbon main chains has also recently become possible due to the precise design of monomers and degradation conditions.^{50–52}

**Figure 5.** The cleavable units used for the degradable polymers.

The alternating cationic copolymerization of vinyl ethers (VEs) and benzaldehyde (BzA) derivatives has been reported to yield a copolymer consisting of acetal moieties periodically located along the main chain.⁵³ Since BzA derivatives do not homopolymerize, only a VE monomer adds to the BzA derivative-derived propagating carbocation. The use of a BzA monomer that has a higher reactivity towards the VE-derived carbocation than the VE monomer is indispensable for alternating propagation. The obtained alternating copolymer is degradable into a single molecule, cinnamaldehyde derivative, by the scission of acetal moieties in the main chain with acid (Figure 6).

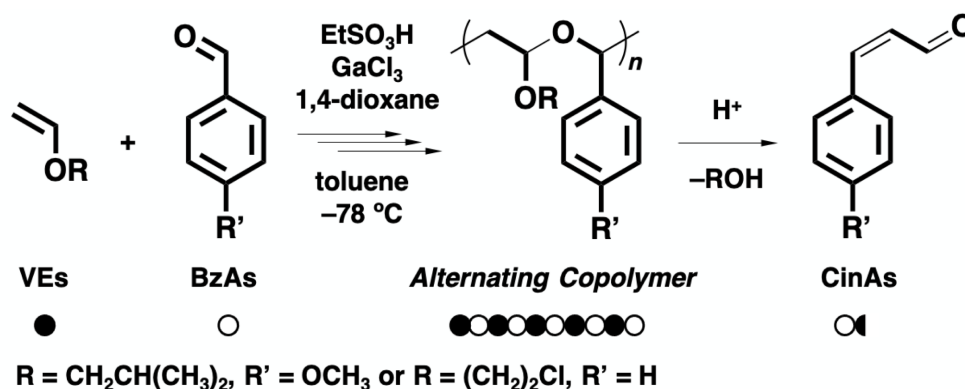


Figure 6. Alternating cationic copolymerization of VEs with BzAs and the degradation by acid.

Based on this system, polymers with cleavable units at predetermined positions were synthesized by adding a small amount of BzA derivatives during the living cationic polymerization of VE.⁵⁴ Desilylation-triggered degradable polymers that are cleavable by mild conditions were also synthesized from trimethylsilyl vinyl ether and cyclic acetals⁵⁵ (Figure 7).

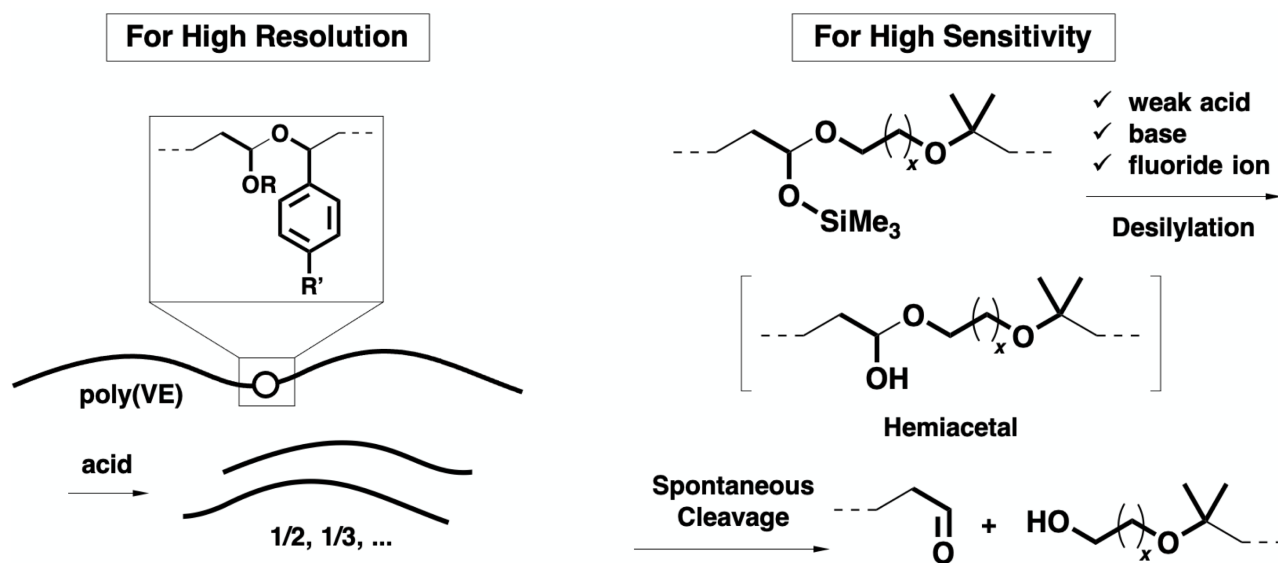


Figure 7. Precisely designed degradable polymers.

1.5 Cationic polymerization

Cationic polymerization is an effective method to obtain polymers from electron-donating vinyl monomers, such as vinyl ethers, styrene (St) derivatives, and isobutene, or cyclic monomers, such as oxiranes and cyclic acetals. However, due to the high reactivity and instability of the propagating carbocation, living cationic polymerization of vinyl monomers is difficult. In 1984, Higashimura and coworkers first reported the living cationic polymerization of isobutyl vinyl ether (IBVE) by using an HI/I₂ system.^{56,57} The key for living polymerization is to cap the propagating carbocation by forming a carbon–halogen bond called a “dormant” species and reactivate the dormant species using a Lewis acid catalyst. Living cationic polymerization of isobutene was also reported by Kennedy and coworkers in 1986^{58,59} (**Figure 8**). Since the first report of living cationic polymerization, various initiating systems have been reported to be effective for living cationic polymerization^{60–65}, which allowed for the polymerization of various monomers, such as VEs with polar moieties^{66,67}, α - or β -substituted VE and St derivatives^{25,26,68–71}, cyclic dienes^{72,73}, plant-derived terpenes^{74,75}, and *N*-vinylcarbazole.^{76,77} Recently, living cationic polymerization has been developed to allow for various systems, such as the alternating copolymerization of VEs with conjugated aldehydes^{53,78,79}, interconvertible living radical and cationic polymerization⁸⁰, ring expansion polymerization of VE^{81–83}, or stereospecific polymerization.⁷⁷

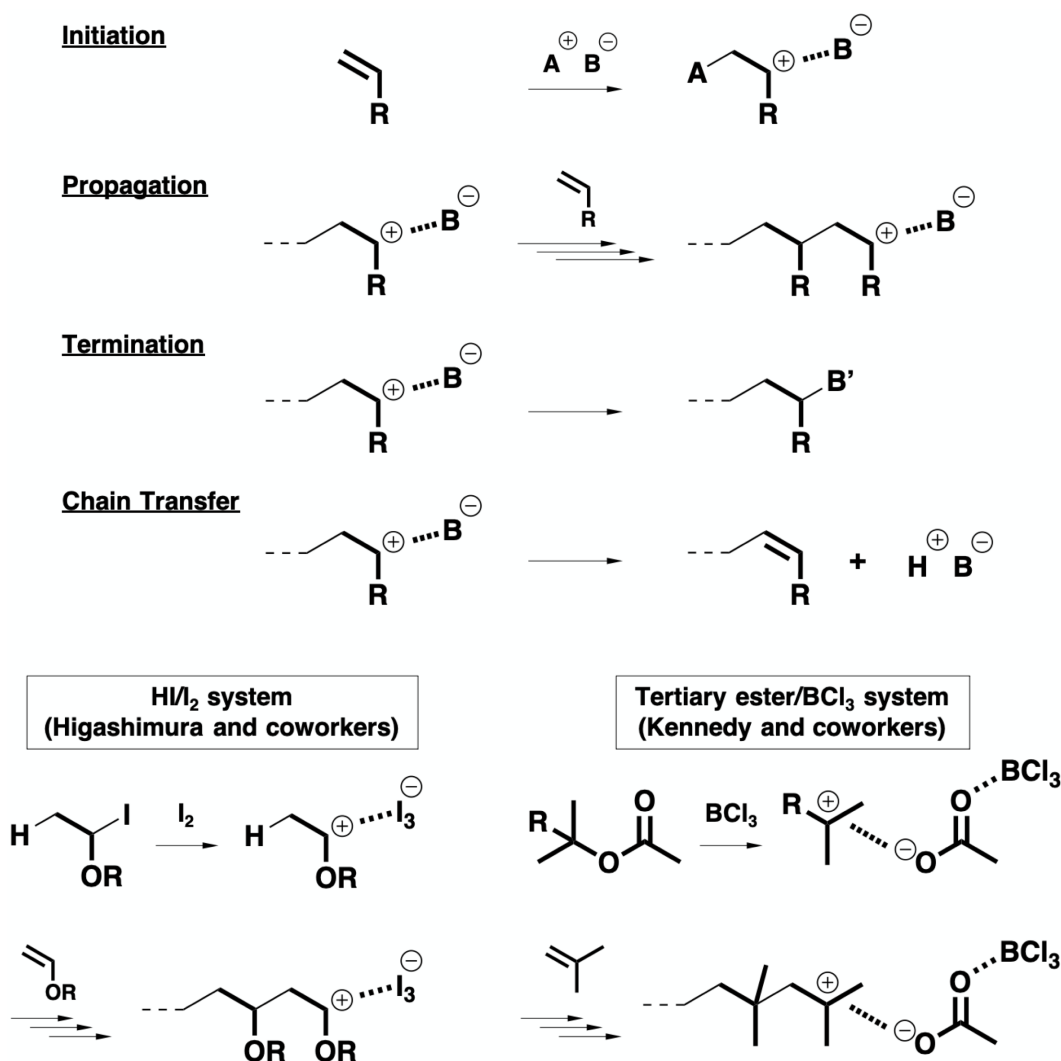


Figure 8. Elementary reactions for cationic polymerization and examples of living cationic polymerization.

1.6 Precise control of the primary structure of synthetic polymers

Biopolymers have precisely programmed molecular weights, monomer sequences, and degradability at predetermined positions. In polymer synthesis, the ultimate goal is to control the molecular weights and monomer sequence, as in the case of biopolymers. The degradability of the obtained polymers also needs to be imparted via the use of degradable unit-incorporated monomers or the generation of degradable units by crossover reactions (**Figure 9**). One or two of the three factors (precise molecular weight, sequence, and degradability) are already accomplished by the progress of living and precision polymerization; however, it is still difficult to simultaneously satisfy all the factors.

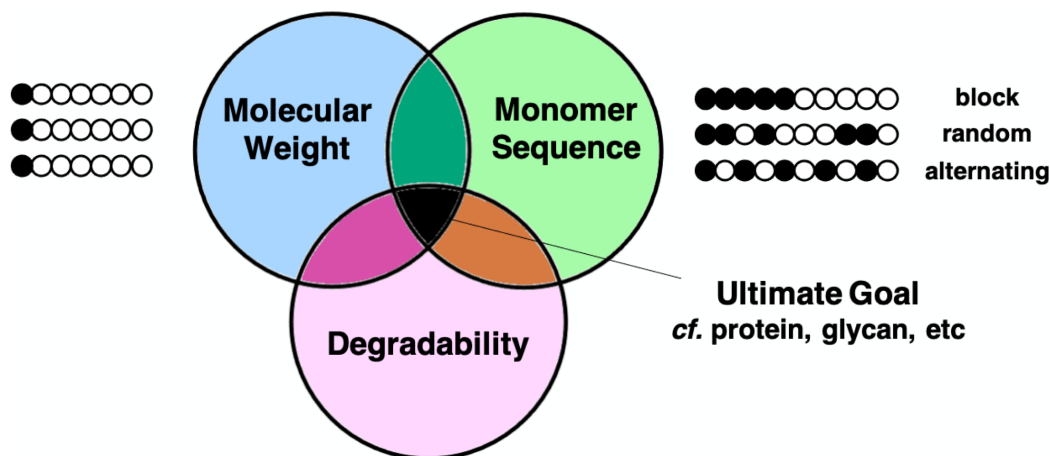
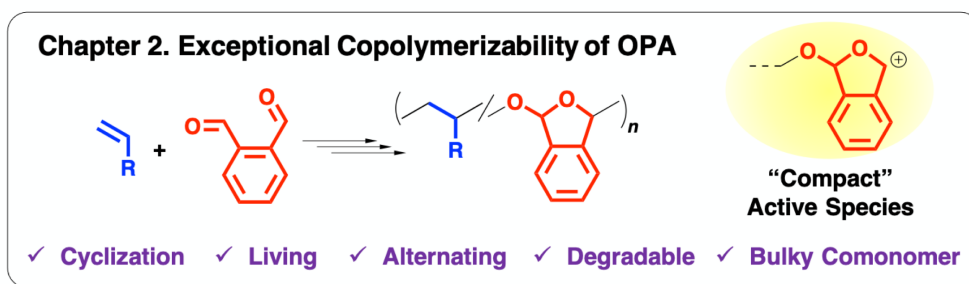


Figure 9. Multifactor control in the polymer synthesis.

2. Objective and Outline of This Thesis

As demonstrated in the background section, there are still many problems and limitations to be overcome in copolymerization using different kinds of monomers, such as inefficient crossover reactions, difference in the reactivity of monomers, or steric hindrance. The objective of this thesis is to develop a new copolymerization system that overcomes the problems and limitations of conventional copolymerization and enables highly programmed molecular weights, monomer sequences, and degradability. The author has focused on the cyclic propagating carbocation of OPA, which has quite a different structure and reactivity than the carbocations of conventional monomers, which can potentially lead to novel copolymerization.

Part I: Understanding the Nature of Cyclic Active Species Derived from OPA



Part II: New Copolymerization Based on the Copolymerizability of OPA

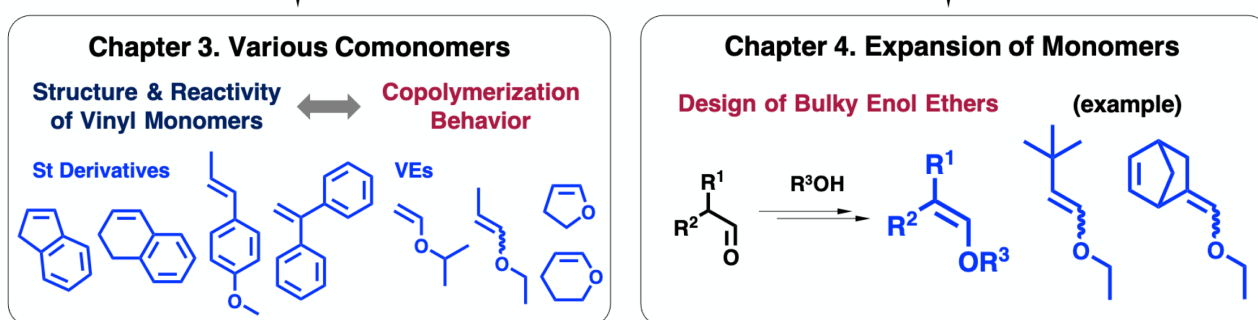


Figure 10. Objective and outline of this thesis.

This thesis consists of two parts. Part I (Chapter 2) describes the unique nature of the OPA-derived propagating carbocation in the cationic copolymerization with vinyl monomers. In particular, the copolymerizability with bulky vinyl monomers that can neither homopolymerize nor copolymerize with BzA derivatives is examined in detail. In Part II (Chapters 3 and 4), copolymerization based on OPA-derived propagating species is investigated, particularly focusing on the relationship between the structure and reactivity of vinyl monomers and the copolymerization behavior (**Figure 10**).

In Chapter 2, the cationic copolymerization behavior of OPA with vinyl monomers is investigated with a particular focus on the copolymerizability difference between OPA and BzA derivatives (**Figure 11**). Living copolymerization with IBVE proceeded to yield copolymers with OPA homosequences. Moreover, copolymerization with very bulky monomers such as β,β -dimethyl VE or 1,1-diphenylethylene successfully proceed, unlike the exclusive generation of cyclic trimers from those monomers with BzA. The unique nature of the OPA-derived propagating carbocation is demonstrated.

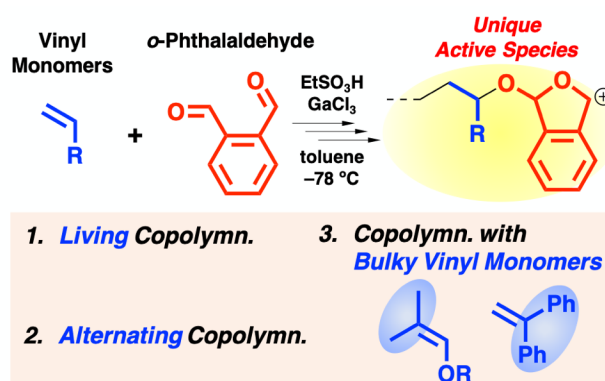


Figure 11. Exceptional cationic copolymerization behavior of OPA with vinyl monomers.

In Chapter 3, to extend the range of monomers copolymerizable with OPA, copolymerization of OPA with St derivatives and VEs that have various substituents on the vinyl group or in the pendant is examined (**Figure 12**). The factors that affect the frequency of the crossover reactions are systematically investigated, and the differences between St derivatives and VEs are revealed. In addition, a copolymer that degrades into low-molecular-weight compounds is demonstrated to be obtained from St derivative monomers.

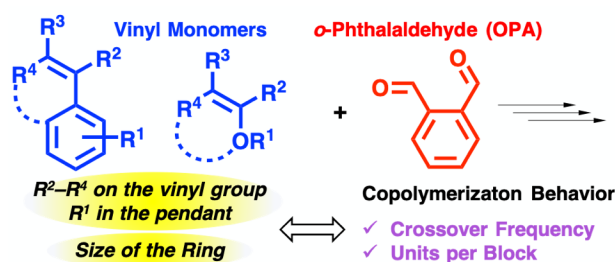


Figure 12. Cationic copolymerization of OPA with vinyl monomers with various substituents in the pendant or on the vinyl group.

In Chapter 4, to further expand the range of polymerizable monomers, enol ethers that have various substituents at the β -carbon site and various alkoxy groups are designed from aliphatic aldehydes and alcohols (**Figure 13**). Some β,β -dialkyl enol ethers are found to undergo living and alternating copolymerization with OPA under appropriate polymerization conditions. In addition, very bulky enol ethers that have not been previously reported to polymerize are demonstrated to be copolymerizable with OPA.

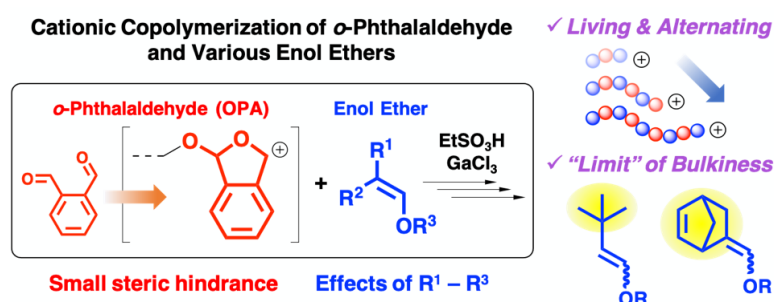


Figure 13. Design of bulky enol ether monomers and expanding the range of polymerizable monomers.

References

1. Swarc, M.; Levy, M.; Milkovich, R. *J. Am. Chem. Soc.* **1956**, *78*, 2656–2657.
2. Dreyfuss, M. P.; Dreyfuss, P. *Polymer* **1965**, *6*, 93–95.
3. Hawker, C. J. *J. Am. Chem. Soc.* **1994**, *116*, 11185–11186.
4. Wang, J. -S.; Matyjaszewski, K. *J. Am. Chem. Soc.* **1995**, *117*, 5614–5615.
5. Bates, F. S.; Fredrickson, G. H. *Phys. Today* **1999**, *52*, 32–38.
6. Kataoka, K.; Harada, A.; Nagasaki, Y. *Adv. Drug. Deliv. Rev.* **2001**, *47*, 113–131.
7. Discher, D. E.; Eisenberg, A. *Science* **2002**, *297*, 967–973.
8. Akovali, G.; Biliyard, K.; Shen, M. *J. Appl. Polym. Sci.* **1976**, *20*, 2419–2427.
9. Kryszewski, M. *Polym. Adv. Technol.* **1998**, *9*, 244–259.
10. Matyjaszewski, K.; Ziegler, M. J.; Arehart, S. V.; Greszta, D.; Pakula, T. *J. Phys. Org. Chem.* **2000**, *13*, 775–786.
11. Hirooka, M.; Yabuuchi, H.; Iseki, J.; Nakai, Y. *J. Polym. Sci., Part A: Polym. Chem.* **1968**, *6*, 1381–1396.
12. Yuki, H.; Hatada, K.; Inoue, T. *J. Polym. Sci., Part A: Polym. Chem.* **1968**, *6*, 3333–3343.
13. Drent, E.; Budzelaar, P. H. M. *Chem. Rev.* **1996**, *96*, 663–681.
14. Huang, J.; Turner, S. R. *Polymer* **2017**, *116*, 572–586.
15. Nishimori, K.; Ouchi, M. *Chem. Commun.* **2020**, *56*, 3473–3483.
16. Sawamoto, M.; Ohtoyo, T.; Higashimura, T.; Gührs, K. H.; Heublein, G. *Polym. J.* **1985**, *17*, 929–933.
17. Yamada, M.; Yoshizaki, T.; Kanazawa, A.; Kanaoka, S.; Aoshima, S. *J. Polym. Sci., Part A: Polym. Chem.* **2019**, *57*, 2166–2174.
18. Ishido, Y.; Kanazawa, A.; Kanaoka, S.; Aoshima, S. *J. Polym. Sci., Part A: Polym. Chem.* **2014**, *52*, 1334–1343.
19. Price, C. J.; Reich, B. J. E.; Miller, S. A. *Macromolecules* **2006**, *39*, 2751–2756.
20. Cubbon, R. C. P. *Polymer* **1965**, *6*, 419–426.
21. Otsu, T.; Matsumoto, A.; Kubota, T.; Mori, S. *Polym. Bull.* **1990**, *23*, 43–50.
22. Matsumoto, A.; Otsu, T. *Macromol. Symp.* **1995**, *98*, 139–152.
23. Barr, D. A.; Rose, J. B. *J. Chem. Soc.* **1954**, 3766–3769.
24. Ogawa, Y.; Sawamoto, M.; Higashimura, T. *Polym. J.* **1984**, *16*, 415–422.
25. Thomas, L.; Polton, A.; Tardi, M.; Sigwalt, P. *Macromolecules* **1992**, *25*, 5886–5892.
26. Kennedy, J. P.; Midha, S.; Keszler, B. *Macromolecules* **1993**, *26*, 424–428.
27. Graham, R. K.; Moore, J. E.; Powell, J. A. *J. Appl. Polym. Sci.* **1967**, *11*, 1797–1805.
28. Ute, K.; Asada, T.; Nabeshima, Y.; Hatada, K. *Polym. Bull.* **1993**, *30*, 171–178.
29. Higashimura, T.; Tanizaki, A.; Sawamoto, M. *J. Polym. Sci., Part A: Polym. Chem.* **1984**, *22*, 3173–3181.
30. Crivello, J. V.; Jo, K. D. *J. Polym. Sci., Part A: Polym. Chem.* **1993**, *31*, 1483–1491.
31. Okuyama, T.; Fueno, T.; Furukawa, J.; Uyeo, K. *J. Polym. Sci., Part A-1: Polym. Chem.* **1968**, *6*, 1001–1007.
32. Okuyama, T.; Fueno, T. *Kobunshi Kagaku* **1971**, *28*, 369–380.
33. Overberger, C. G.; Tanner, D.; Pearce, E. M. *J. Am. Chem. Soc.* **1958**, *80*, 4566–4568.
34. D’Alelio, G. F.; Finestone, A. G.; Taft, L.; Miranda, T. J. *J. Polym. Sci.* **1960**, *45*, 83–89.
35. Mizote, A.; Tanaka, T.; Higashimura, T.; Okamura, S. *J. Polym. Sci., Part A: Gen. Pap.* **1965**, *3*, 2567–

2578.

36. Price, C. C.; Berti, G. *J. Am. Chem. Soc.* **1954**, *76*, 1219–1221.
37. Brackman, D. S.; Plesch, P. H. *J. Chem. Soc.* **1958**, 3563–3573.
38. Flowers, R. G.; Miller, H. F. *J. Am. Chem. Soc.* **1947**, *69*, 1388–1389.
39. Imoto, M.; Takemoto, K. *J. Polym. Sci.* **1955**, *15*, 271–276.
40. Ureta, E.; Smid, J.; Szwarc, M. *J. Polym. Sci., Part A-1: Polym. Chem.* **1966**, *4*, 2219–2228.
41. Yuki, H.; Hotta, J.; Okamoto, Y.; Murahashi, S. *Bull. Chem. Soc. Jpn.* **1967**, *40*, 2659–2663.
42. Nakano, T.; Takewaki, K.; Yade, T.; Okamoto, Y. *J. Am. Chem. Soc.* **2001**, *123*, 9182–9183.
43. Aso, C.; Tagami, S.; Kunitake, T. *Kobunshi Kagaku* **1966**, *23*, 63–68.
44. Aso, C.; Tagami, S.; Kunitake, T. *J. Polym. Sci., Part A-1: Polym. Chem.* **1969**, *7*, 497–511.
45. Kaitz, J. A.; Diesendruck, C. E.; Moore, J. S. *J. Am. Chem. Soc.* **2013**, *135*, 12755–12761.
46. Kaitz, J. A.; Diesendruck, C. E.; Moore, J. S. *Macromolecules* **2013**, *46*, 8121–8128.
47. Lim, L. -T.; Auras, R.; Rubino, M. *Prog. Polym. Sci.* **2008**, *33*, 820–852.
48. Cohn, D.; Hotovelly, S. A. *Biomaterials* **2005**, *26*, 2297–2305.
49. Tomlinson, R.; Heller, J.; Brocchini, S.; Duncan, R. *Bioconjugate Chem.* **2003**, *14*, 1096–1106.
50. Kazama, A.; Kohsaka, Y. *Polym. Chem.* **2019**, *10*, 2764–2768.
51. Shimomoto, H.; Tsunematsu, S.; Itoh, T.; Ihara, E. *Polym. Chem.* **2021**, *12*, 689–701.
52. Kimura, T.; Kuroda, K.; Kubota, H.; Ouchi, M. *ACS Macro Lett.* **2021**, *10*, 1535–1539.
53. Ishido, Y.; Aburaki, R.; Kanaoka, S.; Aoshima, S. *Macromolecules* **2010**, *43*, 3141–3144.
54. Kawamura, M.; Kanazawa, A.; Kanaoka, S.; Aoshima, S. *Polym. Chem.* **2015**, *6*, 4102–4108.
55. Kato, R.; Kanazawa, A.; Aoshima, S. *ACS Macro Lett.* **2019**, *8*, 1498–1503.
56. Miyamoto, M.; Sawamoto, M.; Higashimura, T. *Macromolecules* **1984**, *17*, 265–268.
57. Miyamoto, M.; Sawamoto, M.; Higashimura, T. *Macromolecules* **1984**, *17*, 2228–2230.
58. Faust, R.; Kennedy, J. P. *Polym. Bull.* **1986**, *15*, 317–323.
59. Faust, R.; Kennedy, J. P. *J. Polym. Sci., Part A: Polym. Chem.* **1987**, *25*, 1847–1869.
60. Sawamoto, M. *Prog. Polym. Sci.* **1991**, *16*, 111–172.
61. Kennedy, J. P. *J. Polym. Sci., Part A: Polym. Chem.* **1999**, *37*, 2285–2293.
62. Puskas, J. E.; Kaszas, G. *Prog. Polym. Sci.* **2000**, *25*, 403–452.
63. Goethals, E. J.; Du Prez, F. *Prog. Polym. Sci.* **2007**, *32*, 220–246.
64. Aoshima, S.; Yoshida, T.; Kanazawa, A.; Kanaoka, S. *J. Polym. Sci., Part A: Polym. Chem.* **2007**, *45*, 1801–1813.
65. Aoshima, S.; Kanaoka, S. *Chem. Rev.* **2009**, *109*, 5245–5287.
66. Aoshima, S.; Nakamura, T.; Uesugi, N.; Sawamoto, M.; Higashimura, T. *Macromolecules* **1985**, *18*, 2097–2101.
67. Hashimoto, T.; Ibuki, H.; Sawamoto, M.; Higashimura, T. *J. Polym. Sci., Part A: Polym. Chem.* **1988**, *26*, 3361–3374.
68. Higashimura, T.; Kamigaito, M.; Kato, M.; Hasebe, T.; Sawamoto, M. *Macromolecules* **1993**, *26*, 2670–2673.
69. Kwon, Y.; Cao, X.; Faust, R. *Macromolecules* **1999**, *32*, 6963–6968.
70. Yonezumi, M.; Kanaoka, S.; Aoshima, S. *J. Polym. Sci., Part A: Polym. Chem.* **2008**, *46*, 4495–4504.

71. Yonezumi, M.; Takaku, R.; Kanaoka, S.; Aoshima, S. *J. Polym. Sci., Part A: Polym. Chem.* **2008**, *46*, 2202–2211.
72. Ouchi, M.; Kamigaito, M.; Sawamoto, M. *Macromolecules* **2001**, *34*, 3176–3181.
73. Mizuno, N.; Satoh, K.; Kamigaito, M.; Okamoto, Y. *Macromolecules* **2006**, *39*, 5280–5285.
74. Lu, J.; Kamigaito, M.; Sawamoto, M.; Higashimura, T.; Deng, Y. -X. *Macromolecules* **1997**, *30*, 22–26.
75. Satoh, K.; Nakahara, A.; Mukunoki, K.; Sugiyama, H.; Saito, H.; Kamigaito, M. *Polym. Chem.* **2014**, *5*, 3222–3230.
76. Sawamoto, M.; Fujimori, J.; Higashimura, T. *Macromolecules* **1987**, *20*, 916–920.
77. Watanabe, H.; Kanazawa, A.; Aoshima, S. *ACS Macro Lett.* **2017**, *6*, 463–467.
78. Ishido, Y.; Kanazawa, A.; Kanaoka, S.; Aoshima, S. *Macromolecules* **2012**, *45*, 4060–4068.
79. Ishido, Y.; Kanazawa, A.; Kanaoka, S.; Aoshima, S. *J. Polym. Sci., Part A: Polym. Chem.* **2013**, *51*, 4684–4693.
80. Aoshima, H.; Uchiyama, M.; Satoh, K.; Kamigaito, M. *Angew. Chem. Int. Ed.* **2014**, *53*, 10932–10936.
81. Kammiyada, H.; Konishi, A.; Ouchi, M.; Sawamoto, M. *ACS Macro Lett.* **2013**, *2*, 531–534.
82. Kammiyada, H.; Ouchi, M.; Sawamoto, M. *Macromol. Symp.* **2015**, *62*, 400–408.
83. Daito, Y.; Kojima, R.; Kusuyama, N.; Kohsaka, Y.; Ouchi, M. *Polym. Chem.* **2021**, *12*, 702–710.

Part I

Understanding the Nature of Cyclic Active Species

Derived from *o*-Phthalaldehyde

Chapter 2

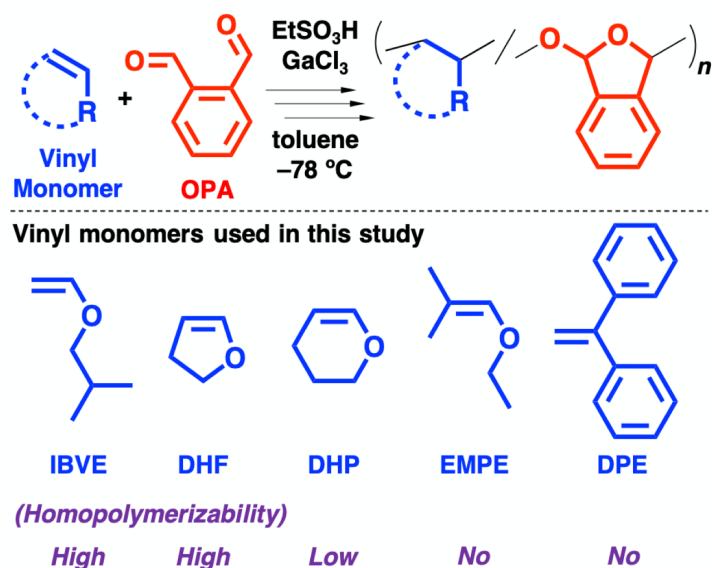
Exceptional Copolymerizability of *o*-Phthalaldehyde in Cationic Copolymerization with Vinyl Monomers

Introduction

Copolymerization is an effective strategy for the synthesis of polymers with characteristic properties and functions that the corresponding homopolymers do not possess.¹⁻⁵ The potential incorporation of nonhomopolymerizable monomers is also another attractive advantage of copolymerization. In many cases, nonhomopolymerizable monomers are incorporated into polymer chains through the mitigation of the effects of steric hindrance when combined with comonomers with suitable steric environments and reactivities. For example, 1,1-diphenylethylene⁶⁻¹¹ and β -methylstyrene¹²⁻¹⁵ can be incorporated into polymer chains *via* copolymerization with other monomers, such as maleimides, styrene, and *p*-methylstyrene.

In the cationic copolymerization of VEs and benzaldehyde derivatives (BzAs)^{16,17} or naturally occurring conjugated aldehydes,¹⁸ acid-labile acetal units are introduced into the main chain through crossover reactions from the VE-derived growing cation chain to an aldehyde monomer. Moreover, alternating copolymerizations proceed via the complete suppression of the homopropagation reactions of VEs using an appropriate combination of VE and aldehyde monomers. The alternating copolymers, which have alternating acetal moieties in the main chain, are selectively degraded into alcohol and cinnamaldehyde derivatives by acid hydrolysis. In addition, the alternating copolymerization of BzAs with 3,4-dihydro-2*H*-pyran (DHP), which is a monomer with low homopolymerizability, also proceeded in a controlled manner.¹⁹ Efficient alternating copolymerizations were feasible due to the appropriate reactivities of the monomers and propagating species and suppression of the undesirable homosequences of each monomer. However, copolymerizations of BzAs with very bulky vinyl monomers, such as β,β -dimethyl VE²⁰⁻²² and 1,1-diphenylethylene⁶⁻¹¹, do not proceed, and cyclic trimerization is observed in the reactions of these vinyl monomers and BzAs.^{8,19} The steric hindrance from these bulky monomers was not fully mitigated even in the copolymerization.

To potentially design new copolymerization systems, the author focused on *o*-phthalaldehyde (OPA), which is known to be homopolymerizable by cationic²³⁻²⁵, anionic, coordination, or γ -ray mechanisms.^{26,27} Despite its potential for generating polymers with novel structures by copolymerization, there have been few reports of cationic copolymerization of OPA with vinyl monomers, except for styrene.²⁸ In this study, the author examined the cationic copolymerization of OPA and various vinyl monomers, particularly focusing on the unique active species derived from OPA. Under optimized conditions, OPA copolymerized with an alkyl VE in a living manner. Moreover, OPA successfully copolymerized with very bulky monomers, such as β,β -dimethyl VE and 1,1-diphenylethylene, to yield linear copolymers unlike BzAs (**Scheme 1**).



Scheme 1. Cationic copolymerization of vinyl monomers and OPA.

Experimental Section

Materials.

Isobutyl vinyl ether (IBVE; TCI; >99.0%) was washed with 10% aqueous sodium hydroxide solution and then with water, dried overnight over potassium hydroxide, and distilled twice over calcium hydride. 2,3-Dihydrofuran (DHF; TCI; >98.0%) and 3,4-dihydro-2*H*-pyran (DHP; TCI; >97.0%) were distilled twice over calcium hydride. 1,4-Dioxane (Nacalai Tesque; >99.5%) and tetrahydrofuran (THF; Nacalai Tesque; >99.5%) were distilled over calcium hydride and then lithium aluminum hydride. Ethyl 2-methyl-1-propenyl ether (EMPE) was prepared from isobutyraldehyde diethyl acetal (TCI, >96.0%) according to a previous report²⁹ and then distilled twice over calcium hydride. 1,1-Diphenylethylene (DPE; TCI; >98.0%) was distilled twice over calcium hydride under reduced pressure. *o*-Phthalaldehyde (OPA; TCI; >99.0%) was recrystallized twice from *n*-hexane before use. Ethanesulfonic acid (EtSO₃H; Sigma-Aldrich; 95%) was used as received. 1-(Isobutoxy)ethyl chloride (IBVE-HCl) was prepared from addition reaction of IBVE with HCl.³⁰ For GaCl₃, a stock solution in *n*-hexane was prepared from commercial anhydrous GaCl₃ (Sigma-Aldrich, 99.999%). SnCl₄ (Sigma-Aldrich, 1.0 M solution in heptane) and TiCl₄ (Sigma-Aldrich, 1.0 M solution in toluene) were used as received. Toluene (Wako) and dichloromethane (Wako) were dried by passage through solvent purification columns (Glass Contour). Diethyl malonate (Nacalai Tesque; >99.0%) and sodium hydride (NaH; Nacalai Tesque; 60% dispersion in paraffin) were used as received.

Polymerization procedures.

Polymerization was conducted under dry nitrogen atmosphere in a glass tube equipped with a three-way stopcock. Toluene, 1,4-dioxane, and monomers were first added into the tube using different dry syringes. To this solution, cooled at 0 °C in advance, a prechilled 40 mM EtSO₃H solution (0.3 mL) in toluene was added using a dry syringe. The tube was then placed into a cooling bath set at -78 °C, 2 min after the EtSO₃H addition. The reaction was started by the addition of a prechilled Lewis acid solution (0.3 mL). The reaction mixture

was terminated with methanol containing a small amount of aqueous sodium hydroxide or ammonia solution, or the solution of sodium diethylmalonate prepared according to a previous report.³¹ The quenched reaction mixture was diluted with dichloromethane and then washed with water. The solvents and other volatiles were evaporated under reduced pressure. The residual OPA monomer was removed by reprecipitation into methanol. The monomer conversion was determined by a gravimetric method and ¹H NMR analysis.

Acid hydrolysis of product copolymers.

The purified copolymer (30 mg) was dissolved in 1,2-dimethoxyethane (DME; 3.4 mL), and then the hydrolysis reaction was started by the addition of an aqueous HCl-DME solution (1.0 M, 3.4 mL) at 30 °C. After predetermined reaction time, the reaction was quenched with aqueous sodium hydroxide (1.0 M, 3.4 mL). The quenched reaction mixture was diluted with dichloromethane and then washed with distilled water five times to remove the resulting salt. The volatiles were evaporated under reduced pressure to yield hydrolysis products.

Acid methanolysis of product copolymers.

The purified copolymer (20 mg) was dissolved in dichloromethane (2.0 mL), and then the methanolysis reaction was started by the addition of an HCl-MeOH solution (1.0 M, 2.0 mL) at room temperature. Other procedures were conducted in a manner similar to that in hydrolysis.

Characterization.

The molecular weight distribution (MWD) of the polymers was measured by gel permeation chromatography (GPC) in chloroform at 40 °C with polystyrene columns [TSKgel GMH_{HR}-M × 2 (exclusion limit molecular weight (MW) = 4 × 10⁶, bead size = 5 mm; column size = 7.8 mm id × 300 mm); flow rate = 1.0 mL/min] connected to a JASCO PU-4580 pump, a Tosoh CO-8020 column oven, a Tosoh UV-8020 ultraviolet detector, and a Tosoh RI-8020 refractive-index detector. The number-average molecular weight (M_n) and polydispersity ratio [weight-average molecular weight/number-average molecular weight (M_w/M_n)] were calculated from the chromatographs with respect to 16 polystyrene standards (Tosoh; $M_n = 5.0 \times 10^2$ — 1.09×10^6 , $M_w/M_n < 1.1$). NMR spectra of the products were recorded using a JEOL JNM-ECA 500 spectrometer (500.16 MHz for ¹H and 125.77 MHz for ¹³C) or a JEOL JNM-ECS 400 spectrometer (399.78 MHz for ¹H and 100.53 MHz for ¹³C) in chloroform-*d* at 30 °C. ESI-MS data were recorded on LTQ Orbitrap XL (Thermo Scientific).

Results and Discussion

To examine the cationic copolymerization behavior of OPA, the copolymerization of OPA with IBVE was examined using various Lewis acids, additives, and solvents. Both monomers were consumed and the corresponding copolymers were generated under all the conditions examined; however, the controllability of the copolymerizations differed among the reaction conditions. Copolymers with controlled molecular weights (MWs) and narrow molecular weight distributions (MWDs) were obtained when GaCl₃ was used as a Lewis acid catalyst in conjunction with EtSO₃H as a proton source in the presence of 1,4-dioxane in toluene at -78 °C

(entry 1 in **Table 1**). The details of the controlled copolymerization behavior are described in the next paragraph. Copolymerizations using other Lewis acids, such as SnCl₄ (entry 6) and TiCl₄ (entry 7), yielded products with uncontrolled MWs. The reactions in CH₂Cl₂ (entry 5) or in the absence of 1,4-dioxane (entry 2) proceeded very quickly and resulted in low MWs and broad MWDs. The copolymerization did not proceed at -78 °C in the presence of THF as an added base, which has a higher basicity than 1,4-dioxane (entry 3). In the presence of THF at -45 °C, the polymerization proceeded via mediation by long-lived species; however, MWs were lower than the calculated values (entry 4).

Figure 1 shows the copolymerization results under the most suitable conditions (entry 1 in **Table 1**). The monomers were consumed at similar rates (**Figure 1A**). The detected peak in the GPC chromatograph of the reaction mixture shifted to a higher MW as the reaction proceeded while maintaining the narrow MWD (**Figure 1B**), which indicates that long-lived species were generated. In addition, the M_n values were consistent with the calculated M_n values based on monomer conversion (red symbols in **Figure 1C**). The experimental and calculated values also agreed at different concentrations of the proton source and monomer (green and blue symbols). Moreover, the addition of a fresh batch of IBVE at the later stage of copolymerization resulted in a further increase in the MW of the polymer (**Figure 2**). These results suggest that the copolymerization of OPA and IBVE proceeded in a living manner.

Table 1. Cationic copolymerization of vinyl monomers and OPA^a

entry	vinyl	Lewis Acid	solvent	added Base	temp. (°C)	time	conv. (%) ^b		$M_n \times 10^{-3}$ (calcd)	$M_n \times 10^{-3}$ (obsd)	M_w/M_n ^c	units per Block ^d	
							vinyl	OPA				vinyl	OPA
1	IBVE	GaCl ₃	toluene	1,4-DO	-78	4 h	55	55	19.3	17.5	1.21	1.3	1.2
2				none	-78	1 min	89	40	21.4	2.6	4.12	-	-
3				THF	-78	2 h	9	4	-	-	-	-	-
4				THF	-45	4 h	36	43	14.1	8.2	1.42	-	-
5			CH ₂ Cl ₂	1,4-DO	-78	1 min	78	68	25.4	3.8	3.51	-	-
6		SnCl ₄	toluene	1,4-DO	-78	1 h	90	62	26.0	5.1	1.57	-	-
7		TiCl ₄	toluene	1,4-DO	-78	6 h	25	13	6.4	11.4	2.30	-	-
8	DHF	GaCl ₃	toluene	1,4-DO	-78	20 min	93	70	15.9	5.4	2.12	-	-
9	DHP	GaCl ₃	toluene	1,4-DO	-78	4 h	62	74	15.7	9.0	2.06	1.0	1.1
10	EMPE	GaCl ₃	toluene	1,4-DO	-78	90 min	76	85	19.0	5.8	1.69	1.0	1.0
11 ^e	DPE	SnCl ₄	CH ₂ Cl ₂	None	-78	24 h	48	94	21.3	7.1	1.75	1.0	2.0

^a [Vinyl monomer]₀ = 0.60 M (for entries 1–7), 0.44 M (for entry 9), or 0.40 M (for entries 8, 10 and 11), [OPA]₀ = 0.60 M (for entries 1–7) or 0.40 M (for entries 8–11), [EtSO₃H]₀ = 4.0 mM, [Lewis acid]₀ = 4.0 mM, [added base]₀ = 0.50 M. 1,4-DO: 1,4-dioxane. ^b Determined by ¹H NMR and gravimetry. ^c Determined by GPC (polystyrene standards). ^d Calculated by the ¹H NMR spectrum. ^e [IBVE-HCl]₀ = 4.0 mM, [SnCl₄]₀ = 10 mM.

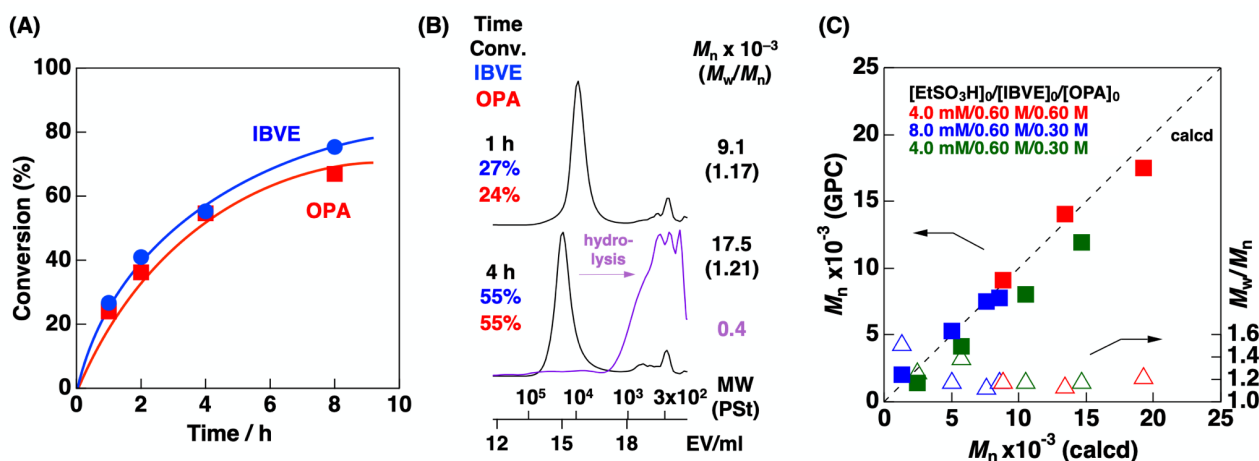


Figure 1. (A) Time-conversion curves for the copolymerization of IBVE (blue) and OPA (red). (B) MWD curves of the obtained polymers (black: original polymers; purple: products obtained by acid hydrolysis). Polymerization conditions: $[\text{IBVE}]_0 = 0.60 \text{ M}$, $[\text{OPA}]_0 = 0.60 \text{ M}$, $[\text{EtSO}_3\text{H}]_0 = 4.0 \text{ mM}$, $[\text{GaCl}_3]_0 = 4.0 \text{ mM}$, $[\text{1,4-dioxane}]_0 = 0.50 \text{ M}$ in toluene at $-78 \text{ }^\circ\text{C}$. (C) M_n and M_w/M_n for the copolymerization of IBVE and OPA. Polymerization conditions: $[\text{GaCl}_3]_0 = 4.0 \text{ mM}$, $[\text{1,4-dioxane}]_0 = 0.50 \text{ M}$ in toluene at $-78 \text{ }^\circ\text{C}$. Quencher: methanol containing a small amount of aqueous sodium-hydroxide solution.

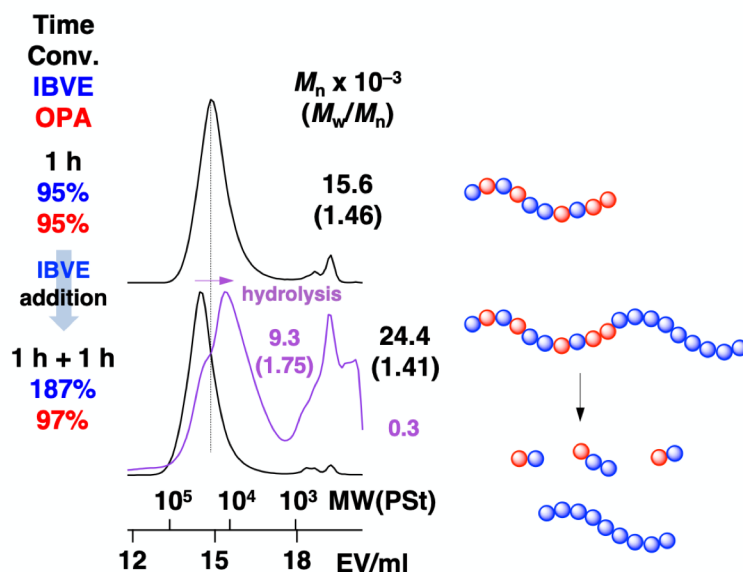


Figure 2. MWD curves of the products before and after IBVE addition ($[\text{IBVE}]_0 = [\text{IBVE}]_{\text{added}} = 0.40 \text{ M}$, $[\text{OPA}]_0 = 0.40 \text{ M}$, $[\text{EtSO}_3\text{H}]_0 = 4.0 \text{ mM}$, $[\text{GaCl}_3]_0 = 4.0 \text{ mM}$, $[\text{1,4-dioxane}]_0 = 0.50 \text{ M}$ in toluene at $-78 \text{ }^\circ\text{C}$).

¹H NMR analysis of the obtained copolymer (**Figure 3A**) indicates that the copolymerization occurred via the selective cyclization of the two aldehyde moieties of OPA and frequent crossover reactions between the monomers. No peaks were observed in the 9–11 ppm region, indicating that all the aldehyde moieties of OPA were incorporated into the main chain. The intramolecular cyclization reactions between two aldehyde moieties most likely proceeded in a manner similar to the homopolymerization of OPA (**Figure 3C**).²³ The

peaks at 5–6 ppm (peaks 2 and 9), which were not detected in the spectra of the homopolymers of either IBVE or OPA (**Figure 3B** and **3C**) were assigned to the structures generated by the crossover reactions from the IBVE-derived carbocation to OPA and from the OPA-derived carbocation to IBVE. In addition, signals from the sodium diethylmalonate fragment³¹, which was used to quench the copolymerization, were observed at 4.2 ppm (11 and 11') and 1.2 ppm (12, 12' and 13) (see **Figure S1** for ESI-MS of the hydrolysis product). The M_n value estimated from the ratio of integrals of the quencher fragment and main chain peaks (1.1×10^4) was comparable to the value by GPC using polystyrene calibration (1.3×10^4). The efficient incorporation of the quencher fragment at the ω -end of the polymer chain confirms the livingness of the copolymerization.

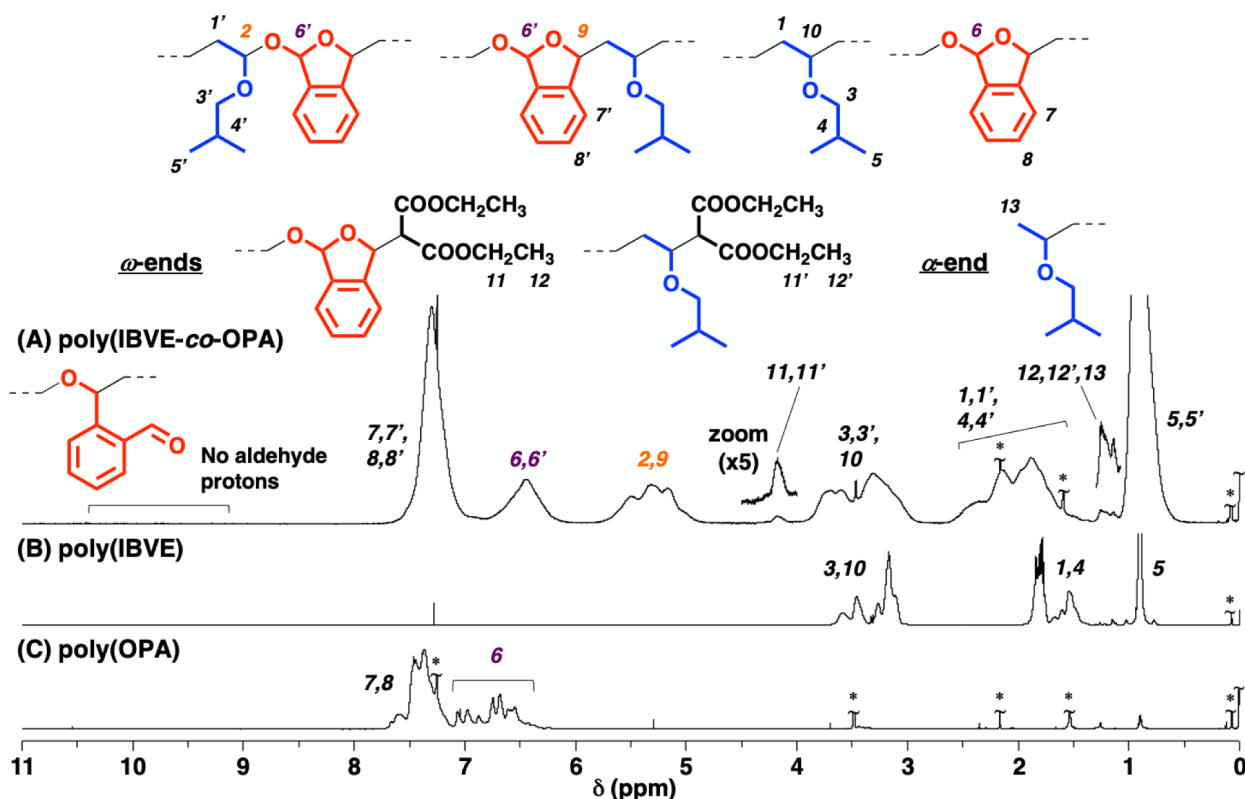


Figure 3. ¹H NMR spectra of (A) poly(IBVE-co-OPA) ($M_n = 13.0 \times 10^3$, $M_w/M_n = 1.23$), (B) poly(IBVE) ($M_n = 12.3 \times 10^3$, $M_w/M_n = 1.10$), and (C) poly(OPA) ($M_n = 2.8 \times 10^3$, $M_w/M_n = 4.05$) recorded in CDCl₃ at 30 °C. Peaks with asterisks are due to TMS, water, acetone, methanol, and CHCl₃. Number written in green: integral ratio. Quencher: sodium diethylmalonate solution for (A) and (C), methanol containing a small amount of aqueous ammonia solution for (B).

The average numbers of IBVE and OPA units per block, which were calculated from the ratios of ¹H NMR integrals, were 1.3 and 1.2, respectively (entry 1 in **Table 1**). Unlike in the copolymerizations of BzAs and IBVE, the homopropagation of the aldehydes does occur in the case of OPA. However, the frequency of the crossover reactions from OPA to IBVE is higher than the homopropagation. The monomer reactivity ratios, which were determined to be less than one ($r_{\text{IBVE}} = 0.49$ and $r_{\text{OPA}} = 0.09$; by the Kelen–Tüdös method; see **Figure 4** and **Table S1** for the detail), are also consistent with the average numbers of units per block.

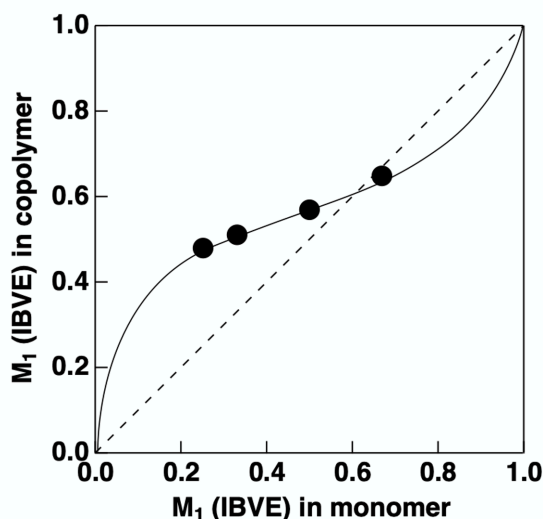
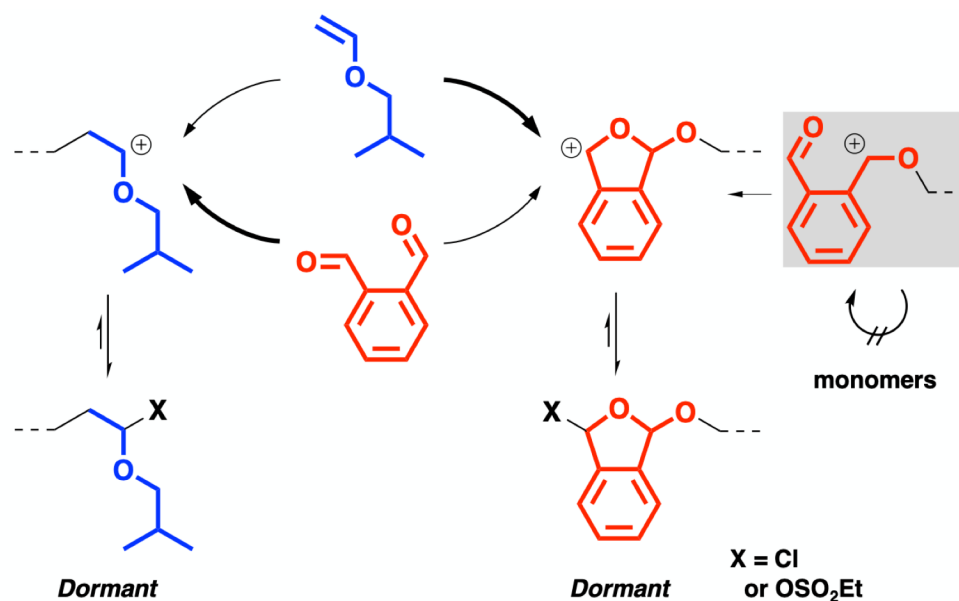
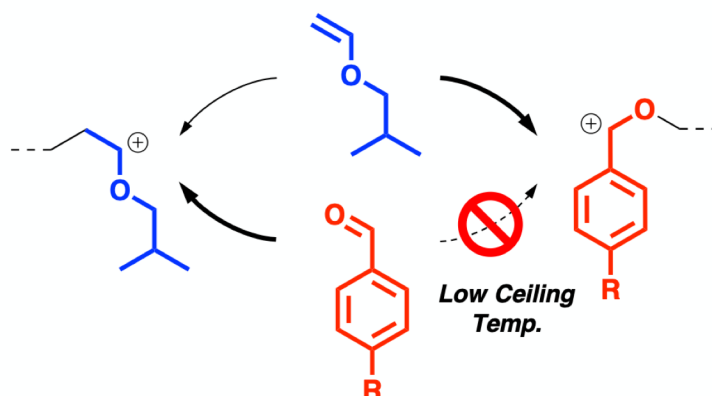


Figure 4. Copolymer compositions in the copolymerization of IBVE and OPA ($[\text{IBVE}]_0 + [\text{OPA}]_0 = 1.20 \text{ M}$, $[\text{EtSO}_3\text{H}]_0/[\text{GaCl}_3]_0 = 4.0/4.0 \text{ mM}$, $[\text{1,4-dioxane}]_0 = 0.50 \text{ M}$ in toluene at $-78 \text{ }^\circ\text{C}$). Solid line: drawn using the r values obtained by the Kelen–Tüdős method; dashed-line: azeotropic line. See **Table S1** for the polymerization data.

Scheme 2 shows plausible propagation mechanisms of the copolymerization. Unlike in the alternating copolymerization of VEs and BzAs, both the homopropagation and crossover reactions proceed. A highly reactive aldehyde, such as pMeOBzA, which has an electron-donating group on the aromatic ring, was necessary to suppress IBVE homopropagation in our previous study¹⁶ in the copolymerization of BzAs. However, OPA, which has electron-withdrawing formyl groups at the *o*-positions, unexpectedly underwent frequent crossover reactions from the IBVE-derived carbocation. The efficient intramolecular cyclization reaction of the two aldehyde moieties of OPA, which potentially occurs in a concerted instead of stepwise manner, is most likely responsible for the frequent crossover reactions. In addition, the copolymerization probably proceeded in a living manner *via* the generation of dormant species at the propagating ends with covalent carbon–Cl or carbon–OSO₂Et bonds. The livingness of the copolymerization is partly derived from the suitable initiating system that is effective for the suppression of side reactions such as β -proton elimination at the IBVE-derived chain end.



cf. Copolymerization of IBVE and BzAs



Scheme 2. Plausible copolymerization mechanisms of IBVE and OPA or BzAs.

The product copolymer was hydrolyzed into low-MW compounds by acid hydrolysis (**Figure 1B** lower and **Figure 5A**). The hydrolysis product had a much lower MW than the original copolymer, which indicates that crossover reactions between IBVE and OPA were quite frequent (**Table S2**). The MW of the hydrolysis products corresponds to the above-estimated average numbers of IBVE and OPA units per block. However, the hydrolysis products were not a single molecule but a mixture of oligomers because IBVE homosequences were present a little in the main chain of the copolymer (see **Figure 5A** for $^1\text{H NMR}$).³² A similar result was also obtained in acid alcoholysis of the copolymer with methanol (**Figure 5B**).

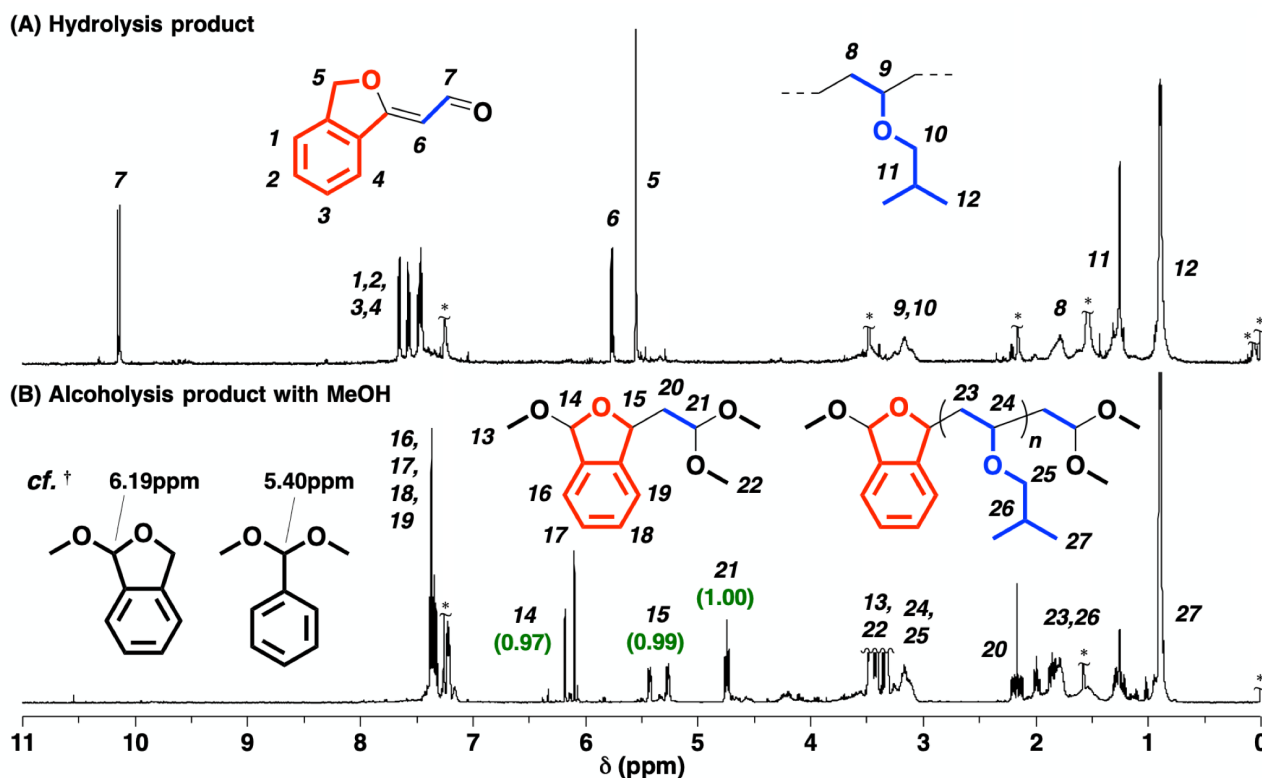


Figure 5. ^1H NMR spectra of (A) the hydrolysis product (a sample prepared under the same conditions to those for **Figure 1B**) or (B) the acid alcoholysis product (0.5 M HCl in MeOH/CH₂Cl₂ (1/1 v/v) solution for 24 h at r.t., 0.5 wt%) of poly(IBVE-*co*-OPA). Peaks with asterisks are due to TMS, grease, water, acetone, methanol, and CHCl₃. † References 33 and 34. Number written in green: integral ratio.

To demonstrate the unique reactivities of both the OPA monomer and the OPA-derived cyclic carbocation, copolymerizations with monomers that also exhibit characteristic reactivities were examined. Cyclic enol ethers, which are cyclic β -substituted VEs, exhibited different copolymerization behaviors depending on the size of the ring. 2,3-Dihydrofuran (DHF), a five-membered cyclic enol ether, which has relatively high cationic homo- and copolymerizabilities^{35–38}, yielded a copolymer with OPA, although the copolymerization was not mediated by long-lived species (entry 8 in **Table 1**; **Figure 6A** and **S2**). The ^1H NMR spectrum of the product indicated that a part of the aldehyde moieties of OPA did not cyclize and remained in the copolymer (**Figure 7A**). The existence of the uncyclized aldehyde moieties was also confirmed by the reduction reaction of the residual formyl group in the copolymer with LiBH₄ (**Figure 7B**). This is partly because DHF has significantly high reactivity and small steric hindrance. Indeed, in the previous report on the cationic copolymerization of DHF and various BzA derivatives¹⁹, the steric repulsion between DHF and the *o*-MeBzA-derived propagating carbocation was found to be small. In the copolymerization with OPA, the reaction of DHF with the OPA-derived acyclic carbocation likely occasionally occurred before the cyclization via the reaction of the carbonyl moiety at the *o*-position proceeds (**scheme 3**).

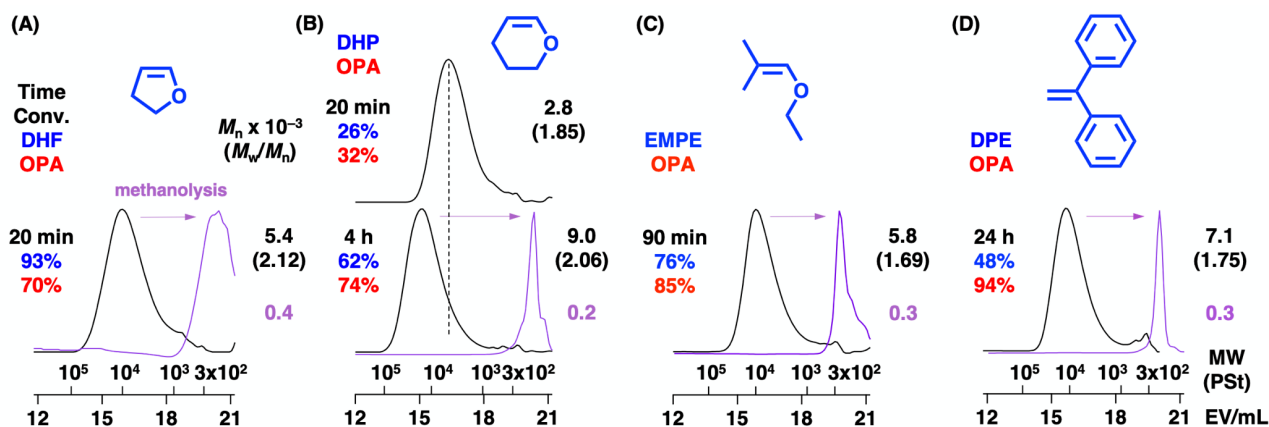


Figure 6. MWD curves of the products obtained by the cationic copolymerization of OPA with (A) DHF (entry 8 in **Table 1**), (B) DHP (entry 9), (C) EMPE (entry 10), and (D) DPE (entry 11) (black: original polymers; purple: products obtained by acid methanolysis). See **Table 1** for the polymerization conditions.

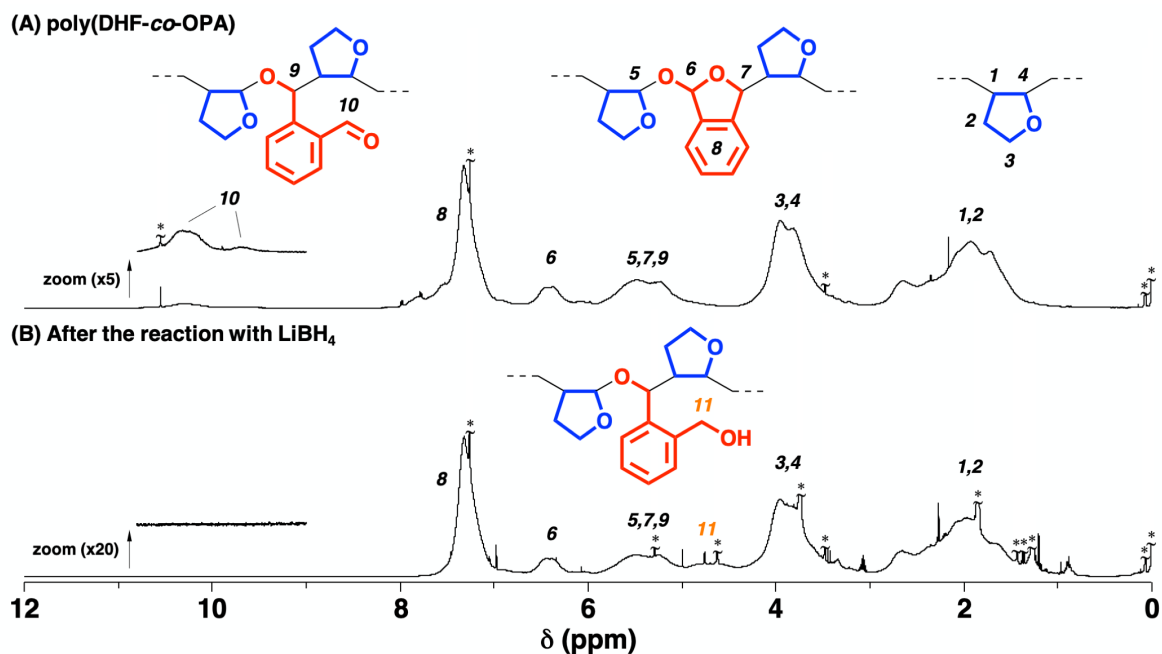
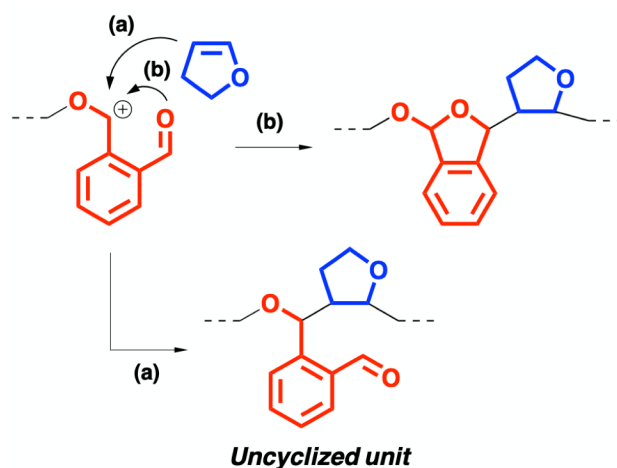
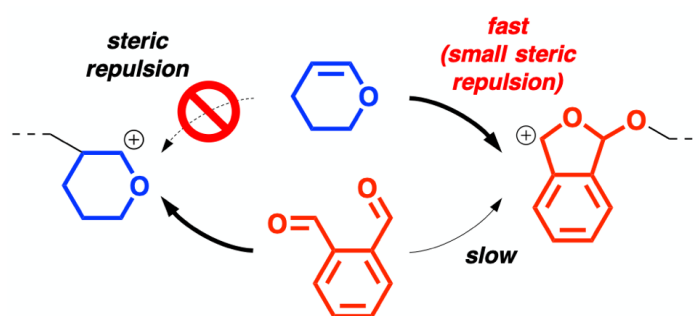


Figure 7. ^1H NMR spectra of (A) poly(DHF-*co*-OPA) (entry 8 in **Table 1**) and (B) the reaction product of the polymer with LiBH_4 recorded in CDCl_3 at 30°C . Peaks with asterisks are due to TMS, grease, water, THF, methanol, CH_2Cl_2 , CHCl_3 and residual OPA.



Scheme 3. Copolymerization of DHF and OPA.

Unlike DHF, 3,4-dihydro-2*H*-pyran (DHP), which is a six-membered cyclic enol ether^{37,38}, efficiently copolymerized with OPA (entry 9 in **Table 1**; **Figure 6B**). Moreover, the homopropagation reactions of DHP and OPA were negligible, resulting in a copolymer with an alternating sequence (**Figure S3**). DHP exhibits low homopolymerizability probably due to the steric hindrance of the DHP homosequences; hence, the reaction with OPA likely helped avoid the effects of steric hindrance (**Scheme 4**), as in the case of the efficient alternating copolymerization of DHP and aromatic aldehydes.¹⁹ Copolymerization with DHP proceeded via the mediation of long-lived species (**Figure 8**), though the MWD was broad. Undesirable side reactions such as chain transfer probably occurred, although the detailed mechanism is not clear.



Scheme 4. Alternating cationic copolymerization of DHP and OPA.

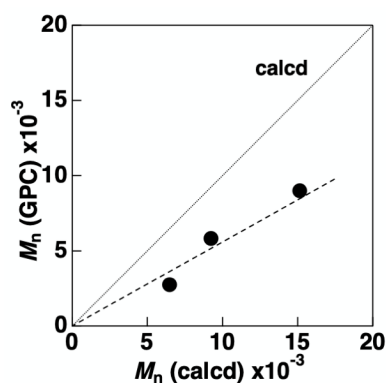


Figure 8. M_n for the copolymerization of DHP and OPA. See **Table 1** for the polymerization conditions.

The unique reactivity of OPA was exerted most effectively in the copolymerization with ethyl 2-methylpropenyl ether (EMPE), a β,β -disubstituted enol ether. EMPE does not homopolymerize²⁰⁻²² (**Figure 9A**) nor does it copolymerize with BzAs¹⁹ (**Figure 9B**) due to the steric hindrance around the β -carbon (the reaction with BzAs resulted in the cyclic trimerization of one EMPE and two aldehyde moieties). Interestingly, the copolymerization of EMPE with OPA successfully produced a copolymer with an alternating sequence (entry 10 in **Table 1**; **Figures 6C, 9C** and **10**). Since the propagating cation derived from OPA has an approximately planar structure, the steric repulsion between the propagating cation and an EMPE monomer is reduced, enabling the addition of EMPE (**Figure 3C**). The intramolecular cyclization reaction of the OPA-derived propagating species is also likely responsible for the efficient propagation reactions through the suppression of depolymerization reaction. The higher ceiling temperature of OPA ($-43\text{ }^{\circ}\text{C}$)²³ than BzA ($-160\text{ }^{\circ}\text{C}$)²³ is probably consistent with these results. In addition, the degree of the resonance effects of the adjacent phenyl ring and oxygen atom on the carbocationic center is possibly different between the acyclic and cyclic carbocation derived from benzaldehyde and OPA, respectively. The difference potentially affects the reactivity of the carbocation toward a vinyl monomer.

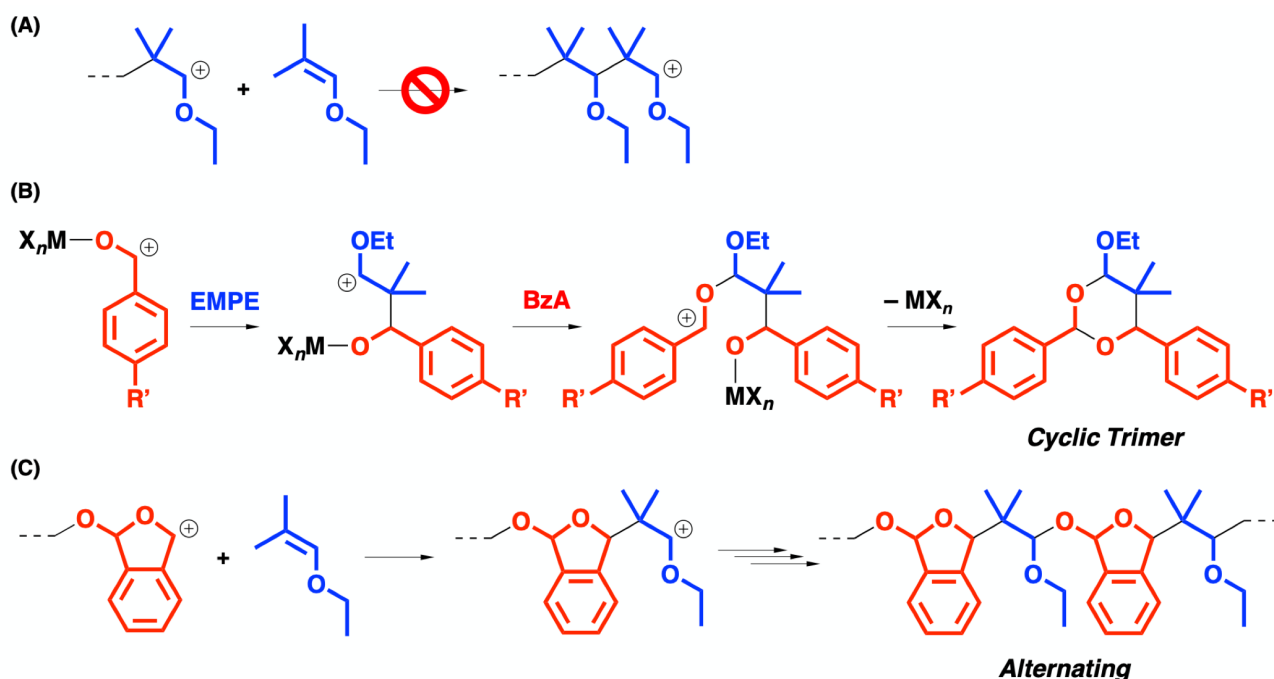


Figure 9. (A) Homopropagation of EMPE, (B) cyclic trimerization reaction of BzAs with EMPE, and (C) crossover reaction from the OPA-derived carbocation to EMPE.

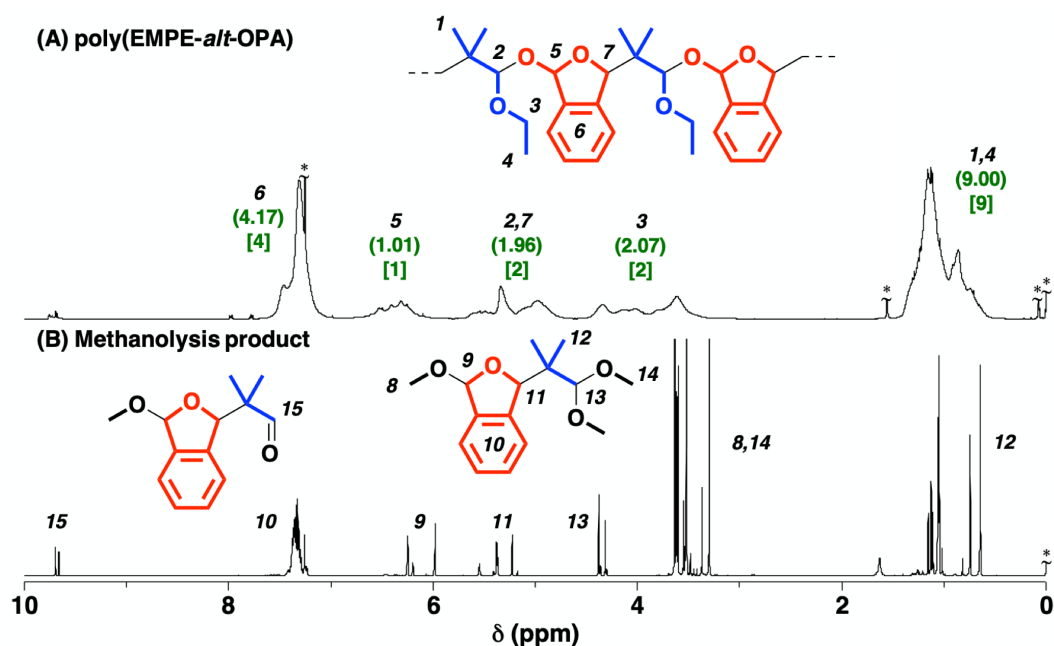


Figure 10. ^1H NMR spectra of (A) poly(EMPE-*alt*-OPA) (entry 10 in **Table 1**) and (B) acid-methanolysis product of (A) recorded in CDCl_3 at 30 $^\circ\text{C}$. Peaks with asterisks are due to TMS, grease, and water.

Importantly, 1,1-diphenylethylene (DPE), which also neither homopolymerize nor copolymerize with BzA⁸ (cyclic trimers are generated in a manner similar to that observed with EMPE), was also an effective comonomer for OPA, although the product copolymer did not have an alternating sequence (entry 11 in **Table 1**; **Figures 6D** and **11A**). In addition, the copolymer did not have DPE homosequences, which was confirmed by the product of acid methanolysis (**Figure 11B**).

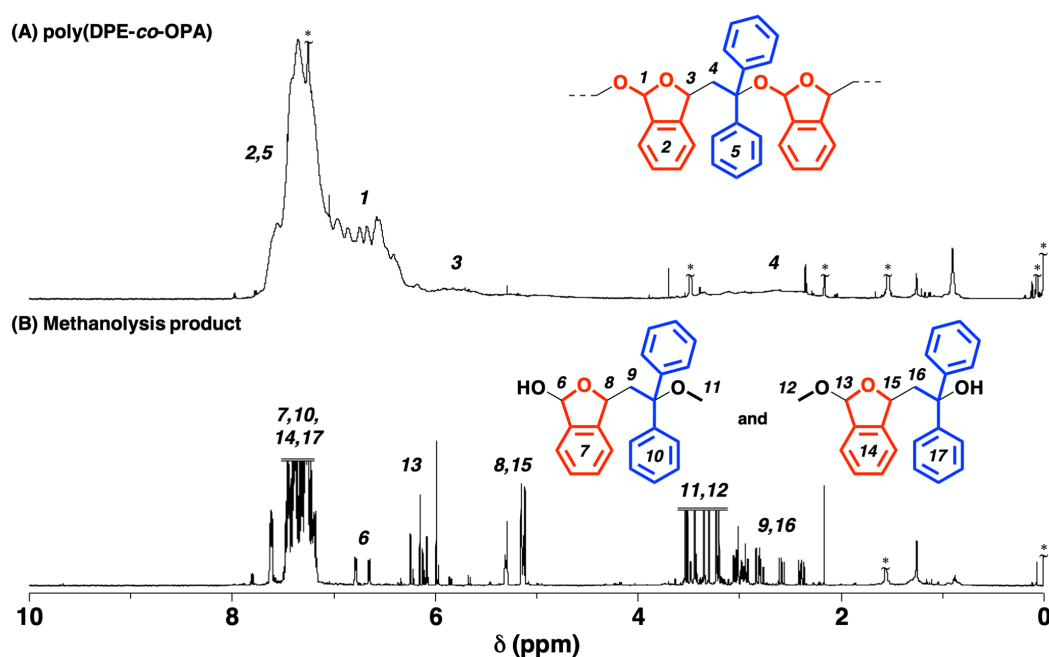


Figure 11. ^1H NMR spectra of (A) poly(DPE-*co*-OPA) (entry 11 in **Table 1**) and (B) its acid-methanolysis product recorded in CDCl_3 at 30 $^\circ\text{C}$. Peaks with asterisks are due to TMS, grease, water, toluene, MeOH, and CHCl_3 .

Conclusion

In conclusion, OPA was demonstrated to exhibit characteristic reactivity in copolymerizations with vinyl monomers. The copolymerization of OPA and IBVE proceeded in a living manner when using a suitable initiating system. Unlike copolymers of VEs and BzAs, the copolymer of IBVE and OPA had homosequences of OPA and IBVE. More interestingly, OPA was successfully copolymerized with vinyl monomers that show neither homopolymerizability nor copolymerizability with BzAs, and linear copolymers with OPA (some of which were alternating) were obtained. Both the intramolecular cyclization and the cyclic propagating cation are most likely responsible for the characteristic reactivity of OPA.

References and Notes

1. Longo, J. M.; Sanford, M. J.; Coates, G. W. *Chem. Rev.* **2016**, *116*, 15167–15197.
2. Herzberger, J.; Niederer, K.; Pohlitz, H.; Seiwert, J.; Worm, M.; Wurm, F. R.; Frey, H. *Chem. Rev.* **2016**, *116*, 2170–2243.
3. Chen, Z.; Brookhart, M. *Acc. Chem. Res.* **2018**, *51*, 1831–1839.
4. Poland, S. J.; Darensbourg, D. J. *Green Chem.* **2017**, *19*, 4990–5011.
5. Nakano, R.; Ito, S.; Nozaki, K. *Nat. Chem.* **2014**, *6*, 325–331.
6. Ureta, E.; Smid, J.; Szwarc, M. *J. Polym. Sci., Part A-1: Polym. Chem.* **1966**, *4*, 2219–2228.
7. Yuki, H.; Hotta, J.; Okamoto, Y.; Murahashi, S. *Bull. Chem. Soc. Jpn.* **1967**, *40*, 2659–2663.
8. Yasuoka, K.; Kanaoka, S.; Aoshima, S. *J. Polym. Sci., Part A: Polym. Chem.* **2012**, *50*, 2758–2761.
9. Hutchings, L. R.; Brooks, P. P.; Parker, D.; Mosely, J. A. Sevinc, S. *Macromolecules* **2015**, *48*, 610–628.
10. Natalello, A.; Hall, J. N.; Eccles, E. A. L.; Kimani, S. M.; Hutchings, L. R. *Macromol. Rapid. Commun.* **2011**, *32*, 233–237.
11. Sang, W.; Ma, H.; Wang, Q.; Hao, X.; Zheng, Y.; Wang, Y.; Li, Y. *Polym. Chem.* **2016**, *7*, 219–234.
12. Overberger, C. G.; Tanner, D.; Pearce, E. M. *J. Am. Chem. Soc.* **1958**, *80*, 4566–4568.
13. D’Alelio, G. F.; Finestone, A. B.; Taft, L.; Miranda, T. J. *J. Polym. Sci.* **1960**, *45*, 83–89.
14. Mizote, A.; Tanaka, T.; Higashimura, T.; Okamura, S. *J. Polym. Sci., Part A: Gen. Pap.* **1965**, *3*, 2567–2578.
15. Satoh, K.; Saitoh, S.; Kamigaito, M. *J. Am. Chem. Soc.* **2007**, *129*, 9586–9587.
16. Ishido, Y.; Aburaki, R.; Kanaoka, S.; Aoshima, S. *Macromolecules* **2010**, *43*, 3141–3144.
17. Aoshima, S.; Oda, Y.; Matsumoto, S.; Shinke, Y.; Kanazawa, A.; Kanaoka, S. *ACS Macro Lett.* **2014**, *3*, 80–85.
18. Ishido, Y.; Kanazawa, A.; Kanaoka, S.; Aoshima, S. *Macromolecules* **2012**, *45*, 4060–4068.
19. Ishido, Y.; Kanazawa, A.; Kanaoka, S.; Aoshima, S. *J. Polym. Sci., Part A: Polym. Chem.* **2014**, *52*, 1334–1343.
20. Okuyama, T.; Fueno, T.; Furukawa, J.; Uyeo, K. *J. Polym. Sci., Part A-1: Polym. Chem.* **1968**, *6*, 1001–1007.
21. Okuyama, T.; Fueno, T.; Furukawa, J. *J. Polym. Sci., Part A-1: Polym. Chem.* **1969**, *7*, 3045–3052.
22. Nuyken, O.; Raether, R. B.; Spindler, C. E. *Macromol. Chem. Phys.* **1998**, *199*, 191–196.

23. Aso, C.; Tagami, S.; Kunitake, T. *J. Polym. Sci., Part A-1: Polym. Chem.* **1969**, *7*, 497–511.
24. Kaitz, J. A.; Diesendruck, C. E.; Moore, J. S. *J. Am. Chem. Soc.* **2013**, *135*, 12755–12761.
25. Schwartz, J. M.; Phillips, O.; Engler, A.; Sutlief, A.; Lee, J.; Kohl, P. A. *J. Polym. Sci., Part A: Polym. Chem.* **2017**, *55*, 1166–1172.
26. Aso, C.; Tagami, S. *Macromolecules* **1969**, *2*, 414–419.
27. Wang, F.; Diesendruck, C. E. *Macromol. Rapid. Commun.* **2018**, *39*, 1700519.
28. Aso, C.; Tagami, S.; Kunitake, T. *J. Polym. Sci., Part A-1: Polym. Chem.* **1970**, *8*, 1323–1336.
29. Mizote, A.; Kusudo, S.; Higashimura, T.; Okamura, S. *J. Polym. Sci., Part A: Polym. Chem.* **1967**, *5*, 1727–1739.
30. Higashimura, T.; Kamigaito, M.; Kato, M.; Hasebe, T.; Sawamoto, M. *Macromolecules* **1993**, *26*, 2670–2673.
31. Sawamoto, M.; Enoki, T.; Higashimura, T. *Macromolecules* **1987**, *20*, 1–6.
32. A main compound in the hydrolysis product most likely has a structure shown in **Figure 5A**, which was suggested by the comparison with the compounds reported in the reference: Bunse, P.; Wuerthwein, E. U.; Wuensch, B. *Eur. J. Org. Chem.* **2018**, 1806–1812. However, the mechanism of the generation of the generation of this compound is unclear.
33. Hobson, S. J.; Parkin, A.; Marquez, R. *Org. Lett.* **2008**, *10*, 2813–2816.
34. Sakurai, H.; Sasaki, K.; Hayashi, J.; Hosomi, A. *J. Org. Chem.* **1984**, *49*, 2808–2809.
35. Barr, D. A.; Rose, J. B. *J. Chem. Soc.* **1954**, 3766–3769.
36. Ogawa, Y.; Sawamoto, M.; Higashimura, T. *Polym. J.* **1984**, *16*, 415–422.
37. Nuyken, O.; Aechtner, S. *Polym. Bull.* **1992**, *28*, 117–122.
38. Yonezumi, M.; Kanaoka, S.; Aoshima, S. *J. Polym. Sci., Part A: Polym. Chem.* **2008**, *46*, 4495–4504.

Supporting Information

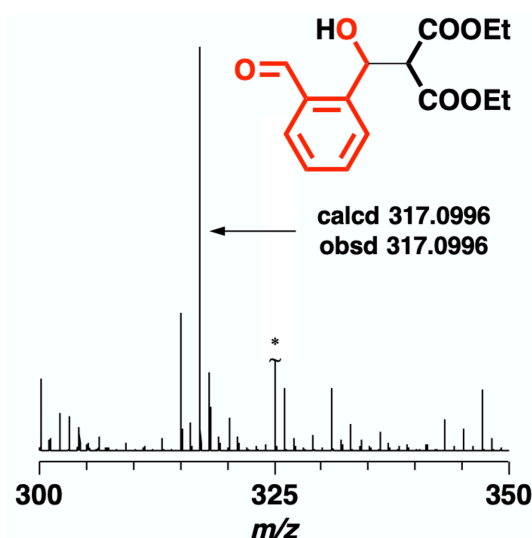


Figure S1. ESI-MS spectrum of the hydrolysis product of poly(IBVE-*co*-OPA) quenched by sodium diethylmalonate solution. * contamination.

Table S1. The data for the determination of monomer reactivity ratio.

entry	IBVE conc. [M]	OPA conc. [M]	time	total conv. (%) ^b	$M_n \times 10^{-3}$ ^c	M_w/M_n ^c	IBVE in copolymer ^d
1	0.81	0.40	10 min	15	5.8	1.70	0.65
2	0.60	0.60	10 min	12	3.2	1.14	0.57
3	0.40	0.80	10 min	6	3.2	1.73	0.54
4	0.30	0.90	10 min	10	1.4	2.22	0.49

^a $[\text{EtSO}_3\text{H}]_0 = 4.0$ mM, $[\text{GaCl}_3]_0 = 4.0$ mM, $[\text{1,4-dioxane}]_0 = 0.50$ M in toluene at -78 °C. ^b By gravimetry. ^c By GPC (polystyrene calibration). ^d By ^1H NMR.

Table S2. The number of each sequence per chain^a

$M_n \times 10^{-3}$	M_w/M_n	OPA content in copolymer (%)	IBVE-IBVE	IBVE-OPA	OPA-IBVE	OPA-OPA
13.0	1.23	49	14	45	46	12

^a The same sample as that shown in **Figure 3A**.

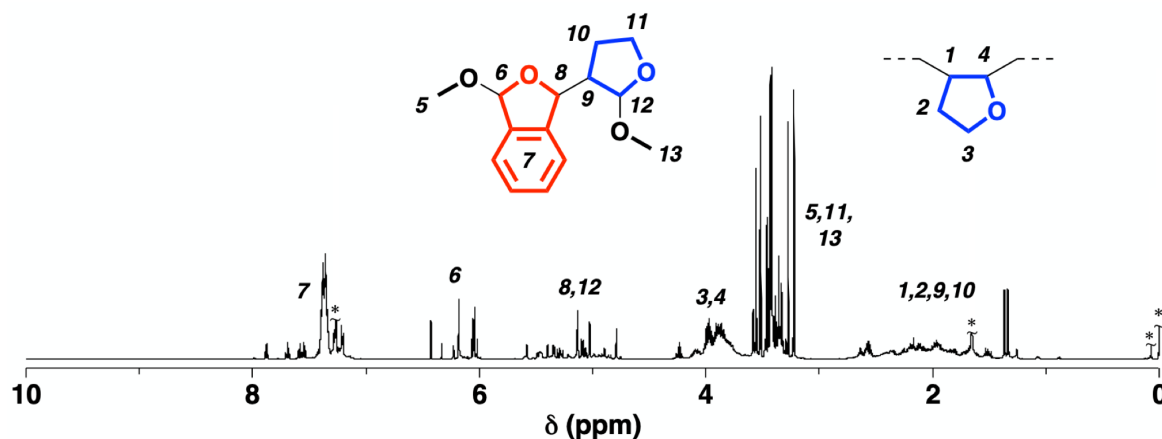
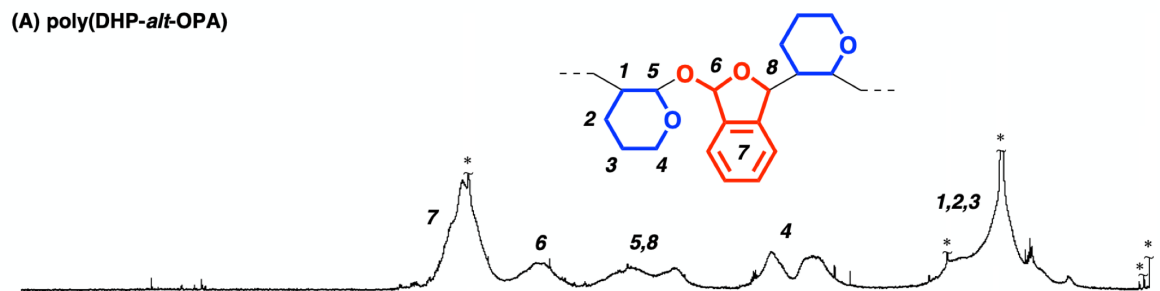


Figure S2. ^1H NMR spectrum of the acid-methanolysis product of poly(DHF-*co*-OPA) recorded in CDCl_3 at 30 °C. Peaks with asterisks are due to TMS, grease, water, and CHCl_3 .

(A) poly(DHP-*alt*-OPA)



(B) Methanolysis product

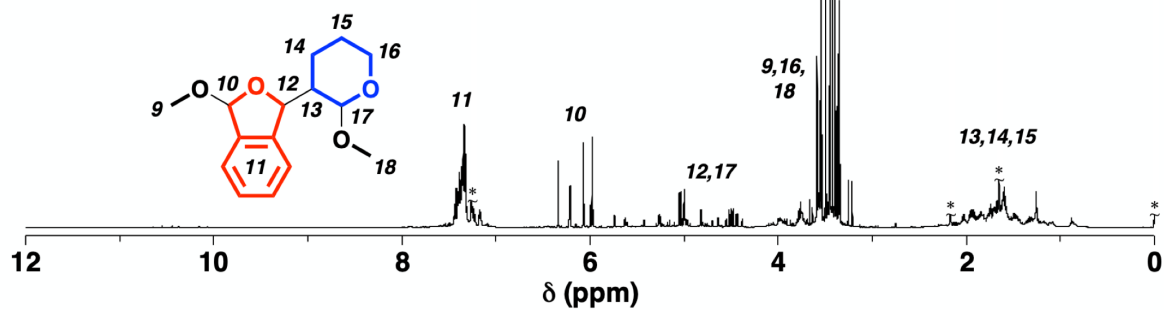


Figure S3. ¹H NMR spectra of (A) poly(DHP-*alt*-OPA) (entry 9 in Table 1) and (B) its acid-methanolysis products recorded in CDCl₃ at 30 °C. Peaks with asterisks are due to TMS, grease, water, and CHCl₃.

Part II

New Copolymerization Based on the Copolymerizability of *o*-Phthalaldehyde

Chapter 3

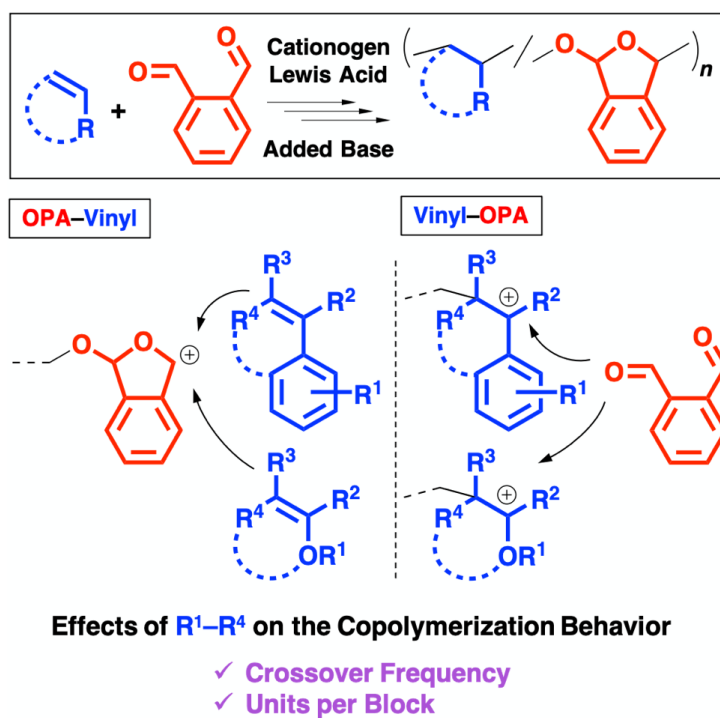
Cationic Copolymerization of *o*-Phthalaldehyde and Vinyl Monomers with Various Substituents on the Vinyl Group or in the Pendant: Effects of the Structure and Reactivity of Vinyl Monomers on Copolymerization Behavior

Introduction

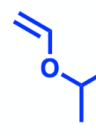
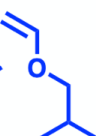
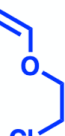
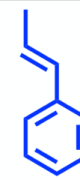
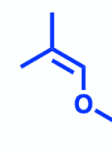
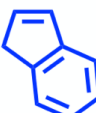
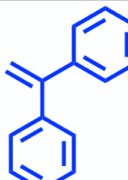
In the copolymerization of monomers that have different structures, the reactivity of each monomer and the stability of each propagating species need to be carefully considered. In radical copolymerization, alternating copolymers are easily obtained from the combination of an electron-rich monomer and an electron-poor monomer. In contrast, frequent crossover reactions between different kinds of monomers are generally difficult in ionic copolymerization. For example, in the anionic copolymerization of styrene (St) and methyl methacrylate (MMA)¹, an MMA monomer can react with the St-derived propagating carbanion, whereas a St monomer cannot react with the MMA-derived propagating carbanion. This observation is due to the high stability of the MMA-derived propagating carbanion and the low reactivity of the St monomer. In the cationic copolymerization of isobutyl vinyl ether (IBVE) and *p*-methoxystyrene (pMOS)^{2,3}, the crossover reaction from the IBVE-derived carbocation to a pMOS monomer negligibly occurs, generating block-like copolymers. Therefore, both monomers are required to react with propagating species derived from both monomers to realize frequent crossover reactions in the copolymerization of different kinds of monomers.

Polymers obtained from monomers that have bulky structures around polymerizable groups are expected to exhibit specific properties compared to those obtained from normal monomers⁴⁻⁶. However, such bulky monomers are generally difficult to polymerize due to the steric hindrance and low ceiling temperature. Consequently, copolymerization is an effective strategy to obtain polymers from such bulky monomers^{7,8}; however, when the comonomer or the bulky monomer does not have sufficient reactivity to react with the propagating species derived from the bulky monomer or the comonomer, respectively, copolymerization does not proceed.⁹ The use of appropriate comonomers, such as monomers with both high reactivity and small steric hindrance, is indispensable for successful copolymerization beyond the limitation of reactivity.

In Chapter 2 of this thesis, the author reports the exceptional copolymerizability of OPA with vinyl monomers. Living copolymerization, alternating copolymerization, and successful copolymerization with bulky monomers such as β,β -dimethyl vinyl ether and 1,1-diphenylethylene (DPE) were demonstrated to proceed due to the special reactivity of the OPA-derived cyclic propagating cation with small steric hindrance. In this chapter, to extend the range of copolymerizable monomers and systematically elucidate the relationships between the structure and reactivity of vinyl monomers and the copolymerization behavior, the author investigated the copolymerization of OPA with various St derivatives and vinyl ethers (VEs) (**Scheme 1**). Vinyl monomers with various substituents in the pendant or on the vinyl group and cyclic structures were used, as shown in **Scheme 2**.



Scheme 1. Cationic copolymerization of vinyl monomers and OPA.

	St derivatives		VEs		
Mono-substituted					
	pMOS	pMeSt	IPVE	IBVE	CEVE
Homo	○	○	○	○	○
BzA	×	○	×	○	○
β -Methyl or β,β -Dimethyl					
	Ane	β MeSt	EPE	EMPE	
Homo	△	×	○	×	
BzA	×	×	○	×	
Cyclic Structure					
	Indene	DHN	DHF	DHP	
Homo	○	△	○	△	
BzA	○*	×	○	○	
α -Methyl or α -Phenyl					
	α MeSt	DPE	MPE	MeDHF	
Homo	○	×	○	○	
BzA	×	×	×	-	

Scheme 2. Vinyl monomers used in this study and the cationic polymerization behavior. Circle: homopolymerizable or copolymerizable alternatingly with BzAs; triangle: oligomer generation; cross: no homopolymerizability, homopolymers of vinyl monomers (for pMOS, IPVE, and MPE), or no copolymerizability with BzAs (others); bar: not examined. * An alternating copolymer generates at a higher BzA content in monomer feed.

Experimental Section

Materials.

p-Methoxystyrene (pMOS; Wako, >97.0%) was dried overnight over sodium sulfate and then distilled twice over calcium hydride under reduced pressure. *p*-Methylstyrene (pMeSt; Aldrich, >96.0%) and 2-chloroethyl vinyl ether (CEVE; TCI, >97%) were washed with a 10% aqueous sodium hydroxide solution and then with water, dried overnight over sodium sulfate, and distilled twice over calcium hydride under reduced

pressure. *trans*-Anethole (Ane; TCI, >98.0%), *trans*- β -methylstyrene (β MeSt; TCI, >97.0%), indene (Aldrich, >98.0%), 1,2-dihydronaphthalene (DHN; TCI, >98.0%), and α -methylstyrene (α MeSt; Nacalai Tesque, >98.0%), and 2,6-di-*tert*-butylpyridine (DTBP; Sigma-Aldrich, 97%) were distilled twice over calcium hydride under reduced pressure. Isopropyl VE (IPVE; Wako, >97.0%) was washed with a 10% aqueous sodium hydroxide solution and then with water, dried overnight over potassium hydroxide, and distilled twice over calcium hydride. Ethyl 1-propenyl ether (EPE; *cis/trans* = 85/15, TCI, >99.0%), methyl 2-propenyl ether (MPE; Aldrich, >97.0%), and 2,3-dihydro-5-methylfuran (MeDHF; Aldrich, >97.0%) were distilled twice over calcium hydride. Other materials were prepared and used as described in Chapter 2.

Polymerization procedures.

Polymerization was conducted under a dry nitrogen atmosphere in a glass tube equipped with a three-way stopcock. Dichloromethane, ethyl acetate, and the monomers were first added into the tube using different dry syringes. To this solution, which was cooled at -78 °C in advance, a prechilled 40 mM IBVE–HCl solution (0.3 mL) in dichloromethane was added using a dry syringe. Other procedures were conducted in a manner similar to that described in Chapter 2.

Acid hydrolysis or methanolysis of product copolymers.

Acid hydrolysis or methanolysis of product copolymers were conducted in a manner similar to that described in Chapter 2.

Characterization.

The thermal properties of the polymers were examined with a PerkinElmer STA6000 or a Shimadzu DSC-60 Plus differential scanning calorimeter. The MWD, ^1H NMR, and ESI-MS spectra were measured in a manner similar to that described in Chapter 2.

Results and Discussion

Copolymerization of Various St Derivatives with OPA

The author first focused on St derivatives, which are known to be less reactive than VEs in cationic polymerization, as comonomers for copolymerization with OPA. Although there were many reports on the living cationic polymerization of St derivatives, only a few studies on the copolymerization of St derivatives and aldehyde monomers have been examined. Only St and indene are reported to copolymerize alternately with BzA by BF_3OEt_2 .¹⁰ The copolymerization of other St derivatives and BzAs has been examined in our group recently; however, only pMeSt was found to copolymerize alternately with BzA¹¹, and the copolymerization of other St derivatives with BzAs did not proceed (**Scheme 2**).⁷ In contrast, as demonstrated in Chapter 2, OPA could copolymerize with 1,1-diphenylethylene, one of the St derivatives that does not copolymerize with BzAs. The unique reactivity of the OPA monomer and the OPA-derived propagating carbocation are expected to exhibit quite different behavior from BzAs in the copolymerization with St derivatives in terms of the crossover frequency. To systematically elucidate the copolymerizability of OPA with St derivatives, monomers with various structures were used for copolymerization. In addition, acid-cleavable acetal moieties derived from intramolecular cyclization of OPA are introduced into the main chain

of St derivative polymers; hence, the degradation behavior of the obtained copolymers by acid was also investigated.

Table 1. Cationic copolymerization of various St derivatives and OPA^a

entry	monomer	Lewis acid	time	conv. ^b (%)		$M_n \times 10^{-3}$ ^c	M_w/M_n ^c	OPA content in the copolymer (%) ^d	units per block ^d	
				St	OPA				St	OPA
1	pMOS	SnCl ₄	1 h	90	70	3.8	1.84	43	–	–
2 ^e		SnCl ₄	1 h	57	0	3.7	1.75	0	–	–
3		GaCl ₃	20 s	80	21	3.7	1.69	20	–	–
4	pMeSt	SnCl ₄	90 min	0	84	12.1	1.73	100	–	–
5		GaCl ₃	5 min	10	65	4.7	3.14	95	–	–
6	Ane	SnCl ₄	1 h	97	95	11.6	1.70	53	1.2	1.5
7		GaCl ₃	1 h	53	96	9.8	1.91	64	1.2	1.9
8	β MeSt	SnCl ₄	2 h	0	57	2.3	1.48	100	–	–
9	Indene	SnCl ₄	1 h	<1	89	5.8	2.09	>99	–	–
10		GaCl ₃	1 h	94	83	7.5	2.61	46	1.9	1.6
11	DHN	SnCl ₄	1 h	<1	80	4.5	2.37	>99	–	–
12		GaCl ₃	1 h	12	54	3.5	1.99	82	1.5	6.8
13	α MeSt	SnCl ₄	30 min	40	93	7.4	1.71	74	1.4	4.7
14 ^f	DPE	SnCl ₄	24 h	48	94	7.1	1.75	68	1.0	2.0

^a [St derivatives]₀ = 0.40 M, [OPA]₀ = 0.40 M, [IBVE-HCl]₀ = 4.0 mM (for entries 1, 2, 4, 6–14) or [EtSO₃H]₀ = 4.0 mM (for entries 3,5), [SnCl₄]₀ = 10 mM or [GaCl₃]₀ = 4.0 mM, [ethyl acetate]₀ = 1.0 M (for entries 1, 2, 4, 6), [1,4-dioxane]₀ = 0.50 M (for entries 3, 5, 7) in CH₂Cl₂ at –78 °C. ^b Determined by ¹H NMR and gravimetry. ^c Determined by GPC (polystyrene standards). ^d Calculated by ¹H NMR spectra. ^e In toluene. ^f Data from Chapter 2 of this thesis.

To elucidate the effect of pendant groups on the copolymerization behavior, pMOS and pMeSt, which exhibit high and middle reactivity in cationic polymerization, respectively, were used for copolymerization. Copolymerizations of pMOS or pMeSt with OPA were conducted by using IBVE-HCl or EtSO₃H as a cationogen and SnCl₄ or GaCl₃ as a Lewis acid catalyst in toluene or dichloromethane at –78 °C. In the copolymerization with pMOS, only pMOS was consumed and OPA was negligibly consumed in toluene (entry 2 in **Table 1**). In dichloromethane, both monomers were consumed (entries 1 and 3); however, the structures derived from the crossover reactions between pMOS and OPA were not confirmed in the ¹H NMR spectrum of the product (**Figures 1A** and **1C**; no peaks around 4.5–5.5 ppm). The product obtained by acid hydrolysis of the polymer also supported both the existence of long pMOS sequences and the absence of the structures derived from frequent crossover. In contrast, in the copolymerization with pMeSt, only OPA was consumed to yield the OPA homopolymer (entries 4 and 5). The reactivity of pMeSt is likely too low to react with the OPA-derived propagating carbocation.

The monomers with substituents on the vinyl group were next used for copolymerization, since the copolymerization of OPA with pMOS or pMeSt was difficult. *trans*-Anethole (Ane), which has a methyl group on the β -carbon of pMOS, was examined instead of pMOS. Ane had been known to be difficult to

homopolymerize before due to the steric repulsion between the β -methyl group of Ane and the propagating carbocation, whereas the quasi-living cationic homopolymerization of Ane was reported recently.¹² In the copolymerization of OPA and Ane by SnCl₄ or GaCl₃ in dichloromethane, both monomers were consumed to yield a copolymer with an M_n of approximately 10^4 (entries 6 and 7 in **Table 1**; **Figure 1B**). Peaks derived from the crossover reactions (peaks 9 and 14) obviously appeared in the ¹H NMR spectrum of the product copolymer (**Figure 1D**), unlike in the case of pMOS. In addition, when the obtained copolymer was subjected to reaction with HCl in methanol, the copolymer was degraded into low-MW compounds (**Figures S1** and **S2**). The acetal moieties, which were derived from the cyclization of OPA, were responsible for the degradation under acidic conditions (**Scheme 3**). The average units of Ane and OPA per block were estimated to be 1.2 and 1.5, respectively.

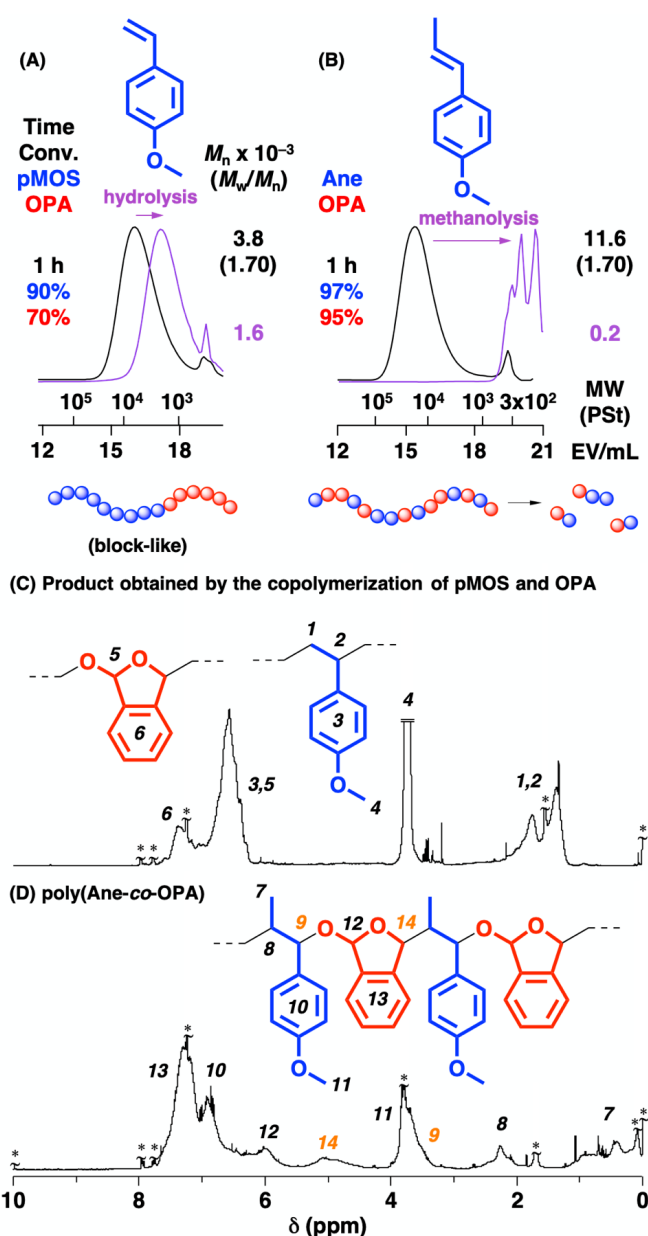
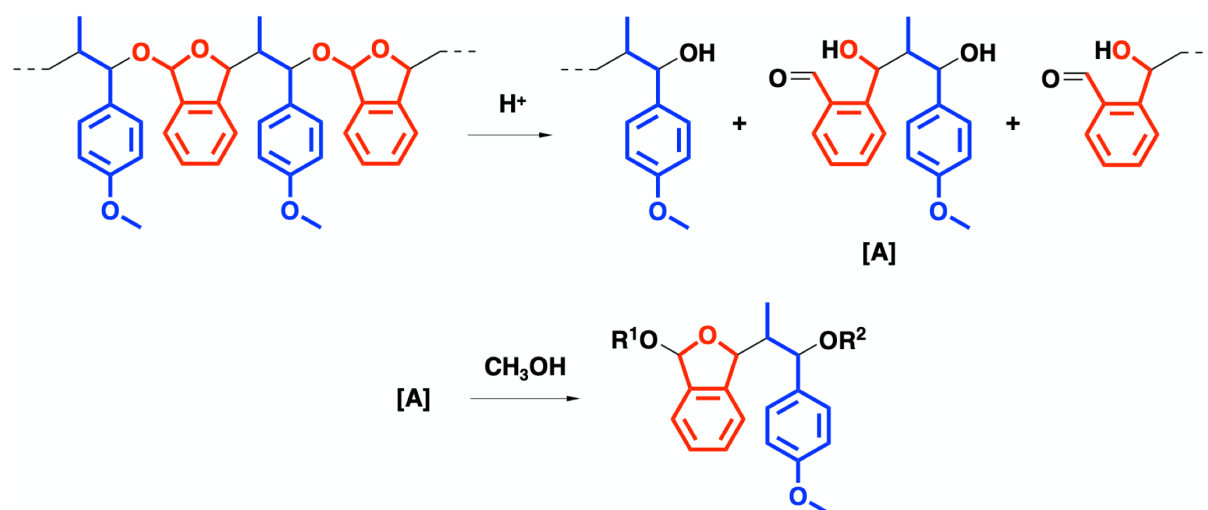
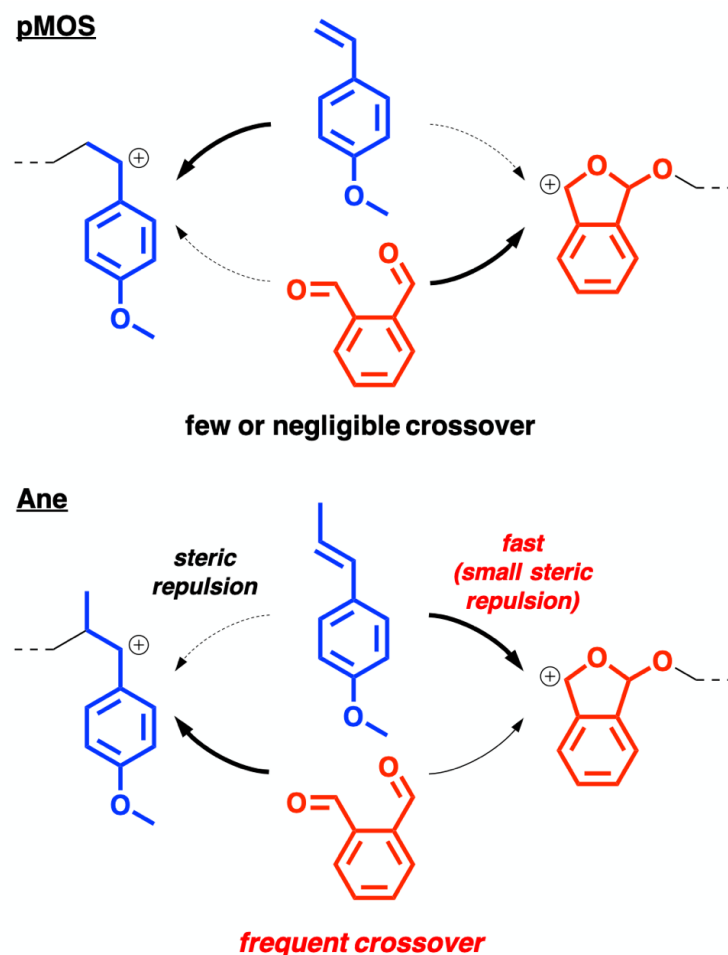


Figure 1. MWD curves of the products obtained by the copolymerization of OPA with (A) pMOS (entry 1 in **Table 1**) or (B) Ane (entry 6), and ¹H NMR spectra of (C) the product obtained by the copolymerization of pMOS and OPA (entry 1) and (D) poly(Ane-co-OPA) (entry 6) recorded in CDCl₃ at 30 °C. Peaks with asterisks are due to TMS, grease, water, methanol, CHCl₃, and residual OPA.



Scheme 3. Acid methanolysis of copolymers via cleavage of acetal moieties ($R^1, R^2 = H$ or Me).

The mechanisms of the copolymerization of OPA with pMOS or Ane are described in **Scheme 4**. In the copolymerization with pMOS, homopropagation of each monomer preferentially occurred rather than crossover reactions. In contrast, copolymerization with Ane proceeded via frequent crossover reactions. The addition of Ane to the Ane-derived propagating carbocation was suppressed due to steric repulsion, and thus, the addition of OPA to the Ane-derived carbocation frequently occurred. For the OPA-derived propagating carbocation, the addition of Ane occurred more smoothly than OPA did because of the high reactivity of Ane and the small steric hindrance between the β -methyl group of Ane and the cyclic carbocation of OPA. In fact, when *trans*- β -methylstyrene (*trans*- β MeSt), which is less reactive than Ane, was used instead of Ane, *trans*- β MeSt did not react with the OPA-derived propagating carbocation, yielding an OPA homopolymer (entry 8 in **Table 1**). Both the β -methyl group and the high reactivity derived from an electron-donating alkoxy group on the aromatic ring were found to be necessary for efficient crossover reactions.



Scheme 4. Plausible copolymerization mechanisms of pMOS or Ane with OPA.

St derivatives with cyclic structures were next examined. Indene, which has a five-membered ring, is known to exhibit homopolymerizability, unlike *cis*- or *trans*- β MeSt. Although indene can be regarded as a β MeSt derivative, the sp^2 orbital of the carbocation derived from indene is highly strained and thus exhibits high reactivity in cationic polymerization. When the copolymerization of indene with OPA was examined using SnCl_4 as a Lewis acid catalyst, indene was negligibly consumed, yielding an OPA homopolymer (entry 9 in **Table 1**). In contrast, both indene and OPA were consumed when GaCl_3 was used as a catalyst instead of SnCl_4 (entry 10). The ^1H NMR spectrum of the product indicated the generation of a random copolymer (indene/OPA units = 1.9/1.6 per block; **Figures 2A** and **3A**). The generation of indene homosequences was also confirmed by acid methanolysis that yielded a degradation product with an MW of approximately 0.5×10^3 (**Figures 3B** and **S3**). A possible reason for unsuccessful copolymerization by SnCl_4 is that SnCl_4 could not cleave the C–Cl bond at the indene-derived propagating end in the presence of OPA, whereas GaCl_3 could activate the C–Cl bond (**Scheme S1**). Both SnCl_4 and GaCl_3 can initiate cationic polymerization by coordination to OPA.

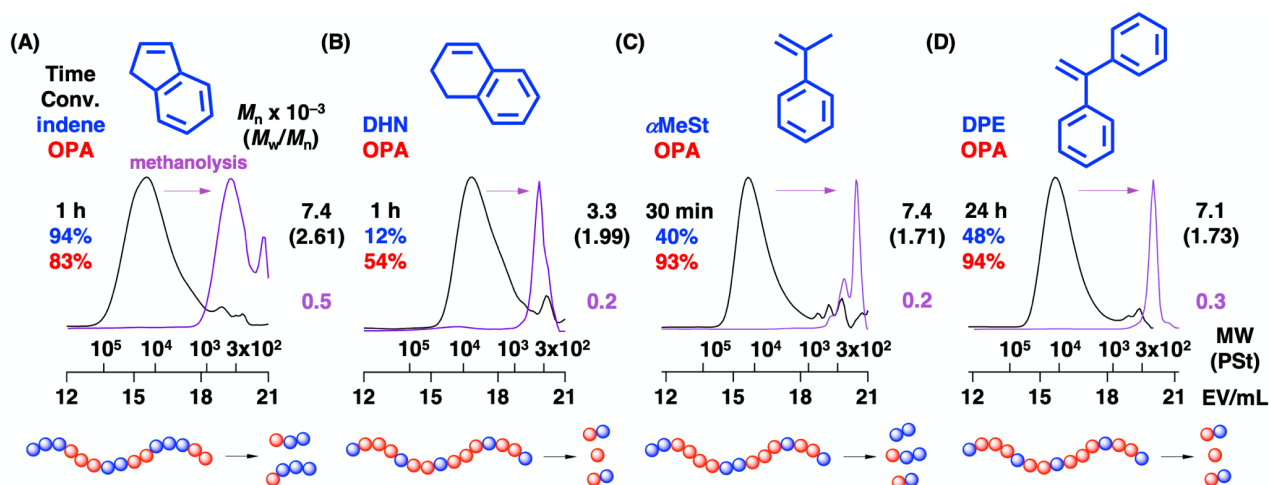


Figure 2. MWD curves of the products obtained by the copolymerization of OPA with (A) indene (entry 10 in **Table 1**), (B) DHN (entry 12), (C) α MeSt (entry 13), or (D) DPE (entry 14) (black: original polymers; purple: products obtained by acid methanolysis). See the footnote of **Table 1** for the polymerization conditions.

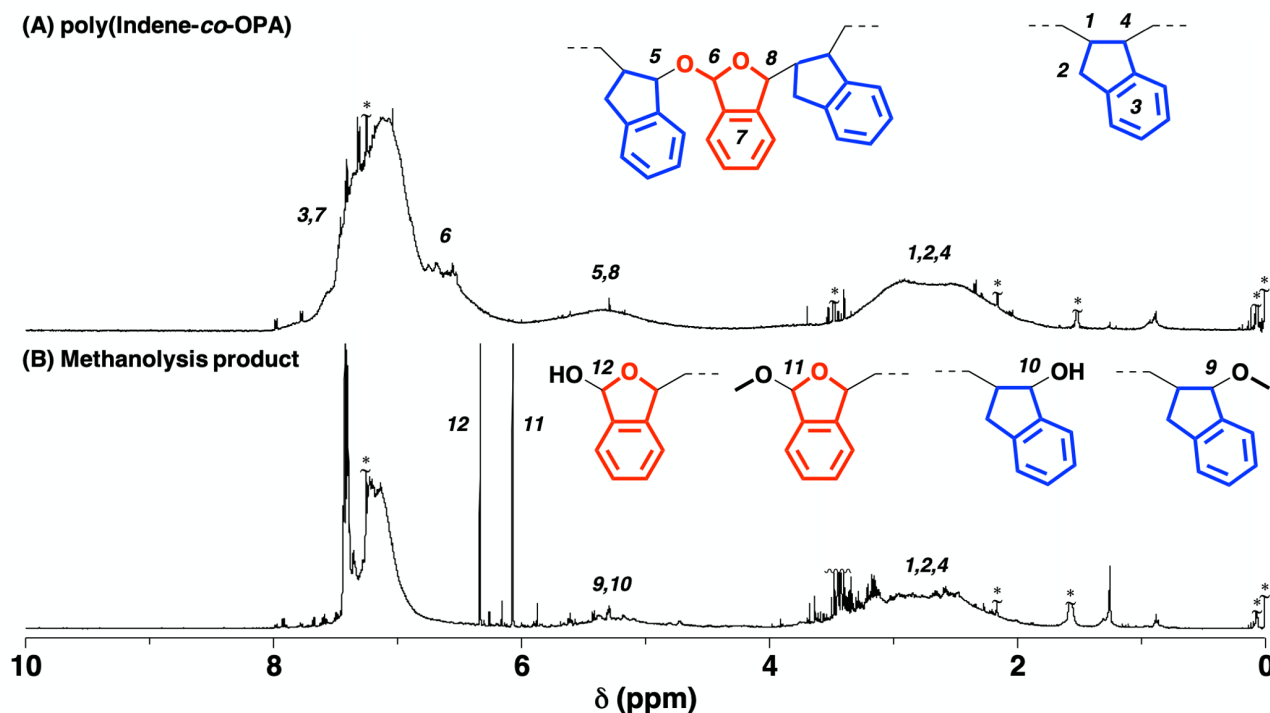


Figure 3. ^1H NMR spectra of (A) poly(indene-*co*-OPA) (entry 10 in **Table 1**) and (B) its acid-methanolysis product recorded in CDCl_3 at 30 $^\circ\text{C}$. Peaks with asterisks are due to TMS, grease, water, acetone, MeOH, and CHCl_3 .

The copolymerization of OPA and 1,2-dihydronaphthalene (DHN), which is a St derivative with a six-membered ring, was also examined. DHN is known to be difficult to homopolymerize due to steric hindrance.¹³ Copolymerization proceeded by GaCl_3 and not by SnCl_4 (entries 11 and 12 in **Table 1**; **Figures 2B** and **S4**), as in the case of indene. The composition of DHN in the copolymer was lower than that of indene, indicating that the reactivity of DHN to the OPA-derived carbocation is not so high.

In Chapter 2 of this thesis, copolymerization of OPA with DPE, which is neither homopolymerizable nor

copolymerizable with BzA derivatives due to the large steric hindrance, was demonstrated to proceed with OPA to yield a copolymer (entry 14 in **Table 1**). The author also examined the copolymerization with α MeSt, which is known to homopolymerize at -78 °C, unlike DPE. Copolymerization of α MeSt and OPA proceeded with SnCl_4 , yielding a copolymer with some α MeSt homosequences (entry 13; **Figures 2C** and **S5**). The generation of α MeSt homosequences was also confirmed by acid methanolysis of the copolymer.

The author investigated the thermal properties of the obtained copolymers of OPA and St derivatives. For example, poly(Ane-*co*-OPA) started to degrade at approximately 200 °C (**Figure 4A** upper panel) and did not exhibit a glass transition below 180 °C (**Figure 4B** upper panel). Poly(DPE-*co*-OPA) was more resistant to heat than poly(Ane-*co*-OPA); however, the T_g was not observed (**Figure 4** lower).

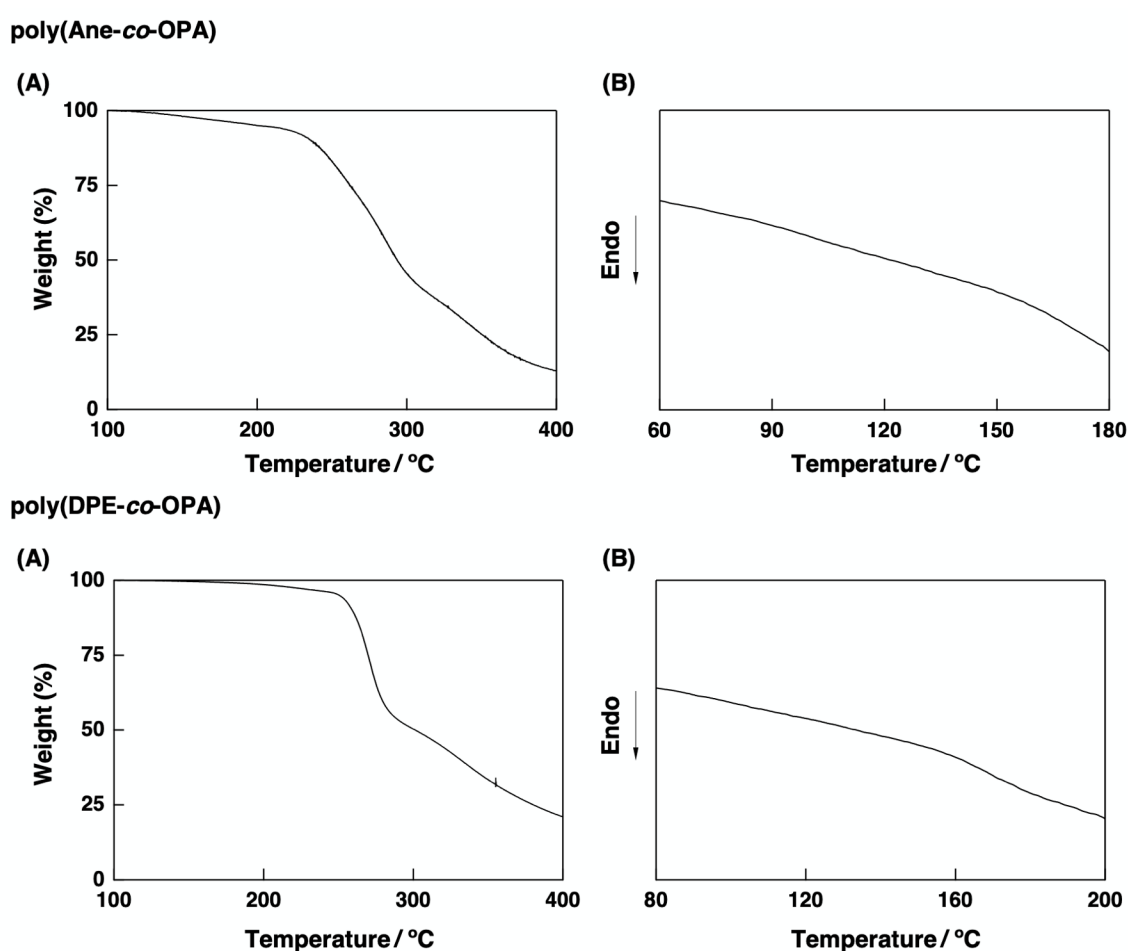


Figure 4. (A) TGA results (heating rate: 10 °C/min) and (B) DSC thermograms (2nd heating scan; heating rate: 10 °C/min) of poly(Ane-*co*-OPA) or poly(DPE-*co*-OPA).

Copolymerization of VEs with OPA

In the cationic copolymerization of St derivatives and OPA, the copolymerization behavior varied depending on the pendant groups, substituents on the vinyl group, and cyclic structures. Copolymerization with St derivatives that have no substituents on the vinyl group did not proceed, whereas the β - or α -

substituents and the cyclic structures were effective for efficient crossover reactions. The author next examined the copolymerization with VEs to elucidate the factors for the efficient crossover reactions and the differences between St derivatives and VEs. In Chapter 2 of this thesis, OPA was found to copolymerize with IBVE via frequent crossover reactions. The incorporated ratio of OPA in the copolymer was 45%, and the average number of IBVE and OPA units per block was 1.3 and 1.2, respectively (entry 2 in **Table 2**; **Figure 5** middle panel; data from chapter 2).

To investigate the effect of the substituents in the pendant of VE on the copolymerization behavior, the author examined the copolymerization of OPA with IPVE or CEVE, which have higher and lower reactivity than IBVE, respectively. In the copolymerization reactions, GaCl₃ was used as a Lewis acid catalyst in conjunction with EtSO₃H as a protonogen in toluene at -78 °C. In the copolymerization with IPVE, both IPVE and OPA were consumed to yield a copolymer (entry 1; **Figure 5** left), although the obtained copolymer had more VE–VE sequences than in the case of IBVE. This result is in sharp contrast to the exclusive generation of IPVE homopolymers in the copolymerization of IPVE with BzA or pMeOBzA. The results indicate that OPA could react with the IPVE-derived carbocation, unlike BzA or pMeOBzA. In the copolymerization with CEVE, a copolymer that has more OPA–OPA sequences than the copolymer of IBVE and OPA was obtained, and the incorporated ratio of OPA in the copolymer exceeded 50% (entry 3; **Figure 5** right). This result is in contrast to the copolymerization of CEVE and BzA. The incorporated ratio of BzA never exceeded 50% because homopropagation of BzA did not occur.

Table 2. Cationic copolymerization of various VEs and OPA^a

entry	VE	time	conv. ^b (%)		$M_n \times 10^{-3}^c$	M_w/M_n^c	OPA content in the copolymer (%) ^d	units per block ^d	
			VE	OPA				VE	OPA
1	IPVE	10 min	95	33	7.1	1.77	24	7.2	2.3
2 ^e	IBVE	4 h	55	55	17.5	1.21	48	1.3	1.2
3 ^f	CEVE	1 h	26	38	4.3	1.88	62	1.2	1.9
4	EPE	5 min	39	33	8.3	1.48	46	1.2	1.0
5 ^e	DHF	20 min	93	70	5.4	2.12	42	1.5	1.1
6 ^e	DHP	4 h	62	74	9.0	2.06	52	1.0	1.1
7 ^e	EMPE	90 min	76	85	5.8	1.69	50	1.0	1.0
8	MPE	1 min	59	22	0.2	–	–	–	–
9	MeDHF	4 h	100	54	0.3	–	–	–	–

^a [VE]₀ = 0.40 M, [OPA]₀ = 0.40 M, [EtSO₃H]₀ = 4.0 mM, [GaCl₃]₀ = 4.0 mM, [1,4-dioxane]₀ = 0.50 M in toluene at -78 °C. ^b Determined by ¹H NMR and gravimetry. ^c Determined by GPC (polystyrene standards). ^d Calculated by ¹H NMR spectra. ^e Data from Chapter 2 of this thesis. ^f [DTBP]₀ = 2.0 mM.

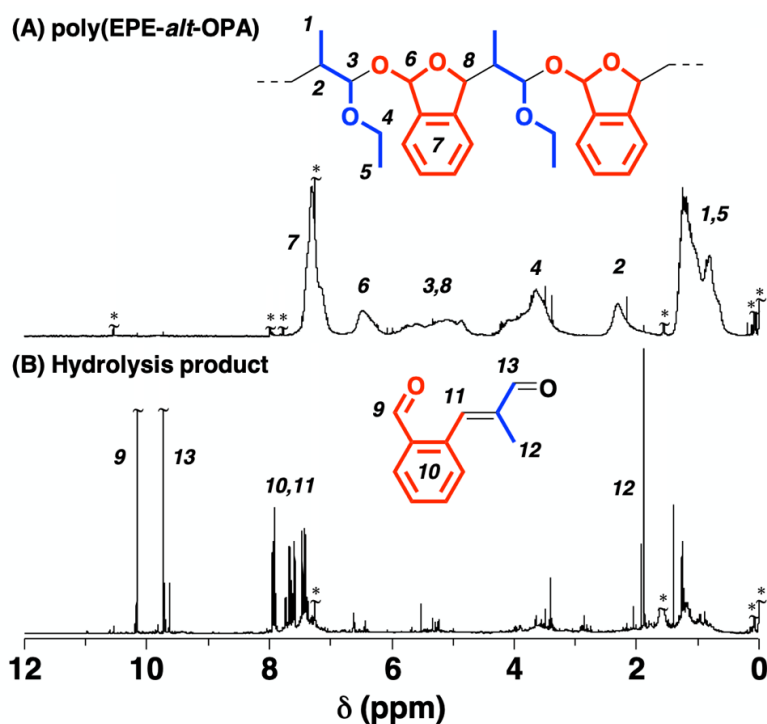
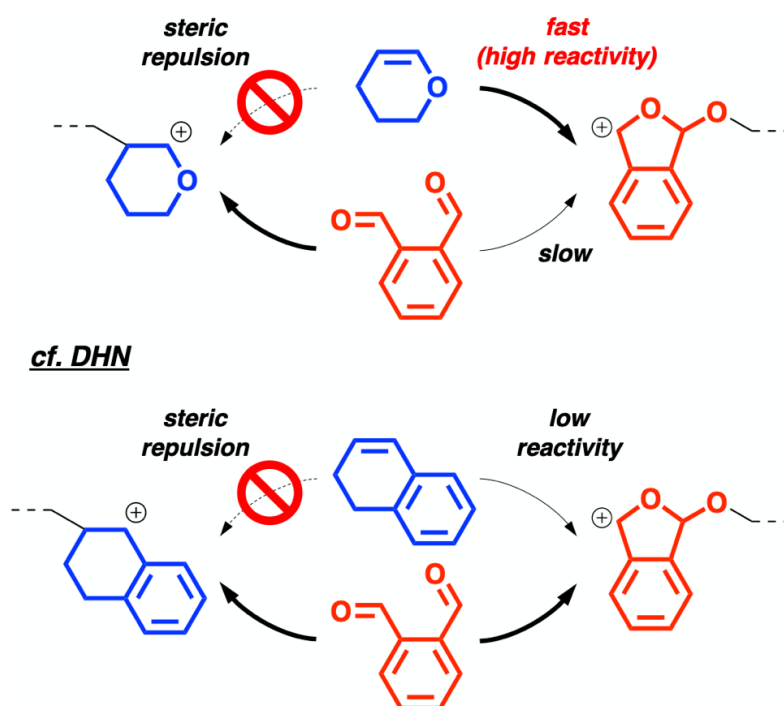


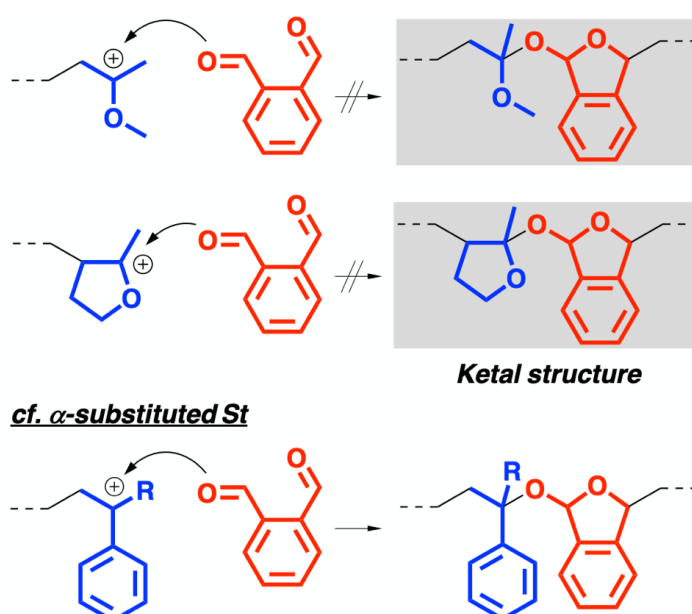
Figure 7. ^1H NMR spectra of (A) poly(EPE-*alt*-OPA) (entry 4 in **Table 2**) and (B) its acid-hydrolysis product recorded in CDCl_3 at 30 °C. Peaks with asterisks are due to TMS, grease, water, CHCl_3 and residual OPA.

2,3-Dihydrofuran (DHF), a five-membered cyclic enol ether, is known to exhibit very high homopolymerizability compared to ethyl VE and EPE.¹⁴ Copolymerization of DHF and OPA proceeded to yield a copolymer, although the copolymerization was not mediated by long-lived species (entry 5 in **Table 2**). The obtained copolymer had random sequences, as in the case of indene. Alternating copolymerization of OPA and DHP, which is a six-membered VE and exhibits very low homopolymerizability, also proceeded (entry 6 in **Table 2**), unlike the styrenic counterpart DHN. The steric strain of the propagating cation of both DHP and DHN is considered to be relatively lower than that of the five-membered counterparts because of the small strain of the sp^2 orbital. The reactivity of the β -carbon of DHP is considered to be larger than that of DHN due to the difference in the electron density of the $\text{C}=\text{C}$ bond (**Scheme 6**). As reported in Chapter 2, alternating copolymerization of OPA with EMPE, which is a β,β -dimethyl VE, successfully proceeded (entry 7 in **Table 2**). Based on this result, the author investigated the copolymerizations of various β,β -disubstituted VEs and OPA in Chapter 4.



Scheme 6. Cationic copolymerization of DHP and OPA.

The copolymerization of OPA with VEs that have a methyl group at the α -carbon did not proceed (entry 8 in **Table 2**). This is due to the unstable ketal structure derived from the crossover reaction from the VE-derived carbocation to OPA (**Scheme 7**). Ketal structures with cyclic moieties are known to be relatively stable compared with their acyclic counterparts¹⁵; however, copolymerization of MeDHF and OPA did not proceed (entry 9). In addition, homopolymers of MPE or DHF were not obtained in the copolymerization with OPA, although both MPE and MeDHF exhibit homopolymerizability. This is possibly because OPA behaved as a Lewis base and suppressed the homopropagation of MPE or DHF.



Scheme 7. Copolymerization of α -substituted VEs and OPA.

Overview

The differences between St derivatives and VEs are discussed in this section (**Figure 10**). The substituents in the pendant had a large effect on the copolymerization behavior. In the case of St derivatives, pMOS, which exhibits high reactivity, was preferentially added to the pMOS-derived carbocation rather than to the OPA-derived carbocation in the copolymerization because the homopropagation of pMOS was much faster than the crossover reaction. This result is probably due to the highly conjugated and stable nature of the pMOS-derived carbocation and the low reactivity of OPA to the pMOS-derived carbocation. pMeSt, which exhibits lower reactivity than pMOS, did not add to the OPA-derived carbocation because the electron density around the β -carbon of pMeSt is too low to react with the OPA-derived carbocation. Recently, nearly alternating copolymerization of pMeSt and BzA was found to proceed¹¹, indicating that pMeSt can add to the BzA-derived carbocation. These results indicate that the reactivity of OPA is higher than that of BzA. In contrast, VEs could undergo copolymerization with OPA, regardless of the kind of pendant group. The incorporated ratio of OPA in the copolymers varied depending on the reactivity of VEs. The high reactivity of OPA compared to BzAs was also indicated by the result of the copolymerization with IPVE: A copolymer of IPVE and OPA was obtained, while an IPVE homopolymer was produced even in the copolymerization with BzAs.

The copolymerization behavior of OPA was quite different between pMOS and VEs. In the previous study on the cationic copolymerization of pMOS and CEVE, the monomer reactivity ratios of both monomers were larger than one (for example, $r_{\text{CEVE}} = 3.08$ and $r_{\text{pMOS}} = 4.55$ by using BF_3OEt_2 as a catalyst in toluene at -78°C)^{16,17}, indicating that the propagating carbocation derived from pMOS preferentially reacted with pMOS rather than with CEVE. This result is most likely because the nature of the propagating carbocation derived from VE and pMOS are different. A possible reason for this difference is that the carbocation derived from pMOS is considered to be a relatively soft acid¹⁸, whereas that from VE is a hard acid. Since the OPA monomer is considered to be a relatively hard base, OPA did not react with the pMOS-derived propagating carbocation.

β -Methyl substituents of both St derivatives and VEs contributed to the increase in the frequency of crossover reactions. The β -methyl group of Ane prevented the homopropagation of Ane and enabled crossover reactions with OPA. High reactivity derived from an electron-donating group on the phenyl ring was also required for efficient crossover reactions, as demonstrated by the inertness of *trans*- β MeSt in the copolymerization with OPA. β -Methyl VE has high homopolymerizability; however, the homopropagation of EPE was suppressed, and nearly alternating copolymerization proceeded with OPA.

Five-membered vinyl monomers exhibited similar copolymerization behavior. Homopropagation of vinyl monomers frequently occurred in the copolymerization of OPA with indene or DHF. Since the homopropagation of indene or DHF is fast, the difference in the rate between the homopropagation and the crossover reaction to the OPA-derived carbocation was not very large, resulting in the generation of random copolymers. Six-membered vinyl monomers also exhibited similar copolymerization behavior. The homopropagation of vinyl monomers negligibly occurred in both the DHP and DHN cases. A nearly alternating copolymer was obtained from DHP and OPA, while the addition of DHN to the OPA-derived carbocation was infrequent, and OPA homosequences were generated in the copolymerization of DHN and OPA. The low electron density of the C=C bond of DHN compared to that of DHP is likely responsible for inefficient crossover reactions from OPA to DHN.

The copolymerization behavior of α -substituted monomers was quite different between St derivatives and

VEs. Copolymerization of OPA with α MeSt or DPE successfully proceeded. OPA could easily approach the propagating carbocation derived from DPE because of the small steric hindrance. However, the copolymers obtained from α MeSt or DPE did not have alternating sequences. The reactivity of the β -carbon of α MeSt and DPE is not so large, which likely contributed to preferential or occasional occurrences of OPA homopropagation. Unlike the α -substituted St derivatives, copolymerization of α -substituted VEs and OPA did not proceed due to the ineffective generation of unstable ketal structures.

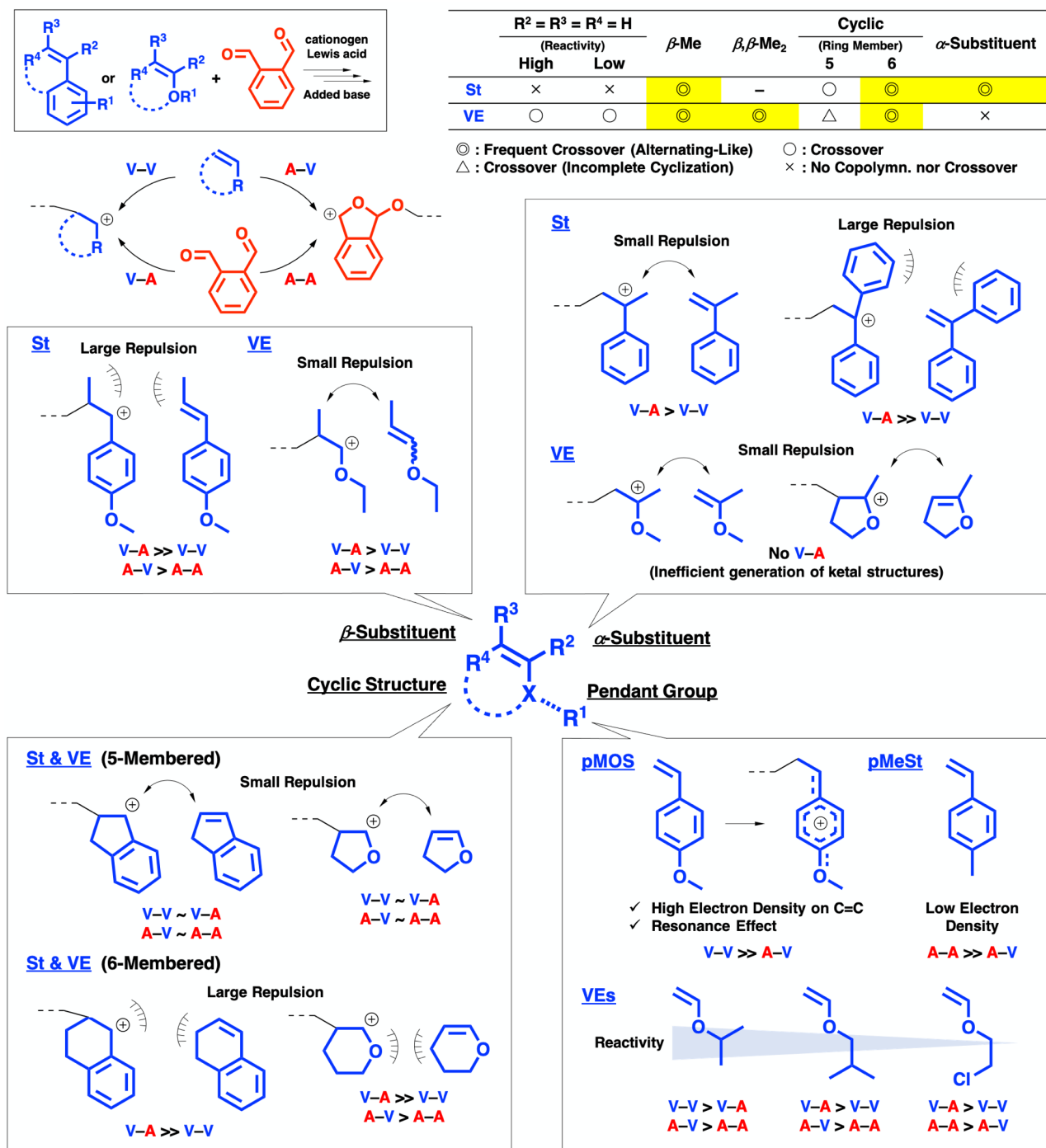


Figure 8. Overview of this study: differences of the copolymerization behavior between VEs and St derivatives.

Conclusion

In the cationic copolymerization of vinyl monomers and OPA, copolymerization behavior varied depending on the structure and reactivity of vinyl monomers. In the case of St derivatives, the β - or α -substituents on the vinyl group and the electron-donating group on the aromatic ring were effective for the frequent crossover reactions, whereas St derivatives that have no substituents on the vinyl group did not undergo copolymerization with OPA. In the case of VEs other than α -substituted VEs, copolymerization with OPA successfully proceeded. The exceptional polymerizability and reactivity of OPA enabled copolymerization with vinyl monomers, such as IPVE, EMPE, Ane, and DPE, that do not copolymerize with BZAs. By demonstrating the copolymerizability of various vinyl monomers with OPA, the author has provided new insight into the copolymerization of different kinds of monomers.

References

1. Graham, R. K.; Dunkelberger, D. L.; Goode, W. E. *J. Am. Chem. Soc.* **1960**, *82*, 400–403.
2. Sawamoto, M.; Ohtoyo, T.; Higashimura, T.; Gührs, K. H.; Heublein, G. *Polym. J.* **1985**, *17*, 929–933.
3. Yamada, M.; Yoshizaki, T.; Kanazawa, A.; Kanaoka, S.; Aoshima, S. *J. Polym. Sci., Part A: Polym. Chem.* **2019**, *57*, 2166–2174.
4. Otsu, T.; Matsumoto, A.; Kubota, T.; Mori, S. *Polym. Bull.* **1990**, *23*, 43–50.
5. Matsumoto, A.; Otsu, T. *Macromol. Symp.* **1995**, *98*, 139–152.
6. Kennedy, J. P.; Midha, S.; Keszler, B. *Macromolecules* **1993**, *26*, 424–428.
7. Yasuoka, K.; Kanaoka, S.; Aoshima, S. *J. Polym. Sci., Part A: Polym. Chem.* **2012**, *50*, 2758–2761.
8. Hutchings, L. R.; Brooks, P. P.; Parker, D.; Mosely, J. A.; Sevinc, S. *Macromolecules* **2015**, *48*, 610–628.
9. Okuyama, T.; Fueno, T.; Furukawa, J.; Uyeo, K. *J. Polym. Sci., Part A-1: Polym. Chem.* **1968**, *6*, 1001–1007.
10. Raff, R.; Cook, J. L.; Etting, B. V. *J. Polym. Sci., Part A: Gen. Pap.* **1965**, *3*, 3511–3517.
11. Nara, T.; Kanazawa, A.; Aoshima, S. Unpublished data.
12. Hulnik, M. I.; Kuharenko, O. V.; Vasilenko, I. V.; Timashev, P.; Kostjuk, S. V. *ACS Sustainable Chem. & Eng.* **2021**, *9*, 6841–6854.
13. Mizote, A.; Tanaka, T.; Higashimura, T.; Okamura, S. *J. Polym. Sci., Part A-1: Polym. Chem.* **1966**, *4*, 869–879.
14. Yonezumi, M.; Kanaoka, S.; Aoshima, S. *J. Polym. Sci., Part A: Polym. Chem.* **2008**, *46*, 4495–4504.
15. Mimura, M.; Kanazawa, A.; Aoshima, S. *Macromolecules* **2019**, *52*, 7572–7583.
16. Masuda, T.; Higashimura, T.; Okamura, S. *Polym. J.* **1970**, *1*, 19–26.
17. Masuda, T.; Higashimura, T. *Polym. J.* **1971**, *2*, 29–35.
18. Boeck, P. T.; Tanaka, J.; Liu, S.; You, W. *Macromolecules* **2020**, *53*, 4303–4311.

Supporting Information

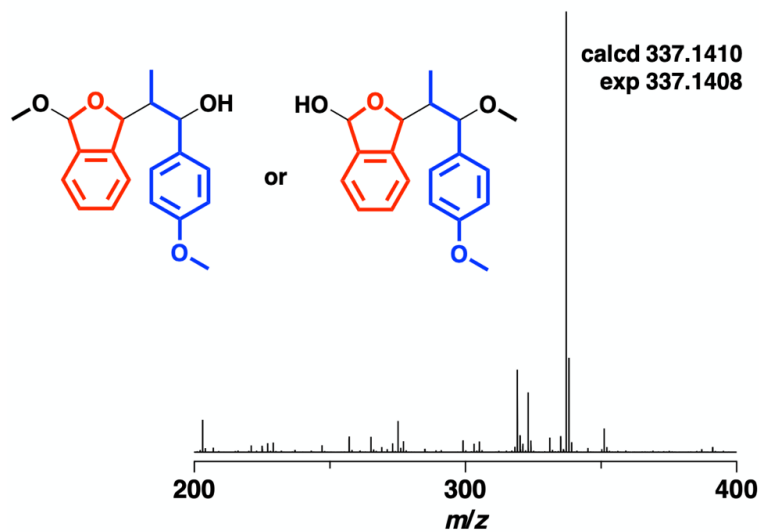


Figure S1. ESI-MS spectrum of the acid-methanolysis product of poly(Ane-co-OPA).

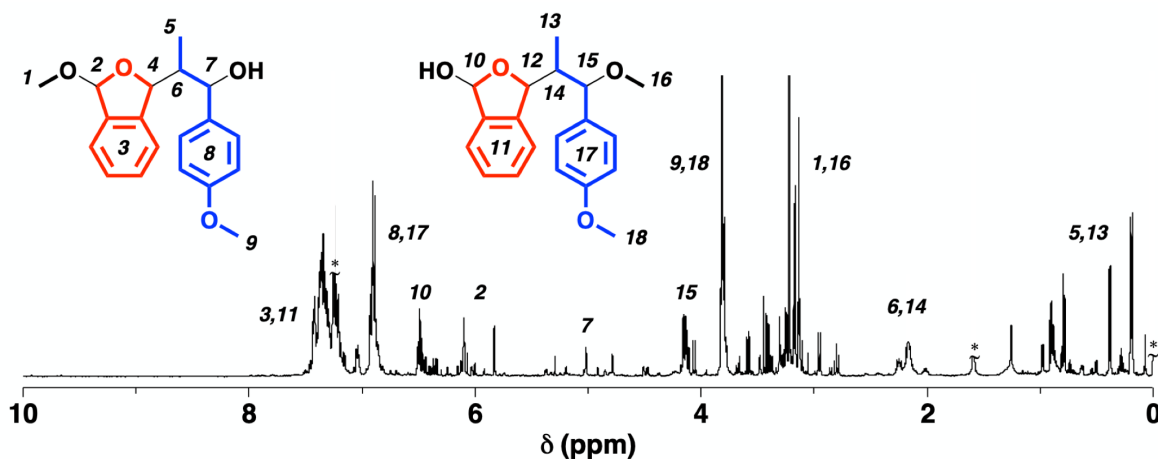


Figure S2. ^1H NMR spectrum of the acid-methanolysis product of poly(Ane-co-OPA). Peaks with asterisks are due to TMS, water, and CHCl_3 .

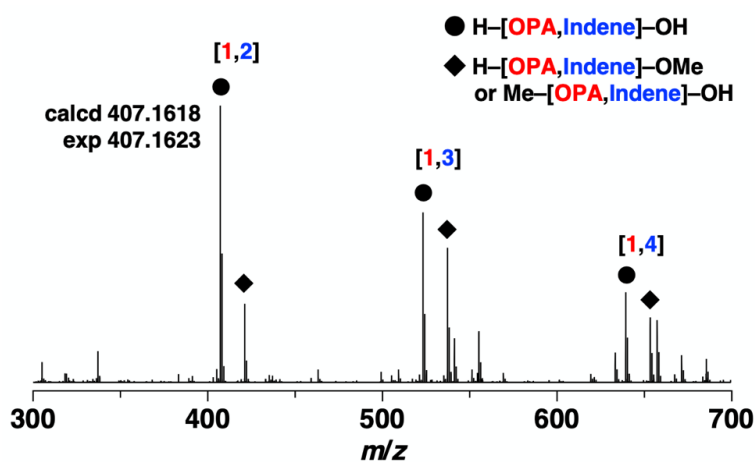
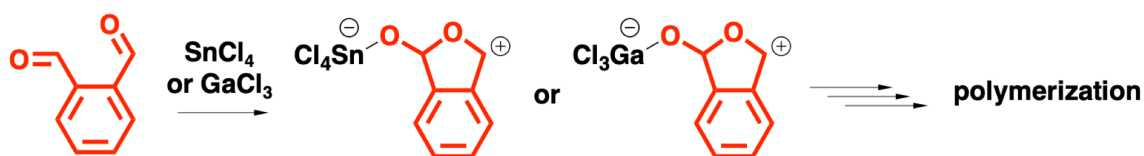


Figure S3. ESI-MS spectrum of the acid-methanolysis product of poly(indene-co-OPA).



in the presence of OPA



Scheme S1. Cationic copolymerization of indene and OPA by SnCl_4 or GaCl_3 .

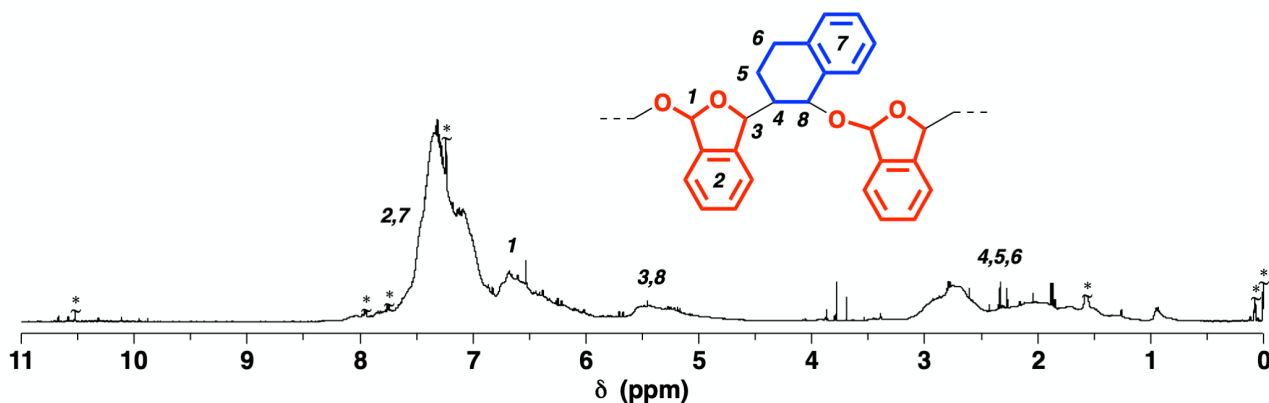


Figure S4. ^1H NMR spectrum of poly(DHN-*co*-OPA) (entry 12 in **Table 1**). Peaks with asterisks are due to TMS, grease, water, CHCl_3 , and residual OPA.

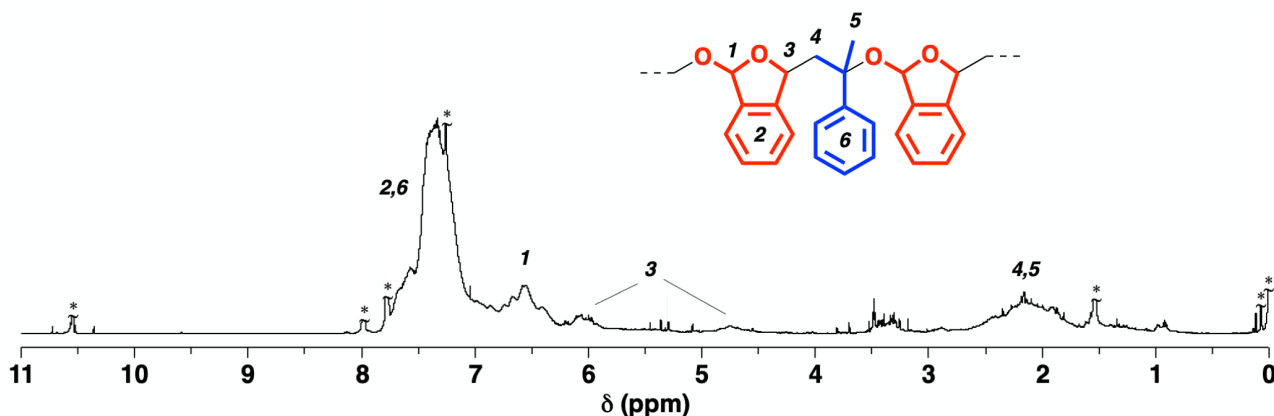


Figure S5. ^1H NMR spectrum of poly(α MeSt-*co*-OPA) (entry 13 in **Table 1**). Peaks with asterisks are due to TMS, grease, water, CHCl_3 , and residual OPA.

Chapter 4

Living and Alternating Cationic Copolymerization of *o*-Phthalaldehyde and Various Bulky Enol Ethers: Expanding the Range of Polymerizable Monomers

Introduction

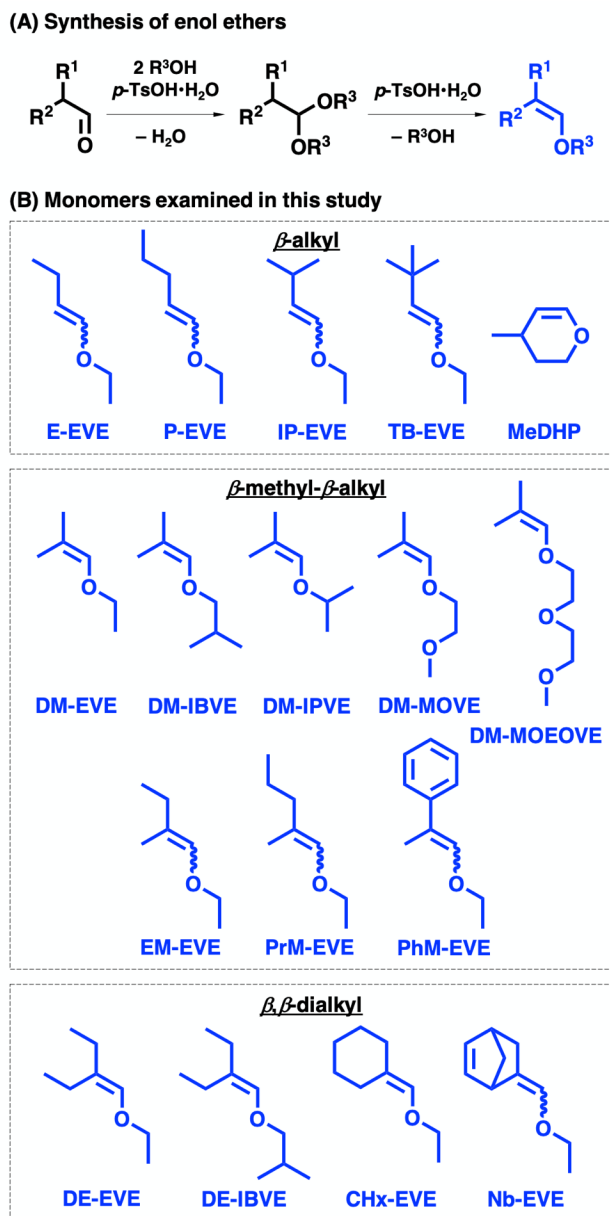
The structure around the polymerizable groups on monomers greatly affects the polymerizability of the monomers and the properties of the resulting polymers. For example, bulky substituents around a polymerizable group are thought to decrease the polymerizability of monomers, which corresponds to a low ceiling temperature, while polymers obtained from monomers with bulky substituents often exhibit good thermal properties. Indeed, polymers obtained from vinyl monomers with substituents on the β -carbon exhibit characteristic properties, such as a high glass-transition temperature, specific conformation of the main chain, and solubility, because such polymers have substituents on every carbon in the main chain. However, β -substituted vinyl monomers, except for maleimides^{1,2}, dialkyl fumarates³, dihydrofuran^{4,5}, indene^{6,7}, and vinyl monomers with a small β -substituent such as crotonates^{8,9} and propenyl ethers^{10,11}, are often difficult to homopolymerize due to steric hindrance.

To form polymers from nonhomopolymerizable monomers with bulky substituents, copolymerization with other monomers has been widely utilized. For example, β -methylstyrene¹²⁻¹⁵ or 1,1-diphenylethylene derivatives¹⁶⁻²¹, which are difficult to homopolymerize, have been copolymerized with styrene derivatives via radical, cationic, or anionic mechanisms. These copolymerizations were feasible due to mitigation of the steric hindrance. In addition, alternating copolymers can be obtained when suitable monomers are used at suitable feed ratios under appropriate polymerization conditions. To obtain copolymers from nonhomopolymerizable monomers, the relationship between the bulkiness of the monomers and the copolymerization behavior is of great importance. According to reports on the cationic copolymerization of isobutyl vinyl ether (IBVE) with enol ethers that have various substituents on the β -carbon, the composition of the bulky monomers in the copolymers decreases with increasing bulkiness of the β -carbon.^{22,23} However, the difference among bulky substituents is difficult to examine because very bulky enol ethers are not incorporated into polymer chains even during copolymerization. Therefore, a suitable comonomer and elaborately designed copolymerization conditions are required to investigate the copolymerizability of bulky monomers.

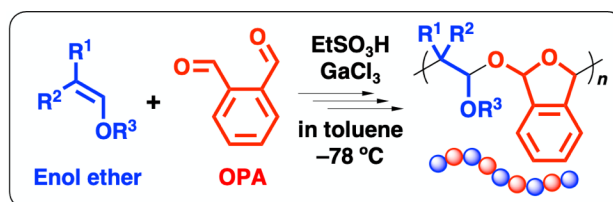
Our group has developed living and alternating cationic copolymerizations of vinyl ethers (VEs) and benzaldehyde derivatives (BzAs). Moreover, the author focused on *o*-phthalaldehyde (OPA), which is a bifunctional aromatic aldehyde, as an aldehyde monomer. OPA was found to undergo alternating copolymerization with a β,β -dimethyl VE, which is a monomer that is neither homopolymerizable nor copolymerizable with BzAs due to its steric hindrance.²⁴ Although there have been reports on the cationic copolymerization of a β,β -dimethyl VE and IBVE, the incorporated ratio of a β,β -dimethyl VE in the copolymer was not so high. The OPA-derived cyclic carbocationic species with small steric hindrance is most likely responsible for the alternating copolymerization of OPA and a β,β -dimethyl VE.

OPA-derived carbocations have great potential to react with enol ethers with various substituents on the β -carbon. Since various enol ethers can be synthesized from aldehydes and alcohols (**Scheme 1A**), the bulkiness of the β -carbon of enol ethers can be finely tuned. Therefore, in this study, the author examined the

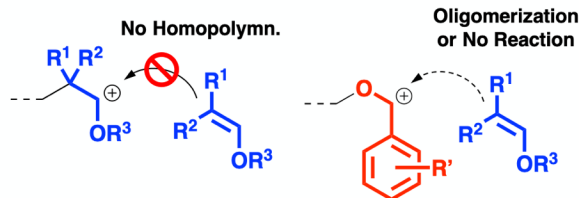
cationic copolymerization of various enol ethers (**Scheme 1B**) with OPA to elucidate the limit of polymerizable monomers, with a particular focus on the relationship between the structure or reactivity of enol ethers and the copolymerization behavior with OPA (**Scheme 2**). As a result, bulky enol ethers such as β -*t*-butyl and β,β -dialkyl monomers were found to be copolymerizable with OPA, and a new method for the polymerization of sterically hindered monomers was demonstrated.



Scheme 1. (A) Synthesis of enol ethers and (B) monomers examined in this study.



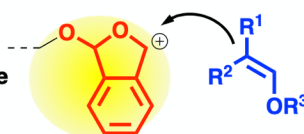
Polymerization Behavior of Bulky Enol Ethers



This Work

Addition toward OPA-Derived Propagating Cation

- ✓ Cyclic, Planar-Like
- ✓ Small Steric Hindrance
- ✓ High Reactivity



Scheme 2. Cationic polymerization behavior of enol ethers toward various active species.

Experimental Section

Materials.

p-Methoxybenzaldehyde (pMeOBzA; Nacalai Tesque, >99%), 4-methyldihydropyran (MeDHP; Kuraray), and 1-butenyl ethyl ether (E-EVE; Wako, >97%) were distilled twice over calcium hydride. Other enol ethers were synthesized according to a previous report²⁵ and then distilled twice over calcium hydride.

Synthesis of enol ethers.

Enol ethers other than E-EVE and MeDHP were synthesized from the corresponding aliphatic aldehydes and alcohols.²⁵ For example, DM-IBVE was synthesized by the following two steps: isobutyraldehyde diisobutyl acetal was synthesized by the reaction of isobutyraldehyde and isobutanol in the presence of a catalytic amount of *p*-TsOH·H₂O (TCI, >98.0%) on calcium chloride at room temperature for 3 days. The organic layer was washed first with aqueous sodium hydrogen carbonate and then with water. Residual isobutyraldehyde was removed by distillation. The obtained isobutyraldehyde diisobutyl acetal and a catalytic amount of *p*-TsOH·H₂O were then heated in a distillation apparatus until the evolution of isobutanol ceased. The crude product was washed with water to remove the alcohol and then distilled twice over calcium hydride.

β-Propyl ethyl vinyl ether (P-EVE; ethyl 1-pentenyl ether).

Synthesized from valeraldehyde (TCI, >95%) and ethanol (Nacalai Tesque, >99%). Distilled under reduced pressure (bp: 54 °C/69 mmHg). Final yield after distillation: 3%. A mixture of isomers (*E/Z* = 22/78). ¹H NMR (CDCl₃, 400 MHz): *E*: δ 6.21 (dt, 12.8 Hz, 1.2 Hz, 1H), 4.77 (dt, 12.8 Hz, 7.2 Hz, 1H), 3.70 (q, 7.2 Hz, 2H), 1.88 (ddt, 7.6 Hz, 7.2 Hz, 1.2 Hz, 2H), 1.36 (tq, 7.6 Hz, 7.6 Hz, 2H), 1.26 (t, 7.2 Hz, 3H), 0.88 (t, 7.6 Hz, 3H). *Z*: δ 5.93 (dt, 6.4 Hz, 1.6 Hz, 1H), 4.34 (dt, 7.2 Hz, 6.4 Hz, 1H), 3.77 (q, 7.2 Hz, 2H), 2.05 (ddt, 7.6 Hz, 7.2 Hz, 1.6 Hz, 2H), 1.36 (tq, 7.6 Hz, 7.6 Hz, 2H), 1.24 (t, 7.2 Hz, 3H), 0.91 (t, 7.6 Hz, 3H). ¹³C NMR (CDCl₃, 125 MHz): *E*: δ 146.1, 104.2, 64.6, 29.9, 23.9, 14.8, 13.5. *Z*: δ 144.6, 107.0, 67.5, 26.1, 23.0, 15.3, 13.8. MS

(ESI) m/z $[M + Na]^+$, calcd: 137.0937, found: 137.0937.

β -Isopropyl ethyl vinyl ether (IP-EVE; 3-methyl-1-butenyl ethyl ether).

Synthesized from isovaleraldehyde (TCI, >98%) and ethanol. Distilled under reduced pressure (bp: 54 °C/110 mmHg). Final yield after distillation: 6%. A mixture of isomers ($E/Z = 40/60$). 1H NMR ($CDCl_3$, 400 MHz): E : δ 6.20 (d, 12.8 Hz, 1H), 4.74 (dd, 12.8 Hz, 7.2 Hz, 1H), 3.68 (q, 7.2 Hz, 2H), 2.22 (dsep, 7.2 Hz, 7.2 Hz, 1H), 1.25 (t, 7.2 Hz, 3H), 0.98 (d, 7.2 Hz, 6H). Z : δ 5.81 (dd, 6.4 Hz, 1.2 Hz, 1H), 4.21 (dd, 6.8 Hz, 6.4 Hz, 1H), 3.75 (q, 7.2 Hz, 2H), 2.75 (ddsep, 7.2 Hz, 6.8 Hz, 1.2 Hz, 1H), 1.23 (t, 7.2 Hz, 3H), 0.96 (d, 7.2 Hz, 6H). ^{13}C NMR ($CDCl_3$, 125 MHz): E : δ 144.4, 112.0, 64.5, 27.6, 23.8, 14.8. Z : δ 142.9, 115.0, 67.5, 24.0, 23.4, 15.3. MS (ESI) m/z $[M + Na]^+$, calcd: 137.0937, found: 137.0936.

β -t-Butyl ethyl vinyl ether (TB-EVE; 3,3-dimethyl-1-butenyl ethyl ether).

Synthesized from 3,3-dimethylbutyraldehyde (TCI, >97%) and ethanol. Distilled under reduced pressure (bp: 51 °C/89 mmHg). Final yield after distillation: 14%. A mixture of isomers ($E/Z = 77/23$). 1H NMR ($CDCl_3$, 500 MHz): E : δ 6.16 (d, 13.0 Hz, 1H), 4.87 (d, 13.0 Hz, 1H), 3.68 (q, 7.0 Hz, 2H), 1.25 (t, 7.0 Hz, 3H), 1.02 (s, 9H). Z : δ 5.72 (d, 7.0 Hz, 1H), 4.21 (d, 7.0 Hz, 1H), 3.72 (q, 7.0 Hz, 2H), 1.23 (t, 7.0 Hz, 3H), 1.11 (s, 9H). ^{13}C NMR ($CDCl_3$, 125 MHz): E : δ 143.4, 116.5, 64.7, 30.6, 30.0, 14.9. Z : δ 143.4, 116.5, 60.4, 30.6, 30.0, 15.4. MS (ESI) m/z $[M + Na]^+$, calcd: 151.1093, found: 151.1093.

β,β -Dimethyl ethyl vinyl ether (DM-EVE; ethyl 2-methyl-1-propenyl ether).

Synthesized from isobutyraldehyde (TCI, >99%) and ethanol. Distilled under atmospheric pressure (bp: 81 °C). Final yield after distillation: 61%. 1H NMR ($CDCl_3$, 400 MHz): δ 5.79 (sep, 1.2 Hz, 1H), 3.71 (q, 7.2 Hz, 2H), 1.61 (d, 1.2 Hz, 3H), 1.54 (d, 1.2 Hz, 3H), 1.23 (t, 7.2 Hz, 3H). ^{13}C NMR ($CDCl_3$, 125 MHz): δ 139.9, 110.2, 67.0, 19.5, 15.2, 14.9. MS (ESI) m/z $[M + Na]^+$, calcd: 123.0780, found: 123.0781.

β,β -Dimethyl isobutyl vinyl ether (DM-IBVE; isobutyl 2-methyl-1-propenyl ether).

Synthesized from isobutyraldehyde and isobutanol (Nacalai Tesque, >99%). Distilled under reduced pressure (bp: 62 °C/78 mmHg). Final yield after distillation: 72%. 1H NMR ($CDCl_3$, 400 MHz): δ 5.77 (sep, 1.2 Hz, 1H), 3.40 (d, 6.8 Hz, 2H), 1.89 (tsep, 6.8 Hz, 6.8 Hz, 1H), 1.61 (d, 1.2 Hz, 3H), 1.53 (d, 1.2 Hz, 3H), 0.92 (d, 6.8 Hz, 6H). ^{13}C NMR ($CDCl_3$, 125 MHz): δ 140.5, 109.8, 78.4, 28.7, 19.5, 19.1, 14.9. MS (ESI) m/z $[M + Na]^+$, calcd: 151.1093, found: 151.1099.

β,β -Dimethyl isopropyl vinyl ether (DM-IPVE; isopropyl 2-methyl-1-propenyl ether).

Synthesized from isobutyraldehyde and 2-propanol (Nacalai Tesque, >99%). Distilled under atmospheric pressure (bp: 105 °C). Final yield after distillation: 65%. 1H NMR ($CDCl_3$, 400 MHz): δ 5.80 (sep, 1.2 Hz, 1H), 3.80 (sep, 6.0 Hz, 1H), 1.60 (d, 1.2 Hz, 3H), 1.55 (d, 1.2 Hz, 3H), 1.19 (d, 6.0 Hz, 6H). ^{13}C NMR ($CDCl_3$, 125 MHz): δ 138.8, 110.7, 73.1, 22.4, 19.6, 15.1. MS (ESI) m/z $[M + Na]^+$, calcd: 137.0937, found: 137.0938.

β,β -Dimethyl 2-methoxyethyl vinyl ether (DM-MOVE; 2-methoxyethyl 2-methyl-1-propenyl ether).

Synthesized from isobutyraldehyde and 2-methoxyethanol (TCI, >99%). Distilled under reduced pressure

(bp: 93 °C/150 mmHg). Final yield after distillation: 19%. ¹H NMR (CDCl₃, 400 MHz): δ 5.82 (sep, 1.2 Hz, 1H), 3.82–3.78 (m, 2H), 3.58–3.54 (m, 2H), 3.39 (s, 3H), 1.61 (d, 1.2 Hz, 3H), 1.54 (d, 1.2 Hz, 3H). ¹³C NMR (CDCl₃, 125 MHz): δ 140.1, 111.1, 71.8, 70.9, 59.2, 19.5, 15.1. MS (ESI) *m/z* [M + Na]⁺, calcd: 153.0886, found: 153.0886.

β,β-Dimethyl 2-(2-methoxyethoxy)ethyl vinyl ether (DM-MOEOVE; 2-(2-methoxyethoxy)ethyl 2-methyl-1-propenyl ether).

Synthesized from isobutyraldehyde and diethylene glycol monomethyl ether (TCI, >99%). Distilled under reduced pressure (bp: 88 °C/15 mmHg). Final yield after distillation: 24%. ¹H NMR (CDCl₃, 500 MHz): δ 5.82 (sep, 1.0 Hz, 1H), 3.84–3.80 (m, 2H), 3.69–3.64 (m, 4H), 3.57–3.53 (m, 2H), 3.38 (s, 3H), 1.60 (d, 1.0 Hz, 3H), 1.54 (d, 1.0 Hz, 3H). ¹³C NMR (CDCl₃, 125 MHz): δ 140.1, 111.0, 72.0, 71.0, 70.7, 70.4, 59.1, 19.5, 15.0. MS (ESI) *m/z* [M + Na]⁺, calcd: 197.1148, found: 197.1149.

β-Ethyl-*β*-methyl ethyl vinyl ether (EM-EVE; 2-methyl-1-butenyl ethyl ether).

Synthesized from 2-methylbutyraldehyde (TCI, >95%) and ethanol. Distilled under reduced pressure (bp: 49 °C/74 mmHg). Final yield after distillation: 9%. A mixture of isomers (*E/Z* = 58/42). ¹H NMR (CDCl₃, 400 MHz): *E isomer*: δ 5.83 (q, 1.2 Hz, 1H), 3.72 (q, 7.2 Hz, 2H), 1.90 (q, 7.6 Hz, 2H), 1.60 (d, 1.2 Hz, 3H), 1.24 (t, 7.2 Hz, 3H), 0.98 (t, 7.6 Hz, 3H). *Z isomer*: δ 5.75 (m, 1H), 3.70 (q, 7.2 Hz, 2H), 2.09 (q, 7.6 Hz, 2H), 1.53 (d, 1.2 Hz, 3H), 1.22 (t, 7.2 Hz, 3H), 0.96 (t, 7.6 Hz, 3H). See **Figure S1** for the Difference NOE NMR spectra. ¹³C NMR (CDCl₃, 125 MHz): *E*: δ 139.6, 116.0, 67.1, 27.1, 15.3, 13.2, 12.3. *Z*: δ 139.4, 116.3, 67.1, 22.1, 16.8, 15.3, 12.8. MS (ESI) *m/z* [M + Na]⁺, calcd: 137.0937, found: 137.0937.

β-Propyl-*β*-methyl ethyl vinyl ether (PrM-EVE; ethyl 2-methyl-1-pentenyl ether).

Synthesized from 2-methylvaleraldehyde (TCI, >95%) and ethanol. Distilled under reduced pressure (bp: 54 °C/41 mmHg). Final yield after distillation: 64%. A mixture of isomers (*E/Z* = 53/47). ¹H NMR (CDCl₃, 400 MHz): *E isomer*: δ 5.81 (q, 1.2 Hz, 1H), 3.71 (q, 7.2 Hz, 2H), 1.84 (t, 7.6 Hz, 2H), 1.58 (d, 1.2 Hz, 3H), 1.39 (tq, 7.6 Hz, 7.6 Hz, 2H), 1.23 (t, 7.2 Hz, 3H), 0.86 (t, 7.6 Hz, 3H). *Z isomer*: δ 5.79 (m, 1H), 3.68 (q, 7.2 Hz, 2H), 2.05 (t, 7.6 Hz, 2H), 1.51 (d, 1.2 Hz, 3H), 1.40 (tq, 7.6 Hz, 7.6 Hz, 2H), 1.21 (t, 7.2 Hz, 3H), 0.89 (t, 7.6 Hz, 3H). See **Figure S2** for the Difference NOE NMR spectra. ¹³C NMR (CDCl₃, 125 MHz): *E*: δ 140.3, 114.2, 67.1, 36.2, 21.1, 15.3, 13.6, 12.8. *Z*: δ 140.2, 114.5, 67.1, 31.0, 20.6, 17.3, 15.3, 13.9. MS (ESI) *m/z* [M + Na]⁺, calcd: 151.1093, found: 151.1093.

β-Phenyl-*β*-methyl ethyl vinyl ether (PhM-EVE; ethyl 2-phenyl-1-propenyl ether).

Synthesized from 2-phenylpropionaldehyde (Sigma-Aldrich, >98%) and ethanol. Distilled under reduced pressure (bp: 92 °C/4 mmHg). Final yield after distillation: 67%. A mixture of isomers (*E/Z* = 85/15). ¹H NMR (CDCl₃, 400 MHz): *E isomer*: δ 7.66–7.62, 7.32–7.23, 7.17–7.12 (m, 5H, aromatic), 6.46 (q, 1.2 Hz, 1H), 3.88 (q, 7.2 Hz, 2H), 2.00 (d, 1.2 Hz, 3H), 1.29 (t, 7.2 Hz, 3H). *Z isomer*: δ 7.66–7.62, 7.32–7.23, 7.17–7.12 (m, 5H, aromatic), 6.16 (q, 1.2 Hz, 1H), 3.85 (q, 7.2 Hz, 2H), 1.91 (d, 1.2 Hz, 3H), 1.28 (t, 7.2 Hz, 3H). See **Figure S3** for the Difference NOE NMR spectra. ¹³C NMR (CDCl₃, 125 MHz): *E*: δ 143.9, 141.0, 128.4, 127.6, 125.9, 125.1, 114.5, 68.2, 15.6, 12.8. *Z*: δ 143.5, 138.6, 129.2, 128.0, 126.0, 125.1, 110.4, 68.6, 18.4, 15.6. MS (ESI)

m/z $[M + Na]^+$, calcd: 185.0937, found: 185.0942.

β,β -Diethyl ethyl vinyl ether (DE-EVE; 2-ethyl-1-butenyl ethyl ether).

Synthesized from 2-ethylbutyraldehyde (TCI, >98%) and ethanol. Distilled under reduced pressure (bp: 62 °C/67 mmHg). Final yield after distillation: 12%. ^1H NMR (CDCl_3 , 400 MHz): δ 5.77 (t, 1.2 Hz, 1H), 3.71 (q, 7.2 Hz, 2H), 2.10 (q, 7.6 Hz, 2H), 1.92 (dq, 7.6 Hz, 1.2 Hz, 2H), 1.23 (t, 7.2 Hz, 3H), 0.97 (t, 7.6 Hz, 3H), 0.96 (t, 7.6 Hz, 3H). ^{13}C NMR (CDCl_3 , 125 MHz): δ 139.4, 122.1, 67.2, 24.4, 20.1, 15.3, 13.3, 12.7. MS (ESI) m/z $[M + Na]^+$, calcd: 151.1093, found: 151.1097.

β,β -Diethyl isobutyl vinyl ether (DE-IBVE; 2-ethyl-1-butenyl isobutyl ether).

Synthesized from 2-ethylbutyraldehyde and isobutanol. Distilled under reduced pressure (bp: 82 °C/56 mmHg). Final yield after distillation: 74%. ^1H NMR (CDCl_3 , 400 MHz): δ 5.76 (t, 1.2 Hz, 1H), 3.41 (d, 6.8 Hz, 2H), 2.10 (q, 7.6 Hz, 2H), 1.91 (dq, 7.6 Hz, 1.2 Hz, 2H), 1.89 (tsep, 6.8 Hz, 6.8 Hz, 1H), 0.97 (t, 7.6 Hz, 6H), 0.92 (d, 6.8 Hz, 6H). ^{13}C NMR (CDCl_3 , 125 MHz): δ 140.0, 121.5, 78.5, 28.7, 24.4, 20.2, 19.2, 13.3, 12.7. MS (ESI) m/z $[M + Na]^+$, calcd: 179.1406, found: 179.1405.

Cyclohexylidenemethyl ethyl ether (abbreviated as CHx-EVE for convenience; ethoxymethylenecyclohexane).

Synthesized from cyclohexanecarboxaldehyde (TCI, >98%) and ethanol. Distilled under reduced pressure (bp: 87 °C/37 mmHg). Final yield after distillation: 23%. ^1H NMR (CDCl_3 , 400 MHz): δ 5.78 (s, 1H), 3.70 (q, 7.2 Hz, 2H), 2.18 (t, 5.6 Hz, 2H), 1.93 (t, 5.6 Hz, 2H), 1.57–1.43 (m, 6H), 1.23 (t, 7.2 Hz, 3H). ^{13}C NMR (CDCl_3 , 125 MHz): δ 137.3, 118.7, 67.2, 30.7, 28.5, 27.1, 27.0, 25.6, 15.2. MS (ESI) m/z $[M + Na]^+$, calcd: 163.1093, found: 163.1093.

5-Norbornenylidenemethyl ethyl ether (abbreviated as Nb-EVE for convenience; 5-ethoxymethylene-2-norbornene).

Synthesized from 5-norbornene-2-carboxaldehyde (TCI, >95%) and ethanol. Distilled under reduced pressure (bp: 74 °C/16 mmHg). Final yield after distillation: 17%. A mixture of isomers ($E/Z = 69/31$). ^1H NMR (CDCl_3 , 400 MHz): *E isomer*: δ 6.11 (dd, 2.0–2.4 Hz, 2.0–2.4 Hz, 1H), 6.06 (dd, 5.6 Hz, 2.8 Hz, 1H), 6.01 (dd, 5.6 Hz, 2.8 Hz, 1H), 3.72 (q, 7.2 Hz, 2H), 3.11–3.07 (m, 1H), 2.99–2.95 (m, 1H), 2.26 (ddd, 14.8 Hz, 3.2 Hz, 2.0–2.4 Hz, 1H), 1.74 (ddd, 14.8 Hz, 2.4 Hz, 2.4 Hz, 1H), 1.55–1.47 (m, 1H), 1.35–1.28 (m, 1H), 1.22 (t, 7.2 Hz, 3H). *Z isomer*: δ 6.10 (dd (overlap), 1H), 6.05 (dd (overlap), 1H), 5.80 (dd, 1.6 Hz, 1.6 Hz, 1H), 3.71 (q, 7.2 Hz, 2H), 3.64–3.60 (m, 1H), 2.96–2.92 (m, 1H), 2.24 (ddd, 13.6 Hz, 3.2 Hz, 1.6 Hz, 1H), 1.64 (ddd, 13.6 Hz, 1.6 Hz, 1.6 Hz, 1H), 1.55–1.47 (m, 1H), 1.35–1.28 (m, 1H), 1.23 (t, 7.2 Hz, 3H). See **Figure S4** for the Difference NOE NMR spectra. ^{13}C NMR (CDCl_3 , 125 MHz): *E*: δ 136.5, 135.7, 134.5, 119.5, 67.3, 50.5, 46.1, 41.9, 30.2, 15.4. *Z*: δ 136.3, 135.7, 134.4, 120.0, 67.4, 49.5, 43.7, 41.6, 30.0, 15.4. MS (ESI) m/z $[M + Na]^+$, calcd: 173.0937, found: 173.0939.

Polymerization procedures.

Polymerization procedures were conducted in a manner similar to that described in the preceding chapters.

Acid methanolysis of product copolymers.

Acid methanolysis of product copolymers was conducted in a manner similar to that described in the preceding chapters.

Characterization.

Characterization data were obtained in a manner similar to that described in preceding chapters.

Results and Discussion

Design and Synthesis of Monomers

To introduce substituents onto the β -carbon of VEs, the author acetalized aliphatic aldehydes and subsequently performed an E1 reaction with acid catalysis. Various enol ethers were designed based on the structures of the precursor aldehydes and alcohols (**Scheme 1**). Specifically, the substituents on the β -carbon of the alkenyl group were derived from the substituents on the α -carbon of the precursor aldehydes, while the alkoxy group was derived from the alcohols used for acetalization. The chemical shifts of the *E*- or *Z*-isomers of EM-EVE, PrM-EVE, PhM-EVE, and Nb-EVE were determined by the difference NOE NMR spectra (**Figures S1–S4**).

Enol Ether Homopolymerizability and Copolymerizability with Aromatic Aldehydes

The author first examined the homopolymerizability and copolymerizability of ethyl VE (EVE) derivatives having an alkyl group at the β -carbon of the alkenyl group. In the polymerization reactions, GaCl₃ was used as a Lewis acid catalyst in conjunction with EtSO₃H as a protonogen in toluene at -78 °C. In our previous studies, EVE and ethyl propenyl ether, which are VEs with no substituent and one methyl group on the β -carbon, respectively, were demonstrated to exhibit both homopolymerizability and copolymerizability with BzAs or OPA.

Table 1. Cationic homo- or copolymerization of enol ethers (EEs)^a

entry	EE	comonomer	time	conv. ^b (%)		$M_n \times 10^{-3}$ ^c	M_w/M_n ^c
				EE	comonomer		
1	P-EVE	none	1 h	37	–	2.4	1.41
2		pMeOBzA	10 min	80	73	8.5	1.27
3 ^d		OPA	1 h	91	94	11.5	1.39
4	IP-EVE	none	24 h	14	–	0.5	–
5		pMeOBzA	1 h	0	0	–	–
6 ^d		OPA	1 h	66	92	9.3	1.68
7	DM-EVE	none	24 h	0	–	–	–
8 ^e		pMeOBzA	6 h	82 (total conv.)		0.4	–
9 ^d		OPA	90 min	76	85	5.8	1.69
10	DE-EVE	none	24 h	0	–	–	–
11		pMeOBzA	2 h	5	11	0.3	–
12 ^d		OPA	2 h	76	89	1.8	1.77

^a [Enol ether]₀ = 0.40 M, [comonomer]₀ = 0 or 0.40 M, [EtSO₃H]₀ = 4.0 mM, [GaCl₃]₀ = 4.0 mM, [1,4-dioxane]₀ = 0.50 M in toluene at –78 °C. ^b Determined by ¹H NMR and gravimetry. ^c Determined by GPC (polystyrene standards). ^d These data are also shown in the subsequent tables. ^e Data from ref 26.

When β -propyl ethyl vinyl ether (P-EVE), which has an *n*-propyl group at the β -carbon, was subjected to homopolymerization and copolymerization with pMeOBzA, a homopolymer (entry 1 in **Table 1**) and an alternating copolymer (entry 2) were successfully obtained, respectively, as in the case of the β -methyl counterpart. In contrast, β -isopropyl ethyl vinyl ether (IP-EVE), which has an isopropyl group, resulted in an oligomeric product upon homopolymerization (entry 4) or no reaction upon copolymerization with pMeOBzA (entry 5). These results indicate that the secondary alkyl group on the β -carbon significantly affects the polymerizability of enol ethers.

Unlike the enol ethers with an alkyl group, those with two alkyl groups on the β -carbon of the alkenyl group were completely unable to homopolymerize. β,β -Dimethyl ethyl vinyl ether (DM-EVE; the abbreviation “EMPE” was used in the preceding chapters) and β,β -diethyl vinyl ether (DE-EVE), which have dimethyl and diethyl groups at the β -carbon, respectively, produced neither polymers nor oligomers during homopolymerization (entries 7 and 10 in **Table 1**). In addition, only cyclic trimers composed of one enol ether and two pMeOBzA molecules were obtained via copolymerization with pMeOBzA (entries 8 and 11).

As demonstrated here, the enol ethers with a bulky alkyl group or two alkyl groups exhibited low or negligible homopolymerizability and copolymerizability with pMeOBzA (**Scheme 2**). In contrast, copolymerization of the enol ethers and OPA proceeded successfully (entries 3, 6, 9 and 12 in **Table 1**). The detailed results are described in the following sections.

Copolymerization of β -Monoalkyl Monomers and OPA

To investigate the effect of the alkyl structures, β -monoalkyl monomers were subjected to cationic copolymerization with OPA. Copolymerization was conducted with the EtSO₃H/GaCl₃ initiating system in the

presence of 1,4-dioxane as a Lewis base in toluene at $-78\text{ }^{\circ}\text{C}$. These conditions are known to be effective for the copolymerization of VEs and OPA, as reported in Chapter 2.²⁴ Copolymerization of OPA with β -ethyl ethyl vinyl ether (E-EVE) or P-EVE, which have an ethyl or propyl group on the β -carbon, respectively, proceeded smoothly to yield polymers with M_n values of approximately 10^4 (entries 1 and 2 in **Table 2**; **Figures 1A**). From the ^1H NMR analysis of the products, the number of enol ether and OPA units per block was estimated to be 1.1 and 1.0–1.1, respectively, which indicates that the copolymers had nearly alternating sequences. These enol ethers exhibited sufficient homopolymerizability (*vide supra*); hence, the results suggest that the addition of OPA to the enol ether-derived propagating carbocation occurred selectively due to the high reactivity of OPA. Since the product copolymers have acetal moieties generated by both the crossover reaction from enol ether to OPA and OPA homopropagation, the copolymers were degraded into low-MW compounds upon reaction with methanol and HCl. The methanolysis product of the copolymer of P-EVE and OPA gave rise to multimodal peaks in the low-MW region in the MWD curve (**Figure 1A**), indicating that the original copolymer did not have completely alternating sequences but had partial P-EVE homosequences. In addition, the copolymerization of P-EVE with OPA proceeded by the mediation of long-lived species. However, the observed MW (11.5×10^3) was lower than the theoretical value (23.0×10^3) calculated from monomer conversions, partly because some side reactions, such as β -proton elimination, occurred during polymerization, although the detailed mechanism is not clear.

Table 2. Cationic copolymerization of β -monoalkyl enol ethers (EEs) and OPA^a

entry	EE	time	conv. ^b (%)		$M_n \times 10^{-3}$ ^c	M_w/M_n ^c	units per block ^d	
			EE	OPA			EE	OPA
1	E-EVE	10 min	86	77	9.0	1.43	1.1	1.1
2	P-EVE	1 h	91	94	11.5	1.39	1.1	1.0
3	IP-EVE	1 h	66	92	9.3	1.68	1.0	1.4
4	TB-EVE	1 h	22	46	0.6 (1.1) ^e	1.69	1.0	2.9
5	MeDHP	1 h	76	87	12.1	1.66	1.0	1.1

^a $[\text{Enol ether}]_0 = 0.40\text{ M}$, $[\text{OPA}]_0 = 0.40\text{ M}$, $[\text{EtSO}_3\text{H}]_0 = 4.0\text{ mM}$, $[\text{GaCl}_3]_0 = 4.0\text{ mM}$, $[\text{1,4-dioxane}]_0 = 0.50\text{ M}$ in toluene at $-78\text{ }^{\circ}\text{C}$. ^b Determined by ^1H NMR and gravimetry. ^c Determined by GPC (polystyrene standards). ^d Calculated by ^1H NMR spectrum. ^e Value for peak top.

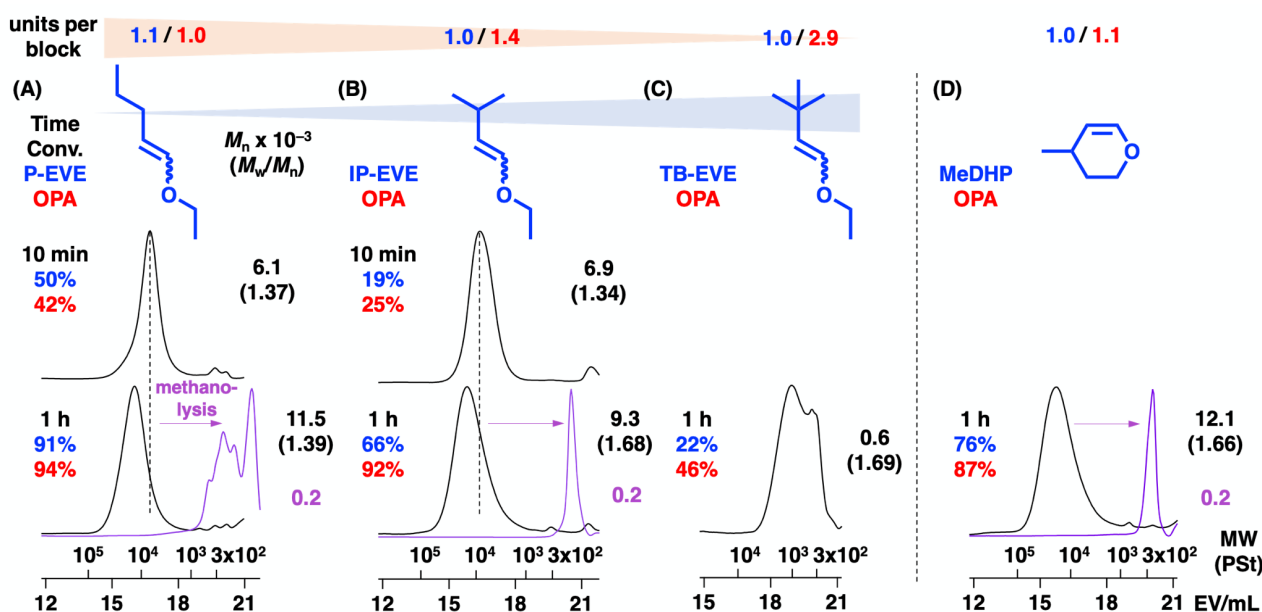


Figure 1. MWD curves of the obtained copolymers (black: original polymers; purple: products obtained by acid methanolysis). Polymerization conditions: $[\text{Enol ether}]_0 = 0.40 \text{ M}$, $[\text{OPA}]_0 = 0.40 \text{ M}$, $[\text{EtSO}_3\text{H}]_0 = 4.0 \text{ mM}$, $[\text{GaCl}_3]_0 = 4.0 \text{ mM}$, $[\text{1,4-dioxane}]_0 = 0.50 \text{ M}$ in toluene at $-78 \text{ }^\circ\text{C}$.

Copolymerization of IP-EVE and OPA also proceeded via frequent crossover reactions (entry 3 in **Table 2**; **Figure 1B**); in contrast, IP-EVE remained inert toward both homopolymerization and copolymerization with pMeOBzA (vide supra). A copolymer composed of IP-EVE and OPA units with a ratio of 1.0/1.4 per block was obtained. The negligible occurrence of IP-EVE homopropagation was also corroborated by the unimodal peak in the MWD curve of the methanolysis product (**Figure 1B**). IP-EVE was reported to form copolymers with IBVE, although long IBVE blocks were likely generated, as determined from the monomer reactivity ratios ($r_{\text{IBVE}} = 1.71$, $r_{\text{IP-EVE}, Z} = 0.09$ or $r_{\text{IBVE}} = 14.44$, $r_{\text{IP-EVE}, E} = 0.09$).^{22,23} The crossover reaction from the OPA-derived carbocation to IP-EVE was more frequent than that from the IBVE-derived carbocation to IP-EVE, partly because the steric hindrance of the OPA-derived carbocation is smaller than that of the IBVE-derived carbocation and the homopropagation of OPA is slower than that of IBVE.

Additionally, the author examined the difference in reactivity between the *E*- and *Z*- isomers of IP-EVE. The NMR spectrum of the polymerization solution after quenching indicated that the *Z*-isomer exhibited higher reactivity than the *E*-isomer in the copolymerization with OPA (**Table S1**). At the early stage of the copolymerization of IP-EVE and OPA, the *Z*-isomer of IP-EVE preferentially reacted with the OPA-derived carbocation, and a nearly alternating copolymer (units per block: EE/OPA = 1.0/1.2) was obtained. At the later stage, the amount of *Z*-isomer decreased, and a copolymer with a low IP-EVE composition (1.0/1.4) was obtained. The higher reactivity of the *Z*-isomer than of the *E*-isomer is most likely because the steric hindrance around the β -carbon of the *Z*-isomer is smaller than that of the *E*-isomer. The result is consistent with the cationic copolymerization of IBVE and IP-EVE.^{22,23}

Copolymerization of β -*t*-butyl ethyl vinyl ether (TB-EVE), which has a *t*-butyl group on the β -carbon, and OPA also proceeded, although the generated copolymer had a low MW and a nonalternating sequence

(entry 4 in **Table 2**; **Figures 1C** and **2**). According to a previous study, TB-EVE, unlike IP-EVE, did not copolymerize with IBVE, which means that TB-EVE cannot react with the IBVE-derived carbocation.^{22,23} In contrast, the obtained results show that TB-EVE can react with the OPA-derived carbocation.

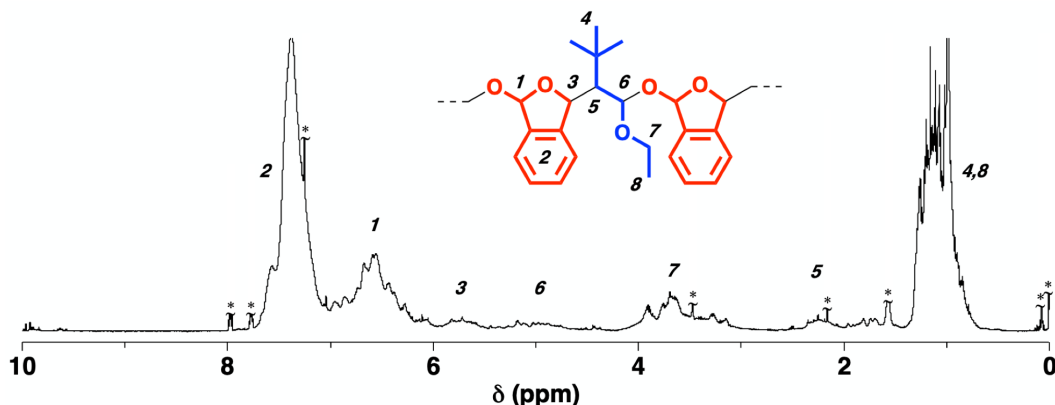


Figure 2. ¹H NMR spectrum of poly(TB-EVE-co-OPA) (entry 4 in **Table 2**) recorded in CDCl₃ at 30 °C. Peaks with asterisks are due to TMS, grease, water, toluene, methanol, CHCl₃ and residual OPA.

Copolymerization of OPA and MeDHP, which can be regarded as a cyclic enol ether possessing a secondary alkyl group on the β-carbon, was also conducted (entry 5 in **Table 2**). The reaction proceeded smoothly to yield a nearly alternating copolymer (**Figure 1D**). The number of OPA units per block was obviously smaller (1.1) than that in the copolymer formed by IP-EVE and OPA (1.4). This is partly because the rotation of the secondary alkyl group was suppressed by the cyclic structure, which facilitated the approach of MeDHP to the OPA-derived carbocation compared to the case of IP-EVE.

Copolymerization of β-Methyl-β-Alkyl Monomers and OPA

The copolymerization of β,β-dimethyl monomers and OPA was examined with a particular focus on alternating propagation and the livingness of polymerization. In Chapter 2, alternating copolymerization of DM-EVE and OPA proceeded under the same polymerization conditions used for the β-monoalkyl monomers, whereas propagation reactions mediated by long-lived species did not proceed (entry 1 in **Table 3**; **Figure 3A**).

Table 3. Cationic copolymerization of β -methyl- β -alkyl enol ethers and OPA^a

entry	EE	time	added base	conv. ^b (%)		$M_n \times 10^{-3}$ ^c	M_w/M_n ^c	units per block ^d	
				EE	OPA			EE	OPA
1 ^e	DM-EVE	90 min	1,4-DO	76	85	5.8	1.69	1.0	1.0
2		90 min	1,4-DO, DTBP	73	81	20.5	1.38	1.0	1.0
3	DM-IBVE	4 h	1,4-DO	69	81	16.1	1.83	1.0	1.2
4		1 h	1,4-DO, DTBP	32	37	9.3	1.61	1.0	1.1
5	DM-IPVE	20 min	1,4-DO	75	82	5.1	1.54	1.0	1.2
6		1 h	1,4-DO, DTBP	66	75	15.9	1.48	1.0	1.2
7	DM-MOVE	2 h	1,4-DO	59	70	4.2	2.05	1.0	1.1
8		30 min	none	82	84	12.6	1.82	1.0	1.0
9		10 min	DTBP	60	62	19.5	1.31	1.0	1.0
10	DM-MOEVE	2 h	1,4-DO	52	63	0.8	1.27	1.0	1.0
11		8 h	none	95	94	2.6	1.78	1.0	1.0
12 ^f		6 h	DTBP	48	55	10.3	1.62	1.0	1.0
13	EM-EVE	30 min	1,4-DO	63	69	12.9	1.47	1.0	1.1
14		25 min	1,4-DO, DTBP	83	96	26.0	1.38	1.0	1.1
15	PrM-EVE	25 min	1,4-DO	67	73	11.5	1.56	1.0	1.0
16		25 min	1,4-DO, DTBP	79	93	27.0	1.45	1.0	1.1
17	PhM-EVE	4 h	1,4-DO	68	79	6.0	1.70	1.0	1.2
18		24 h	1,4-DO, DTBP	58	70	7.7	1.65	1.0	1.2

^a [Enol ether]₀ = 0.40 M, [OPA]₀ = 0.40 M, [EtSO₃H]₀ = 4.0 mM, [GaCl₃]₀ = 4.0 mM, [1,4-dioxane]₀ = 0 or 0.50 M, [DTBP]₀ = 0 or 2.0 mM in toluene at -78 °C. ^b Determined by ¹H NMR and gravimetry. ^c Determined by GPC (polystyrene standards). ^d Calculated by ¹H NMR spectrum. ^e Data from Chapter 2 of this thesis. ^f At -96 °C.

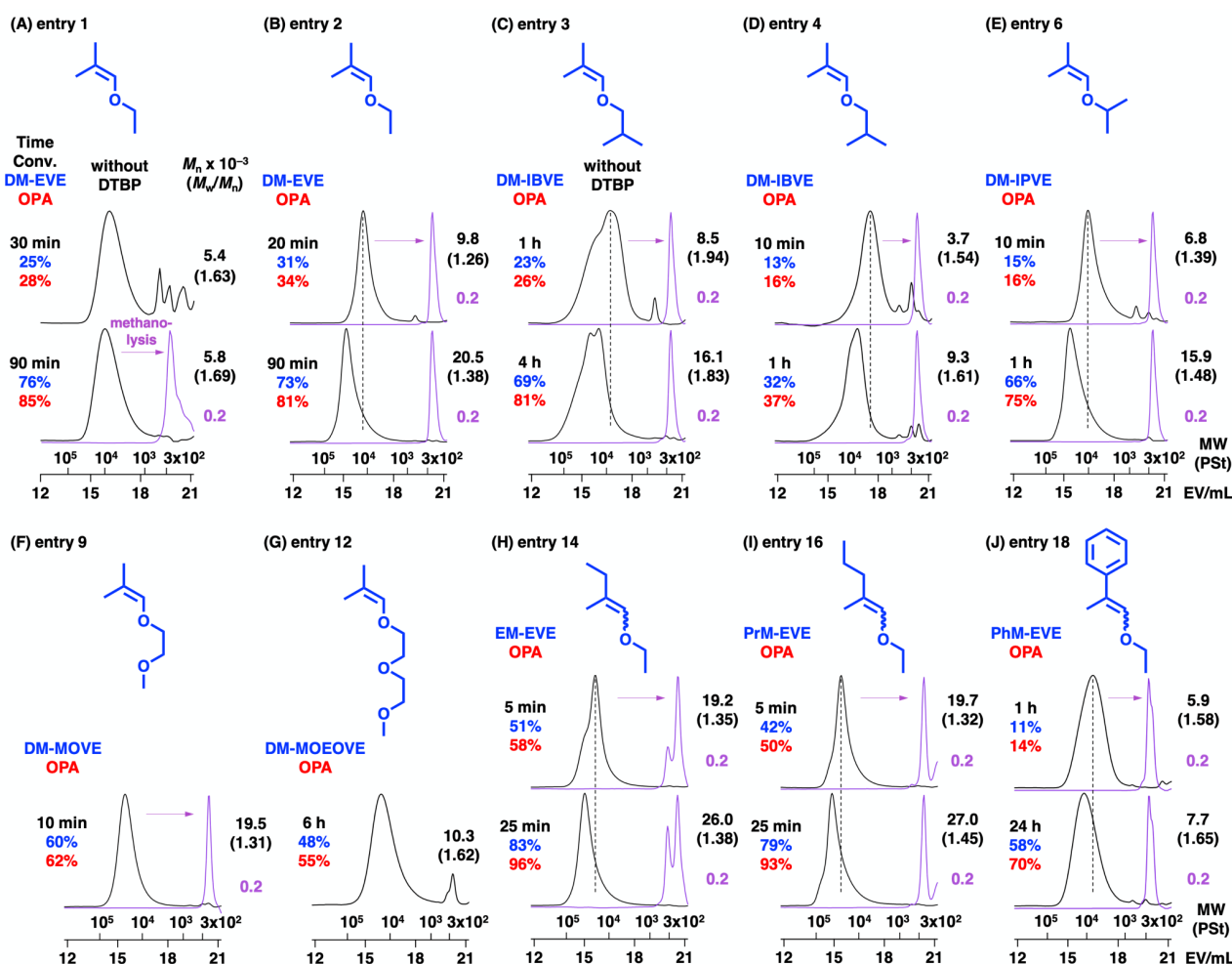


Figure 3. MWD curves of the products obtained by the copolymerization of OPA and (A) DM-EVE without DTBP (entry 1 in Table 3), (B) DM-EVE (entry 2), (C) DM-IBVE without DTBP (entry 3), (D) DM-IBVE (entry 4), (E) DM-IPVE (entry 6), (F) DM-MOVE (entry 9), (G) DM-MOEOVE (entry 12), (H) EM-EVE (entry 14), (I) PrM-EVE (entry 16), and (J) PhM-EVE (entry 18) (black: original polymers; purple: products obtained by acid methanolysis). See the footnote of Table 3 for the polymerization conditions.

The addition of 2,6-di-*tert*-butylpyridine (DTBP) was found to be effective for the living copolymerization of DM-EVE and OPA (entry 2 in Table 3; Figure 3B). The copolymerization was conducted using the EtSO₃H/GaCl₃ initiating system at -78 °C. The MW of the copolymer obtained in the presence of DTBP was higher (approximately 2×10^4) than that of the copolymer obtained without DTBP. Moreover, the MWs increased as the reaction proceeded while maintaining narrow MWDs. In addition, the experimental M_n values were consistent with those calculated from monomer conversions (Figure 4), indicating that polymer chains were generated from protonogen (EtSO₃H) and that chain transfer reactions were negligible during copolymerization. The acid-methanolysis products of the copolymers obtained at both early and late stages of polymerization had a unimodal peak in the MWD curves (purple curves in Figure 3B), indicative of the alternating sequences of the copolymers.

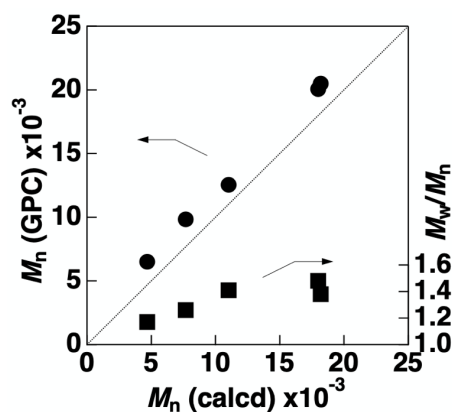
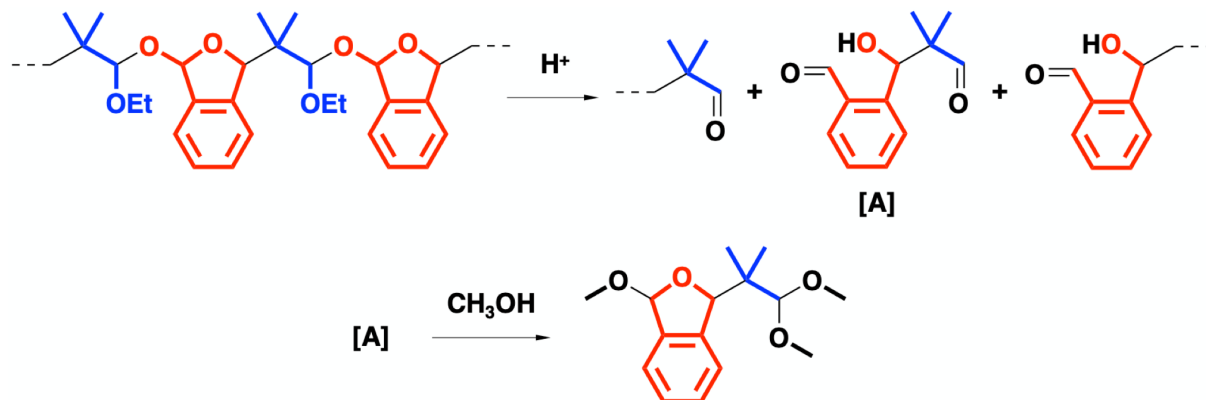


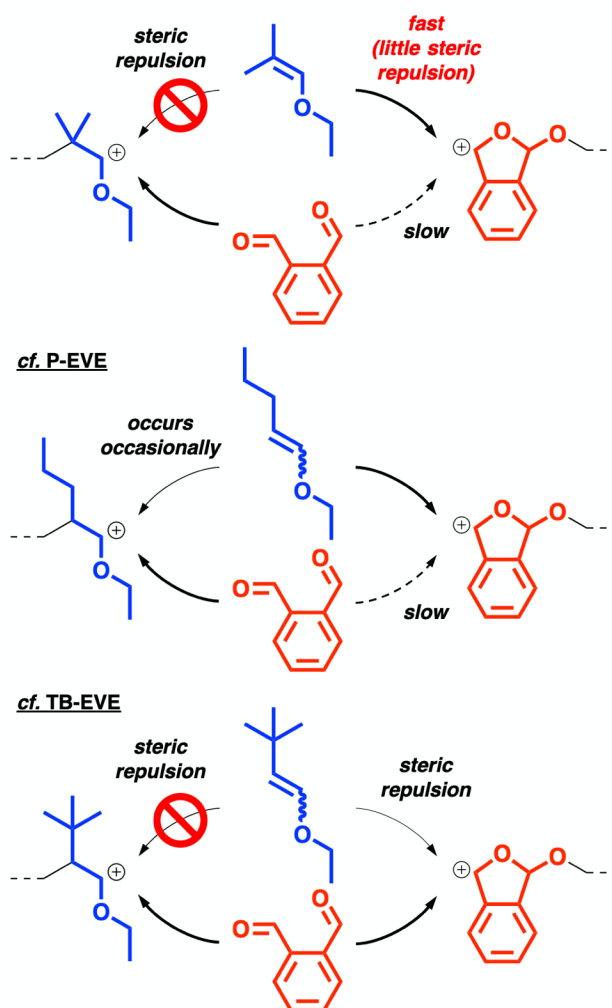
Figure 4. M_n and M_w/M_n plots for the copolymerization of DM-EVE and OPA ($[\text{DM-EVE}]_0 = [\text{OPA}]_0 = 0.40$ M, $[\text{EtSO}_3\text{H}]_0 = 4.0$ mM, $[\text{GaCl}_3]_0 = 4.0$ mM, $[\text{1,4-dioxane}]_0 = 0.50$ M, $[\text{DTBP}]_0 = 2.0$ mM in toluene at -78 °C).

The ^1H NMR spectrum of the product copolymer also suggested the generation of alternating sequences (see **Figure 10** in Chapter 2). The integral ratios of each peak were consistent with the values of an alternating copolymer. The alternating sequence was also confirmed by the ^1H NMR spectrum of the acid-methanolysis product. The spectrum exhibited peaks assignable to the products resulting from the degradation of the OPA–DM-EVE–OPA sequence (**Scheme 3**). Peaks assigned to the structures derived from DM-EVE homosequences were not observed at all.



Scheme 3. Acid methanolysis of copolymers via cleavage of acetal moieties.

Scheme 4 shows the mechanism of alternating copolymerization. DM-EVE could not add to the DM-EVE-derived propagating carbocation due to the steric repulsion of two methyl groups on the β -carbon; hence, only OPA could add to the DM-EVE carbocation. In contrast, both DM-EVE and OPA could add to the OPA-derived propagating carbocation; however, the addition of DM-EVE to the OPA-derived carbocation was much faster than that of OPA because the homopropagation of OPA was relatively slow. As a result, both DM-EVE and OPA homopropagations were suppressed, triggering alternating propagation reactions (the monomer reactivity ratios of DM-EVE and OPA were determined to be approximately zero; **Figure 5** and **Table S2**). DTBP is thought to suppress the chain-transfer reaction mediated by protons (**Scheme 5** and **Figure 6**) or undesired side reactions by tuning the Lewis acidity of GaCl_3 .



Scheme 4. Plausible copolymerization mechanisms of enol ethers and OPA.

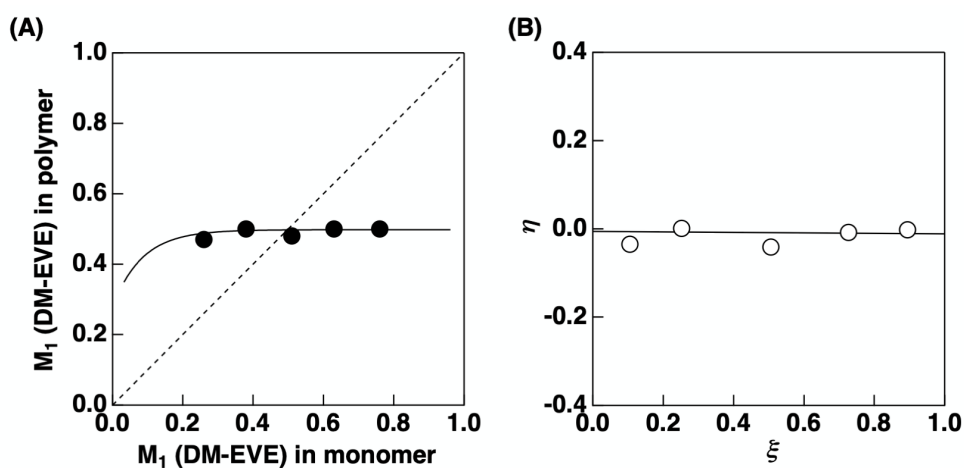


Figure 5. (A) Copolymer compositions for the cationic copolymerization of DM-EVE (M_1) and OPA (M_2). The solid line was drawn using the r values ($r_1 \sim 0$, $r_2 = 0.03$) obtained by the Kelen-Tüdös method. (B) The plots for the determination of the monomer reactivity ratios by the Kelen-Tüdös method [$\eta = (r_1 + r_2/a)x - r_2/a$; the data listed in Table S2 were used for the calculation.].

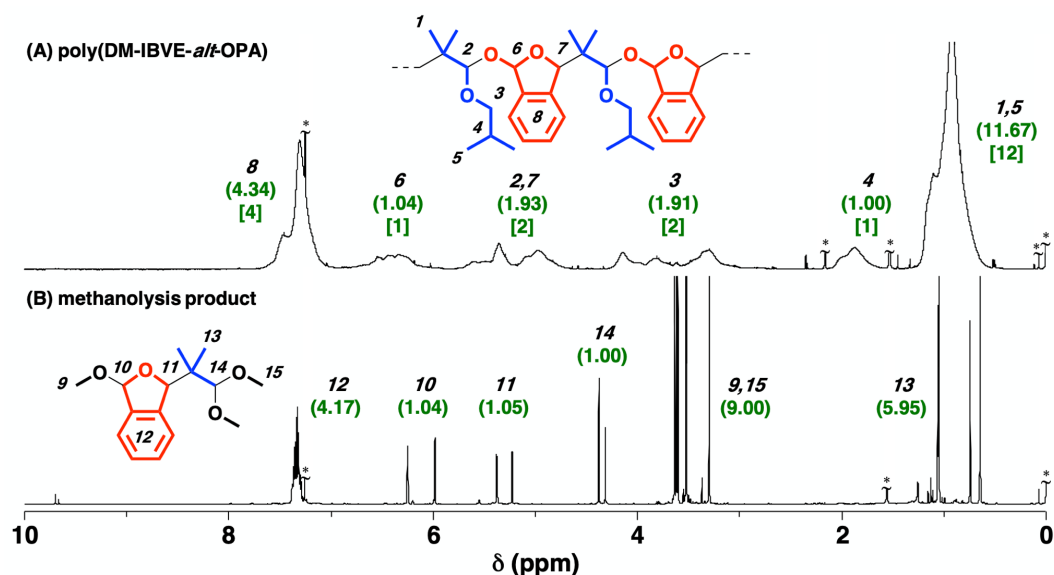


Figure 7. ^1H NMR spectra of (A) poly(DM-IBVE-*alt*-OPA) ($M_n = 20.3 \times 10^3$, $M_w/M_n = 1.32$) and (B) acid-methanolysis product of (A) recorded in CDCl_3 at 30°C . Peaks with asterisks are due to TMS, grease, water, acetone, CHCl_3 and residual OPA. Numbers written in green parentheses: observed integral ratio; written in green square brackets: theoretical integral ratio in alternating copolymers.

Alternating copolymerization of β,β -dimethyl monomers with oxyethylene moieties (β,β -dimethyl 2-methoxyethyl vinyl ether; DM-MOVE and β,β -dimethyl 2-(2-methoxyethoxy)ethyl vinyl ether; DM-MOEOVE) and OPA also proceeded. The polymerization occurred more smoothly in the absence of 1,4-dioxane than in its presence (entries 7–12, **Figures 3F** and **3G**), probably because the oxyethylene moieties acted as a Lewis base instead of 1,4-dioxane. In addition, the copolymerization of DM-MOEOVE with OPA at -96°C resulted in a copolymer with a higher MW than that at -78°C . The 2-methoxyethoxy moiety possibly caused some undesired side reactions at -78°C , although the detailed mechanism is not clear.

Alternating copolymerization of β -methyl- β -alkyl monomers and OPA also proceeded in a similar manner to those of the β,β -dimethyl monomers (entries 13–16 in **Table 3**; **Figures 3H** and **3I**) to yield copolymers with high MWs (up to 2.7×10^4). The introduction of an ethyl group (β -ethyl- β -methyl ethyl vinyl ether; EM-EVE) or a propyl group (β -propyl- β -methyl ethyl vinyl ether; PrM-EVE) onto the β -carbon instead of a methyl group (DM-EVE) did not affect the copolymerizability of enol ethers. The β -methyl- β -phenyl-type monomer (β -phenyl- β -methyl ethyl vinyl ether; PhM-EVE) and OPA also reacted via the mediation of long-lived species, though the MWDs were broader than those of the copolymers obtained from other monomers (entries 17 and 18; **Figure 3J**). PhM-EVE can be regarded as an α -methylstyrene derivative; hence, both alkenyl carbon atoms potentially react with a propagating carbocation. However, the ^1H NMR spectrum of the product copolymer indicated that PhM-EVE reacted with the OPA-derived carbocation exclusively at the carbon with a methyl and a phenyl group, which suggests that the monomer behaved not as a styrene-type monomer but as a VE-type monomer (**Figure 8**). The result is consistent with a previous report of the cationic polymerization of β -alkoxystyrenes.²⁷ To the best of our knowledge, this is the first example of the polymerization of a β -methyl- β -phenyl type monomer.

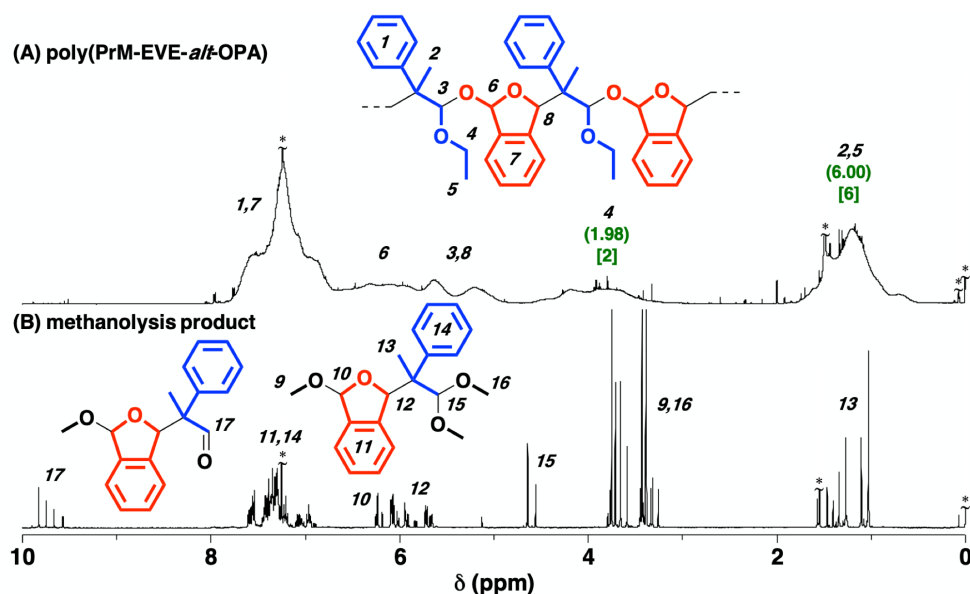


Figure 8. ^1H NMR spectrum of (A) poly(PhM-EVE-*alt*-OPA) (entry 18 in Table 3) and (B) its methanolysis product recorded in CDCl_3 at 30°C . Peaks with asterisks are due to TMS, grease, water and CHCl_3 .

Copolymerization with β,β -Dialkyl Monomers

As demonstrated above, β -methyl- β -alkyl monomers were found to be copolymerizable with OPA in an alternating manner. To investigate the limit of the copolymerizability, β,β -dialkyl monomers with bulkier β -substituents were synthesized and subjected to copolymerization with OPA.

Table 4. Cationic copolymerization of β,β -dialkyl enol ethers and OPA^a

entry	EE	temp. ($^\circ\text{C}$)	time	added base	conv. ^b (%)		$M_n \times 10^{-3}$ ^c	M_w/M_n ^c	units per block ^d	
					EE	OPA			EE	OPA
1	DE-EVE	-78	2 h	1,4-DO	76	89	1.8	1.77	1.0	1.2
2			5 min	1,4-DO, DTBP	50	56	15.9	1.54	1.0	1.1
3		-96	8 h	1,4-DO	67	81	7.4	1.80	1.0	1.2
4			3 h	1,4-DO, DTBP	77	94	20.7	1.66	1.0	1.2
5	DE-IBVE	-78	1 h	1,4-DO, DTBP	23	50	27.2	1.33	1.0	1.0
6		-96	6 h	1,4-DO, DTBP	16	35	15.6	1.44	1.0	1.0
7	CH _x -EVE	-78	90 min	1,4-DO	97	98	1.2	1.56	1.0	1.1
8			5 min	1,4-DO, DTBP	78	78	12.5	1.58	1.0	1.0
9		-96	8 h	1,4-DO	67	81	10.2	1.78	1.0	1.1
10			3 h	1,4-DO, DTBP	83	93	17.5 (30.5) ^e	1.44	1.0	1.1
11	Nb-EVE	-96	8 h	1,4-DO	11	13	2.7	1.58	1.0	1.1
12			8 h	1,4-DO, DTBP	13	17	5.2	1.59	1.0	1.1

^a $[\text{Enol ether}]_0 = 0.40$ (for entries 1–4, 7–12) or 0.81 (for entries 5,6) M, $[\text{OPA}]_0 = 0.40$ M, $[\text{EtSO}_3\text{H}]_0 = 4.0$ mM, $[\text{GaCl}_3]_0 = 4.0$ mM, $[\text{1,4-dioxane}]_0 = 0.50$ M, $[\text{DTBP}]_0 = 0$ or 2.0 mM in toluene. ^b Determined by ^1H NMR and gravimetry. ^c Determined by GPC (polystyrene standards). ^d Calculated by ^1H NMR spectrum. ^e Value for peak top.

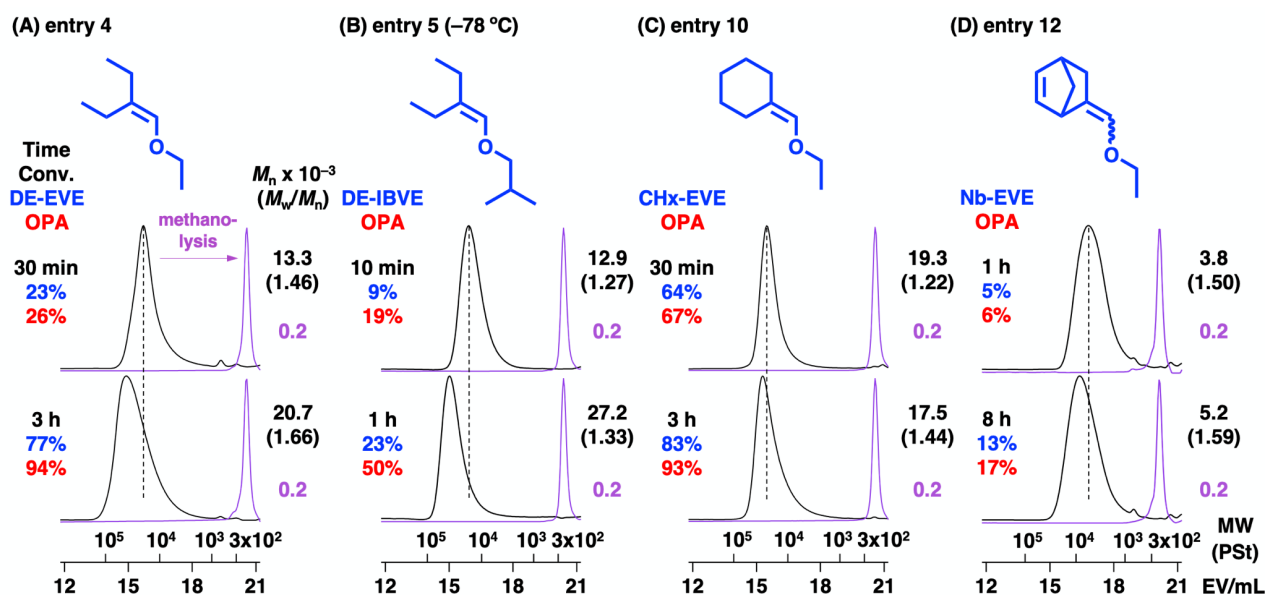


Figure 9. MWD curves of the products obtained by the copolymerization of OPA and (A) DE-EVE (entry 4 in Table 4), (B) DE-IBVE (entry 5), (C) CHx-EVE (entry 10), or (D) Nb-EVE (entry 12) (black: original polymers; purple: products obtained by acid methanolysis). See the footnote of Table 4 for the polymerization conditions.

Interestingly, β,β -diethyl-type (β,β -diethyl ethyl vinyl ether; DE-EVE and β,β -diethyl isobutyl vinyl ether; DE-IBVE), cyclohexylidene-type (cyclohexylidenemethyl ethyl ether; abbreviated as CHx-EVE for convenience), and 5-(2-norbornenylidene)-type (5-norbornenylidenemethyl ethyl ether; abbreviated as Nb-EVE for convenience) monomers also yielded nearly alternating copolymers with OPA (Table 4 and Figures 9 and S7). To the best of our knowledge, these are the first examples of the polymerization of β,β -diethyl-type, cyclohexylidene-type, and 5-norbornenylidene-type monomers. The ^1H NMR spectrum of the copolymer obtained from CHx-EVE and OPA (Figure 10A) suggests the generation of a nearly alternating copolymer. Copolymers with M_n values of approximately 10^4 were obtained at -96 °C (entries 3 and 9 in Table 4). In addition, the use of DTBP improved the controllability of the polymerization (entries 2, 4–6, 8, 10 and 12), similar to the case of the β -methyl- β -alkyl monomers. However, the MWs were not as high and decreased at the later stage of the reaction at -78 °C (entries 1 and 7). This is probably because the depolymerization reaction occurred due to equilibrium polymerization at -78 °C and/or the bulky geminal substituents led to cyclic oligomerization by the back-biting reaction (c.f. the Thorpe-Ingold effect) (Scheme 6). The molecular weight decreased even in the presence of DTBP at the later stage of the reaction at -78 °C, suggesting that the adventitious protons are not the main reason of the decrease of the MWs. Actually, the ESI-MS spectrum of the product obtained at the later stage of copolymerization showed peaks corresponding to the sum of the MWs of both monomers (Figure 11).

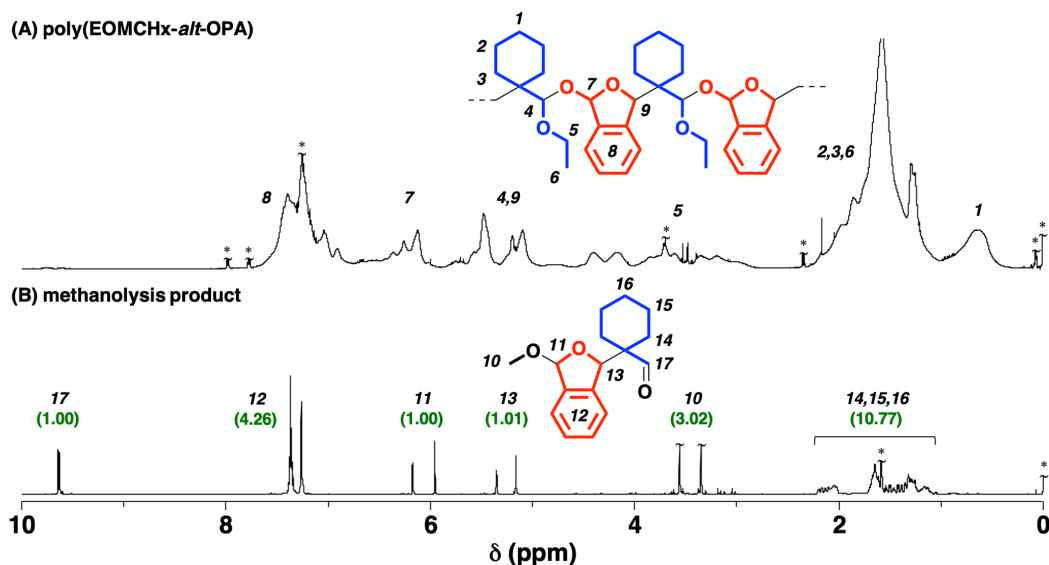
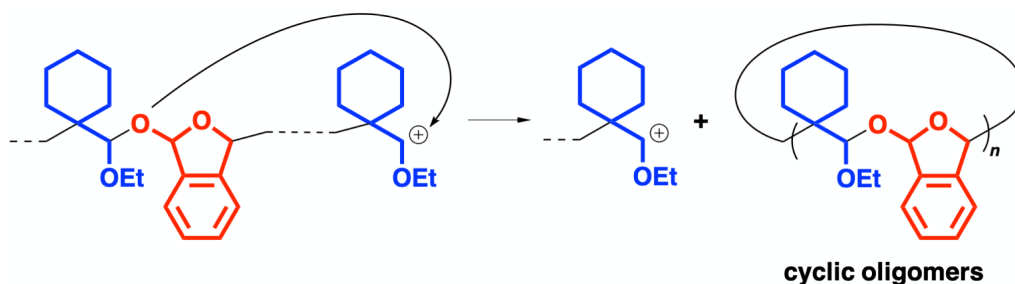


Figure 10. ^1H NMR spectra of (A) poly(CHx-EVE-*alt*-OPA) ($M_n = 17.5 \times 10^3$, $M_w/M_n = 1.44$) and (B) Acid-methanolysis product of (A) recorded in CDCl_3 at 30°C . Peaks with asterisks are due to TMS, grease, water and CHCl_3 . Numbers written in green parentheses: observed integral ratio; written in green square brackets: theoretical integral ratio in alternating copolymers.



Scheme 6. Plausible mechanism of back-biting reaction in the copolymerization of CHx-EVE and OPA.

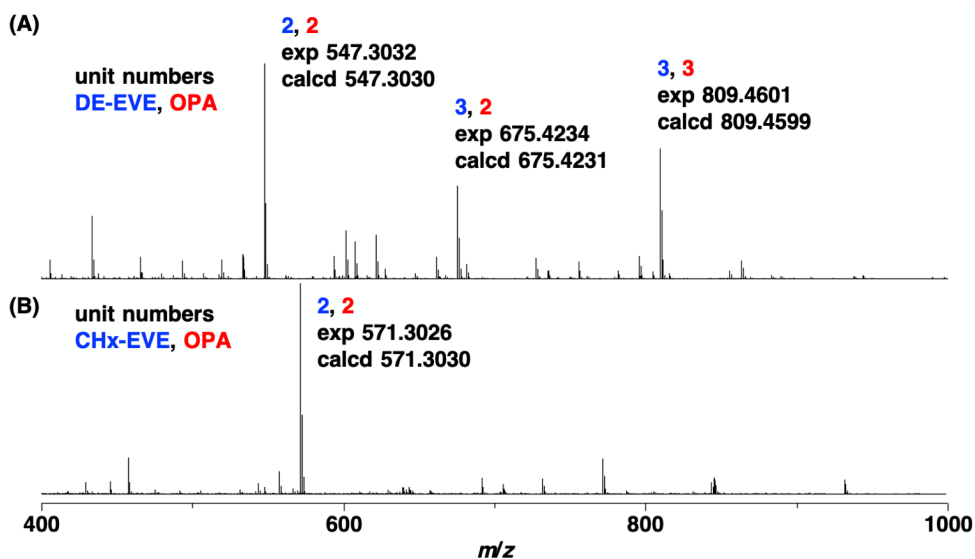


Figure 11. ESI-MS spectra of the products obtained at the later stage of polymerization reaction of OPA and (A) DE-EVE (entry 1 in **Table 4**) or (B) CHx-EVE (entry 7).

The methanolysis of the copolymers also indicated the successful generation of alternating sequences. The spectrum of the methanolysis product of poly(CHx-EVE-*alt*-OPA) was assigned to a single compound that was derived from the alternating sequence of CHx-EVE and OPA (**Figure 10B**). The methanolysis product has an aldehyde structure, unlike the acetal structures in the case of DM-EVE, because the acetal moiety adjacent to the quaternary carbon with large substituents was unstable.

The author also investigated the properties of the obtained poly(DE-EVE-*alt*-OPA) since its structure is quite different from that of conventional polymers. When the OPA homopolymer or copolymers were subjected to acetic acid, which is a weaker acid than HCl, poly(DE-EVE-*alt*-OPA) degraded almost completely into the single compound (**Figure 12C**), in contrast to the incomplete degradation of poly(EVE-*co*-OPA) (**Figure 12B**) or no degradation of poly(OPA) (**Figure 12A**). The acetal moieties derived from the crossover reaction from DE-EVE to OPA is more susceptible to acid than that from EVE to OPA due to the instability of the acetal moieties adjacent to the quaternary carbon with large substituents. In TGA measurement, poly(DE-EVE-*alt*-OPA) started to degrade at approximately 200 °C (**Figure 13A**), which is higher than the degradation temperature of poly(OPA) (150 °C).²⁸ Poly(DE-EVE-*alt*-OPA) did not exhibit glass-transition at the temperature below 190 °C (**Figure 13B**), which suggests that the alternating copolymer has T_g above 190 °C, higher than that of conventional copolymers such as poly(IBVE-*alt*-pMeOBzA) (33 °C)²⁹ and poly(DHP-*alt*-pMeOBzA) (182 °C).²⁶

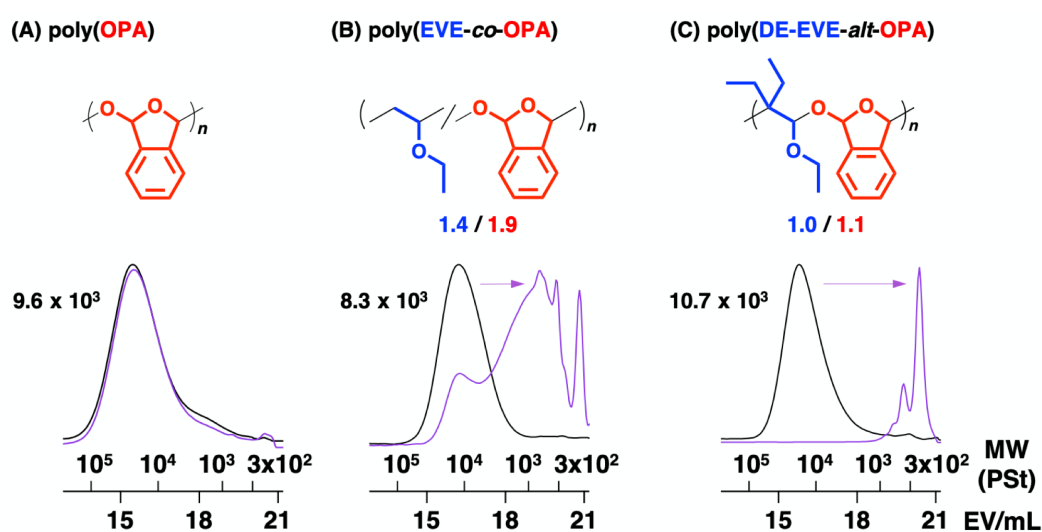


Figure 12. MWD curves of the original polymers (black) and products obtained by the reaction with acetic acid (purple). Acidolysis condition: 0.5 wt% solution in CH₂Cl₂/MeOH/AcOH/H₂O (8/4/3/1 v/v/v/v) at room temperature for 2 h.

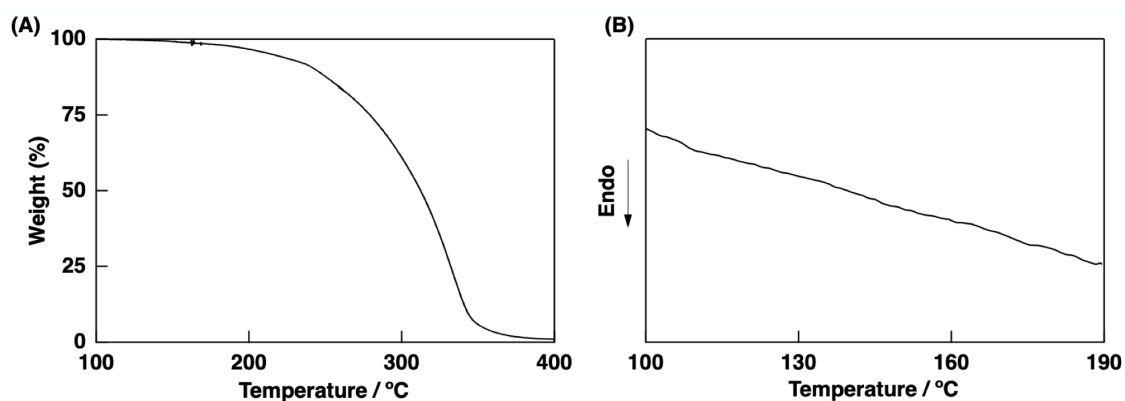


Figure 13. (A) TGA result (heating rate: 10 °C/min) and (B) DSC thermogram (2nd heating scan; heating rate: 10 °C/min) of poly(DE-EVE-*alt*-OPA).

Overview

Enol ethers possessing various alkyl groups on the β -carbon were demonstrated to copolymerize with OPA. Importantly, some of the enol ethers were successfully copolymerized for the first time by using OPA as a comonomer. The small steric hindrance and high reactivity of the OPA-derived cyclic propagating carbocation are most likely responsible for the occurrence of copolymerization.

According to the results, copolymerization behavior can be classified based on the structure of the alkyl groups on the β -carbon or the alkoxy groups (**Figure 14**). For example, methyl or *n*-alkyl groups on the β -carbon of enol ethers do not affect the alternating addition of enol ethers to the OPA-derived carbocation regardless of the number of substitutions. In contrast, a secondary or tertiary alkyl group whose conformation is not fixed decreases the reactivity of enol ethers in the reaction with the OPA-derived carbocation and thus leads to the generation of OPA homosequences as demonstrated by IP-EVE and TB-EVE. Monomers with cyclic, fixed-type secondary alkyl substituents, such as MeDHP and Nb-EVE, resulted in alternating copolymerization with OPA since these secondary alkyl groups are fixed by the cyclic structures. The steric hindrance of MeDHP or Nb-EVE is smaller than that of IP-EVE or TB-EVE. PhM-EVE underwent more frequent crossover reactions than IP-EVE or TB-EVE in the copolymerization with OPA. The steric hindrance around the β -carbon of PhM-EVE is probably not as large since the phenyl ring is considered to be in the same plane as the C=C bond of the enol ether moiety due to conjugation.

The secondary alkoxy group in the pendant had a smaller effect on the alternating copolymerization than did the secondary group on the β -carbon. Nearly alternating copolymerization proceeded regardless of the structures of the alkoxy groups, as demonstrated by the case of DM-IPVE. This is in sharp contrast to the copolymerization of non-substituted VEs with OPA: copolymers with long IPVE blocks were obtained in the copolymerization of IPVE and OPA.

For living copolymerization, methyl or primary alkyl groups on the β -carbon and primary alkoxy groups without polar moieties were suitable. A lower temperature was required for the living copolymerization of β,β -dialkyl monomers than for β,β -dimethyl monomers to suppress the depolymerization and/or back-biting reactions derived from bulky geminal substituents.

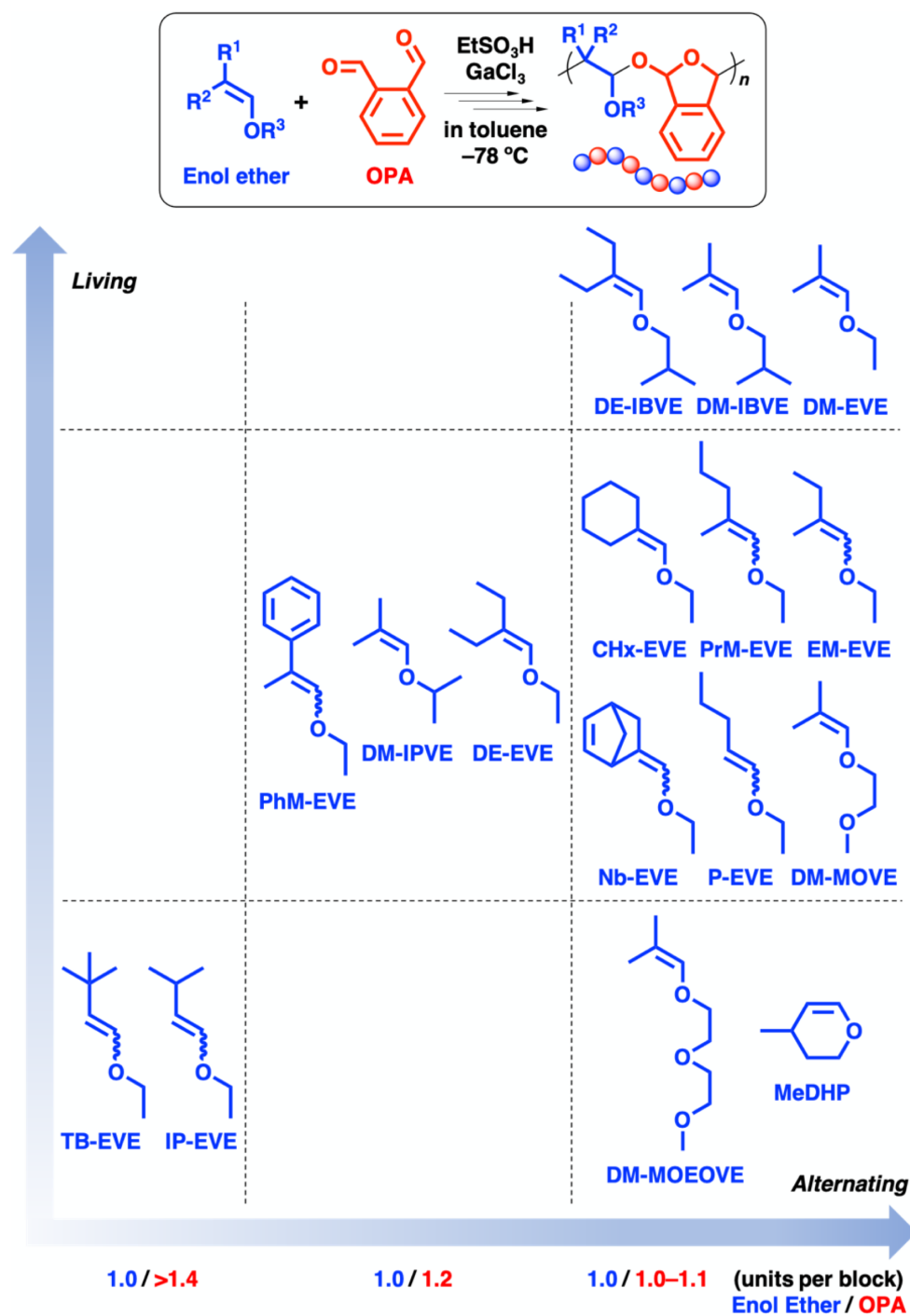


Figure 14. Summary of this study: cationic copolymerization of enol ethers and OPA.

Comparison to the Cyclic Active Species Derived from DHF

To confirm the specificity of the OPA-derived propagating carbocation, the author examined the cationic copolymerization of enol ethers and DHF because DHF generates a five-membered cyclic carbocation similar to OPA (Table 5 and Figure 15). Under conditions similar to those used for the copolymerizations of enol ethers and OPA, both DM-EVE and DE-EVE yielded copolymers in the reaction with DHF. However, the incorporation ratios of the enol ethers into copolymers were obviously lower than those for the alternating copolymers with OPA. The ratios were approximately 20 % or 8 % in the cases of DM-EVE, or DE-EVE, respectively, indicating that DE-EVE is less reactive toward the DHF-derived carbocation than DM-EVE.

Table 5. Cationic copolymerization of DHF and enol ethers^a

entry	EE	time	conv. ^b (%)		$M_n \times 10^{-3}$ ^c	M_w/M_n ^c	units per block ^d	
			DHF	EE			DHF	EE
1	DM-EVE	24 h	19	5	2.9	1.69	4.1	1.0
2	DE-EVE	24 h	29	3	1.4	1.48	11.0	1.0

^a [DHF]₀ = 0.40 M, [enol ether]₀ = 0.40 M, [EtSO₃H]₀ = 4.0 mM, [GaCl₃]₀ = 4.0 mM, [1,4-dioxane]₀ = 0.50 M, [DTBP]₀ = 2.0 mM in toluene at -78 °C. ^b Determined by ¹H NMR and gravimetry. ^c Determined by GPC (polystyrene standards).

^d Calculated by ¹H NMR spectrum.

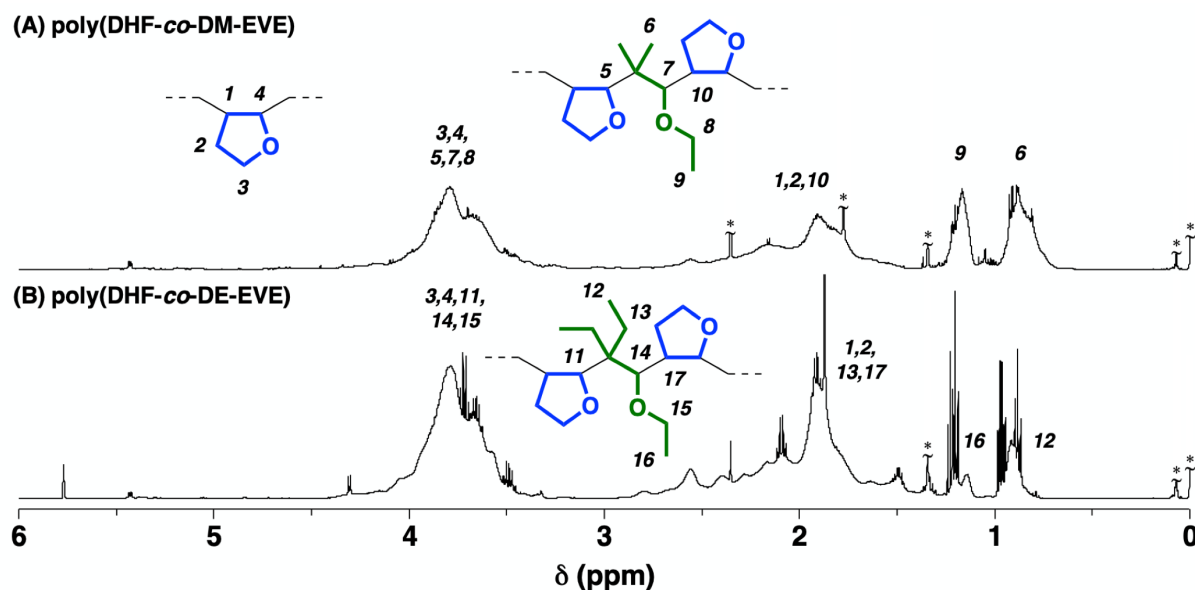


Figure 15. ¹H NMR spectra of (A) poly(DHF-co-DM-EVE) (entry 1 in **Table 5**) and (B) poly(DHF-co-DE-EVE) (entry 2) recorded in CDCl₃ at 30 °C. Peaks with asterisks are due to TMS, grease, water and toluene.

One possible reason of the lower incorporation ratios is that the degree of the planarity of the OPA-derived carbocation is larger than that of the DHF-derived carbocation due to the fused aromatic ring. This planarity is probably responsible for the easier access of an enol ether to the propagating cation. Another reason for the alternating copolymerization with OPA is the homopropagation rate of DHF or OPA. Since the homopolymerization of DHF is very fast, the addition of DHF to the DHF-derived carbocation (**Figure 16a**) is considered to be faster than that of an enol ether (**Figure 16b**). In contrast, since the homopolymerization of OPA is slow, the addition of an enol ether to the OPA-derived carbocation (**Figure 16d**) is much faster than that of OPA (**Figure 16c**).

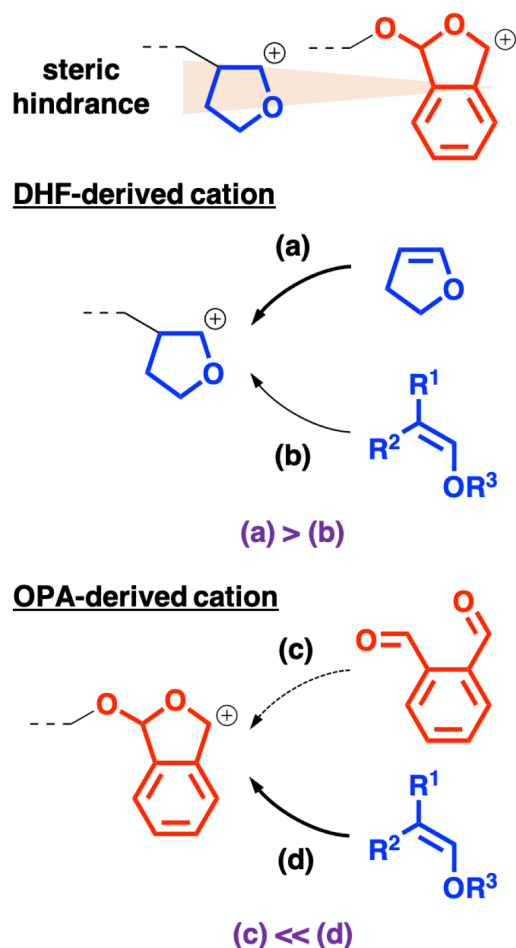


Figure 16. Differences between the DHF-derived and OPA-derived carbocations.

Conclusion

Bulky enol ethers that have been difficult to homopolymerize were successfully copolymerized with OPA. The incorporated ratio of the enol ethers into the copolymers was higher than that reported in other studies on the copolymerization of bulky enol ethers, suggesting that OPA is a suitable comonomer for the efficient copolymerization of bulky enol ethers. The copolymerization behavior varied depending on the structure of the enol ethers. Freely rotatable secondary or tertiary alkyl groups on the β -carbon of enol ethers were found to decrease the reactivity of the enol ethers toward the OPA-derived carbocation. In contrast, monomers with one or two methyl and/or primary alkyl groups on the β -carbon were copolymerized with OPA in an alternating manner, regardless of the structure of alkoxy moieties in the pendant. In addition, by designing the appropriate polymerization conditions, such as the addition of DTBP or the polymerization temperature, living and alternating copolymerization of β,β -dimethyl or dialkyl monomers with OPA was demonstrated to proceed. To elucidate the limit of polymerizable monomers, the author designed bulky monomers such as β -*t*-butyl or norbornenylidene-type monomers. However, copolymerization of those monomers proceeded successfully with OPA despite the very bulky structures. The success of these copolymerizations is most likely due to the cyclic propagating cation with small steric hindrance derived from OPA. By demonstrating the copolymerizability of enol ethers with OPA, the author has provided new insight into the polymerization of sterically hindered monomers.

References

1. Cubbon, R. C. P. *Polymer* **1965**, *6*, 419–426.
2. Otsu, T.; Matsumoto, A.; Kubota, T.; Mori, S. *Polym. Bull.* **1990**, *23*, 43–50.
3. Matsumoto, A.; Otsu, T. *Macromol. Symp.* **1995**, *98*, 139–152.
4. Barr, D. A.; Rose, J. B. *J. Chem. Soc.* **1954**, 3766–3769.
5. Ogawa, Y.; Sawamoto, M.; Higashimura, T. *Polym. J.* **1984**, *16*, 415–422.
6. Thomas, L.; Polton, A.; Tardi, M.; Sigwalt, P. *Macromolecules* **1992**, *25*, 5886–5892.
7. Kennedy, J. P.; Midha, S.; Keszler, B. *Macromolecules* **1993**, *26*, 424–428.
8. Graham, R. K.; Moore, J. E.; Powell, J. A. *J. Appl. Polym. Sci.* **1967**, *11*, 1797–1805.
9. Ute, K.; Asada, T.; Nabeshima, Y.; Hatada, K. *Polym. Bull.* **1993**, *30*, 171–178.
10. Higashimura, T.; Tanizaki, A.; Sawamoto, M. *J. Polym. Sci., Part A: Polym. Chem.* **1984**, *22*, 3173–3181.
11. Crivello, J. V.; Jo, K. D. *J. Polym. Sci., Part A: Polym. Chem.* **1993**, *31*, 1483–1491.
12. Overberger, C. G.; Tanner, D.; Pearce, E. M. *J. Am. Chem. Soc.* **1958**, *80*, 4566–4568.
13. D’Alelio, G. F.; Finestone, A. G.; Taft, L.; Miranda, T. J. *J. Polym. Sci.* **1960**, *45*, 83–89.
14. Mizote, A.; Tanaka, T.; Higashimura, T.; Okamura, S. *J. Polym. Sci., Part A: Gen. Pap.* **1965**, *3*, 2567–2578.
15. Satoh, K.; Saitoh, S.; Kamigaito, M. *J. Am. Chem. Soc.* **2007**, *129*, 9586–9587.
16. Ureta, E.; Smid, J.; Szwarc, M. *J. Polym. Sci., Part A-1: Polym. Chem.* **1966**, *4*, 2219–2228.
17. Yuki, H.; Hotta, J.; Okamoto, Y.; Murahashi, S. *Bull. Chem. Soc. Jpn.* **1967**, *40*, 2659–2663.
18. Yasuoka, K.; Kanaoka, S.; Aoshima, S. *J. Polym. Sci., Part A: Polym. Chem.* **2012**, *50*, 2758–2761.
19. Hutchings, L. R.; Brooks, P. P.; Parker, D.; Mosely, J. A.; Sevinc, S. *Macromolecules* **2015**, *48*, 610–628.
20. Natalello, A.; Hall, J. N., Alex, E.; Eccles, L.; Kimani, S. M.; Hutchings, L. R. *Macromol. Rapid. Commun.* **2011**, *32*, 233–237.
21. Sang, W.; Ma, H.; Wang, Q.; Hao, X.; Zheng, Y.; Wang, Y.; Li, Y. *Polym. Chem.* **2016**, *7*, 219–234.
22. Okuyama, T.; Fueno, T.; Furukawa, J.; Uyeo, K. *J. Polym. Sci., Part A-1: Polym. Chem.* **1968**, *6*, 1001–1007.
23. Okuyama, T.; Fueno, T. *Kobunshi kagaku* **1971**, *28*, 369–380.
24. Hayashi, K.; Kanazawa, A.; Aoshima, S. *Polym. Chem.* **2019**, *10*, 3712–3717.
25. Mizote, A.; Kusudo, T.; Higashimura, T.; Okamura, S. *J. Polym. Sci., Part A: Polym. Chem.* **1967**, *5*, 1727–1739.
26. Ishido, Y.; Kanazawa, A.; Kanaoka, S.; Aoshima, S. *J. Polym. Sci., Part A: Polym. Chem.* **2014**, *52*, 1334–1343.
27. Mizote, A.; Higashimura, T.; Okamura, S. *J. Macromol. Sci., Chem.* **1968**, *2*, 717–726.
28. Fineberg, E. C.; Hernandez, H. L.; Plantz, C. L.; Mejia, E. B.; Sottos, N. R.; White, S. R.; Moore, J. S. *ACS Macro Lett.* **2018**, *7*, 47–52.
29. Ishido, Y.; Aburaki, R.; Kanaoka, S.; Aoshima, S. *Macromolecules* **2010**, *43*, 3141–3144.

Supporting Information

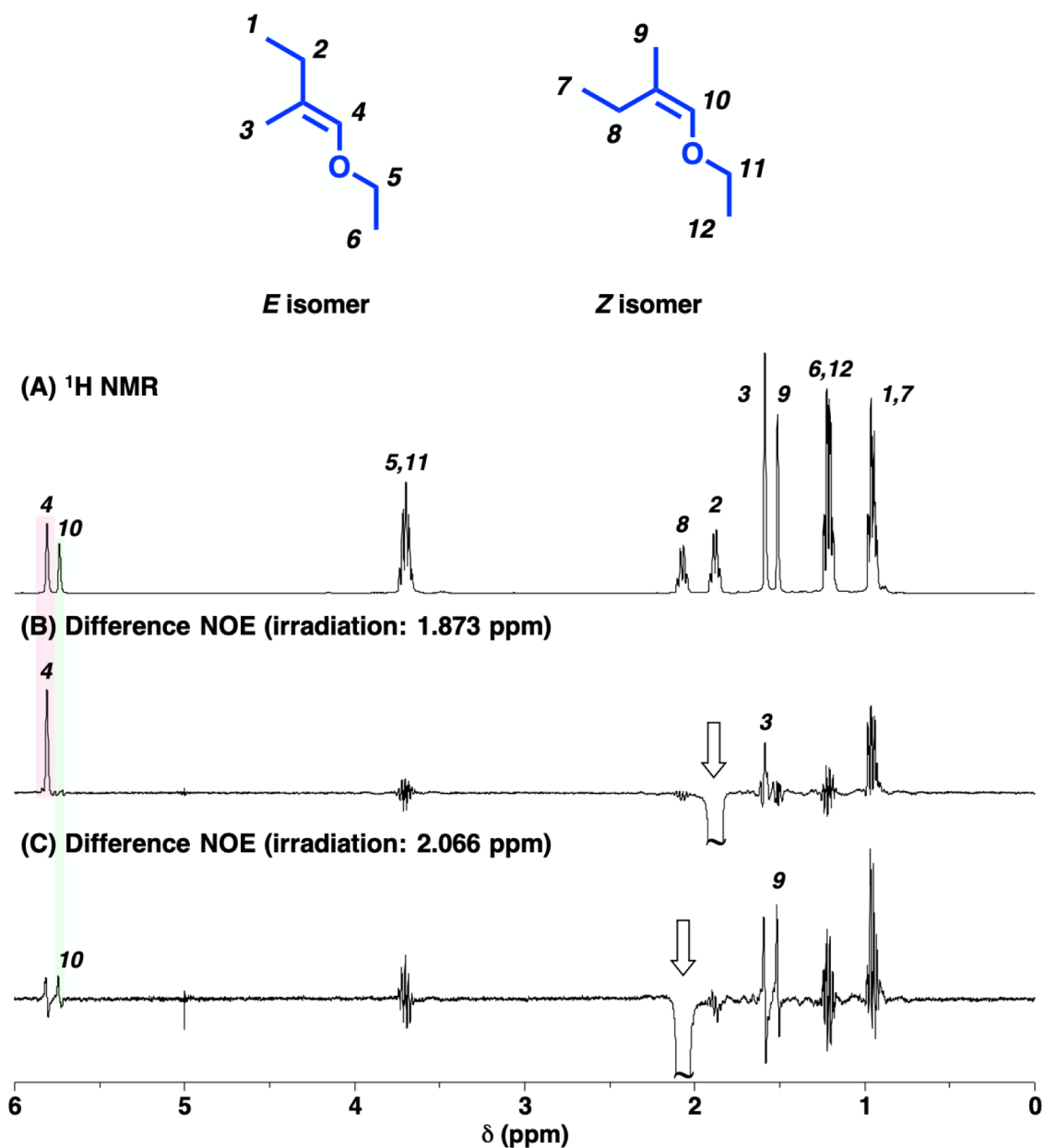


Figure S1. Difference NOE NMR spectra of EM-EVE recorded in CDCl₃ at 30 °C.

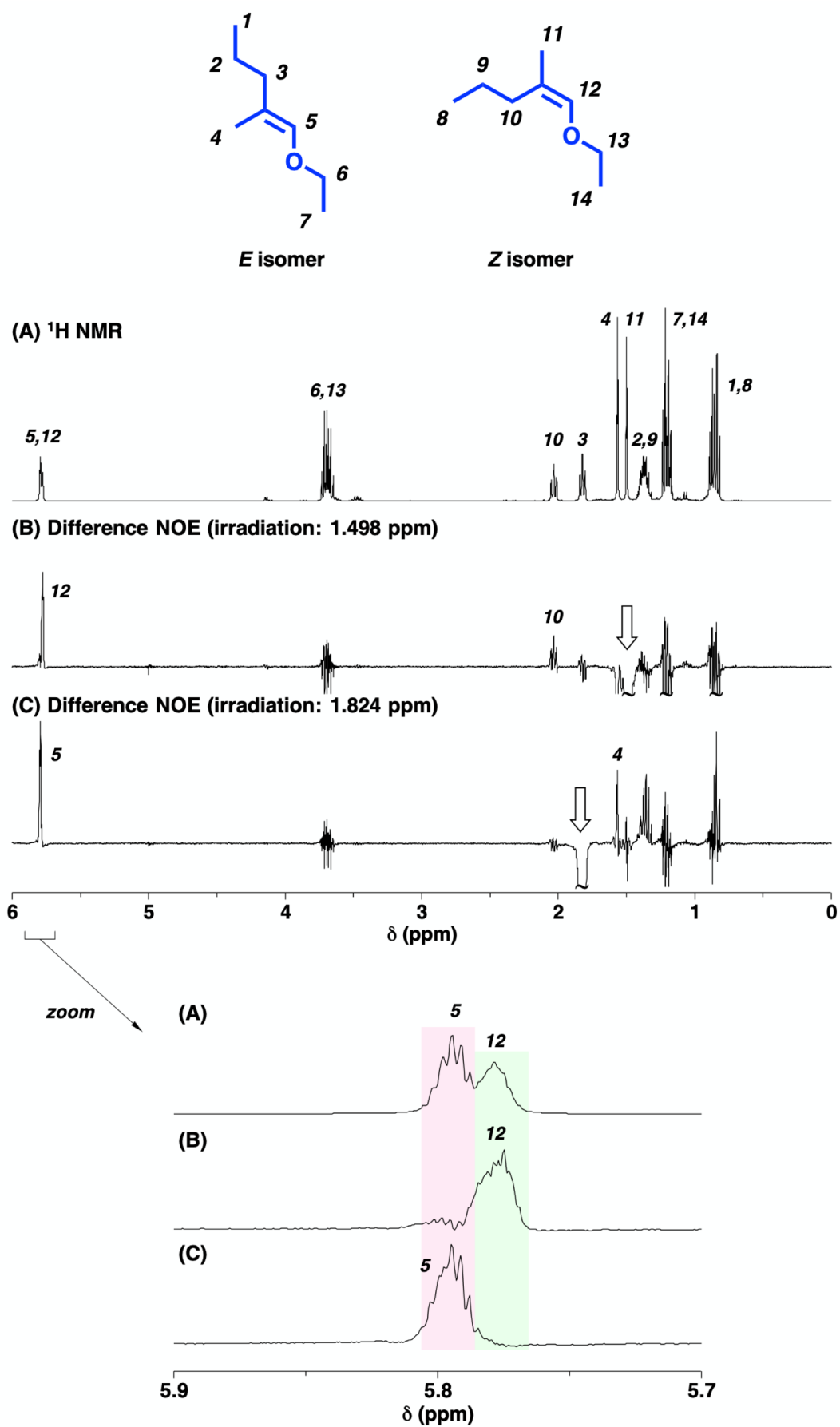


Figure S2. Difference NOE NMR spectra of PrM-EVE recorded in CDCl_3 at 30 °C.

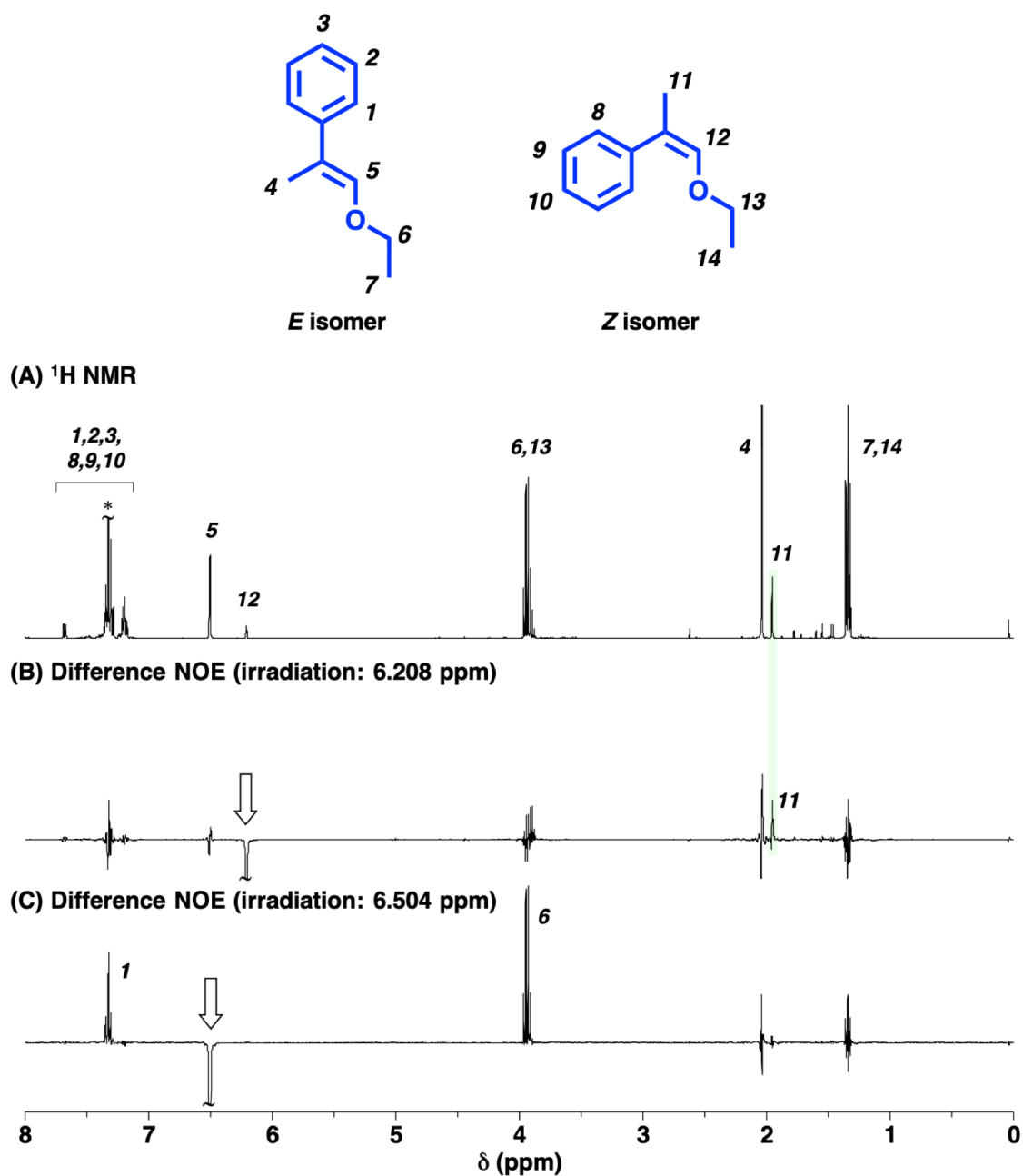


Figure S3. Difference NOE NMR spectra of PhM-EVE recorded in CDCl_3 at 30 $^\circ\text{C}$.

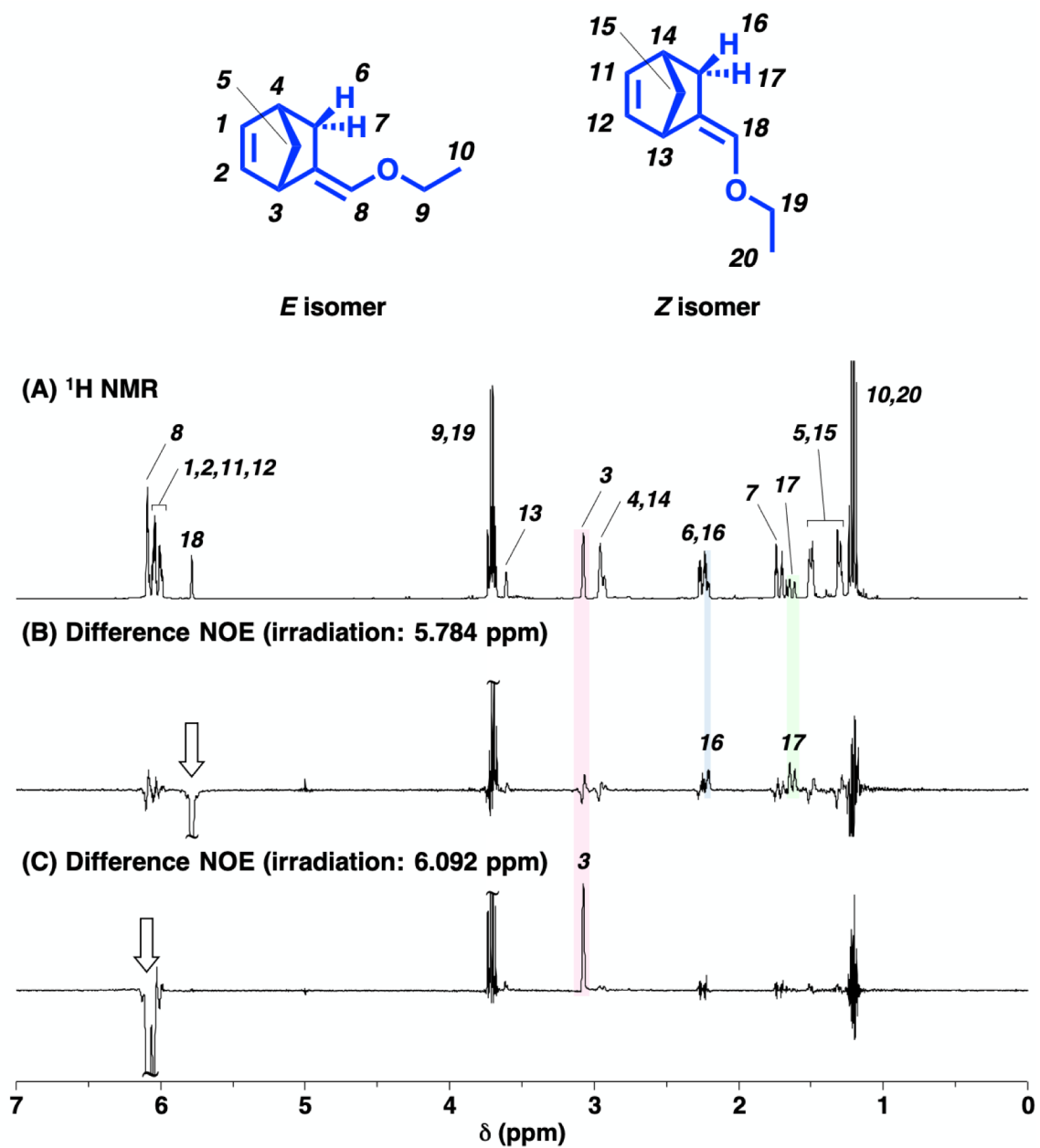


Figure S4. Difference NOE NMR spectra of Nb-EVE recorded in CDCl_3 at 30 $^\circ\text{C}$.

Table S1. Conversion of each isomer of IP-EVE in the copolymerization with OPA.^a

time	total Conv. ^b of IP-EVE (%)	conv. ^c (%)	
		<i>E</i>	<i>Z</i>
10 min	19	10	27
1 h	66	26	>99

^a [IP-EVE]₀ = 0.40 M (*E/Z* ratio = 40/60), [OPA]₀ = 0.40 M, [EtSO₃H]₀ = 4.0 mM, [GaCl₃]₀ = 4.0 mM, [1,4-dioxane]₀ = 0.50 M in toluene at -78 °C. ^b Determined by gravimetry. ^c Determined by ¹H NMR.

Table S2. Copolymerization of DM-EVE and OPA for the determination of monomer reactivity ratios.^a

DM-EVE conc [M]	OPA conc [M]	time	total conv. (%) ^b	<i>M_n</i> × 10 ⁻³ ^c	<i>M_w</i> / <i>M_n</i> ^c	DM-EVE in copolymer ^d
0.620	0.199	1 min	5	2.5	1.84	0.50
0.516	0.299	1 min	4	3.4	1.35	0.50
0.413	0.398	2 min	7	2.5	1.73	0.48
0.310	0.499	1 min	6	6.6	1.73	0.50
0.207	0.598	1 min	4	4.0	1.66	0.47

^a [EtSO₃H]₀ = 4.0 mM, [GaCl₃]₀ = 4.0 mM, [1,4-dioxane]₀ = 0.50 M, [DTBP]₀ = 2.0 mM in toluene at -78 °C.

^b By gravimetry. ^c By GPC (polystyrene calibration). ^d By ¹H NMR.

Table S3. Copolymerization of DM-IBVE and OPA for the determination of monomer reactivity ratios.^a

DM-IBVE conc [M]	OPA conc [M]	time	total conv. (%) ^b	<i>M_n</i> × 10 ⁻³ ^c	<i>M_w</i> / <i>M_n</i> ^c	DM-IBVE in copolymer ^d
0.622	0.200	1 min	8	2.2	1.52	0.50
0.518	0.299	1 min	5	1.3	2.14	0.51
0.414	0.401	1 min	5	1.4	1.50	0.51
0.311	0.500	1 min	4	1.4	1.61	0.45
0.207	0.599	1 min	3	1.2	1.95	0.42

^a [EtSO₃H]₀ = 4.0 mM, [GaCl₃]₀ = 4.0 mM, [1,4-dioxane]₀ = 0.50 M, [DTBP]₀ = 2.0 mM in toluene at -78 °C.

^b By gravimetry. ^c By GPC (polystyrene calibration). ^d By ¹H NMR.

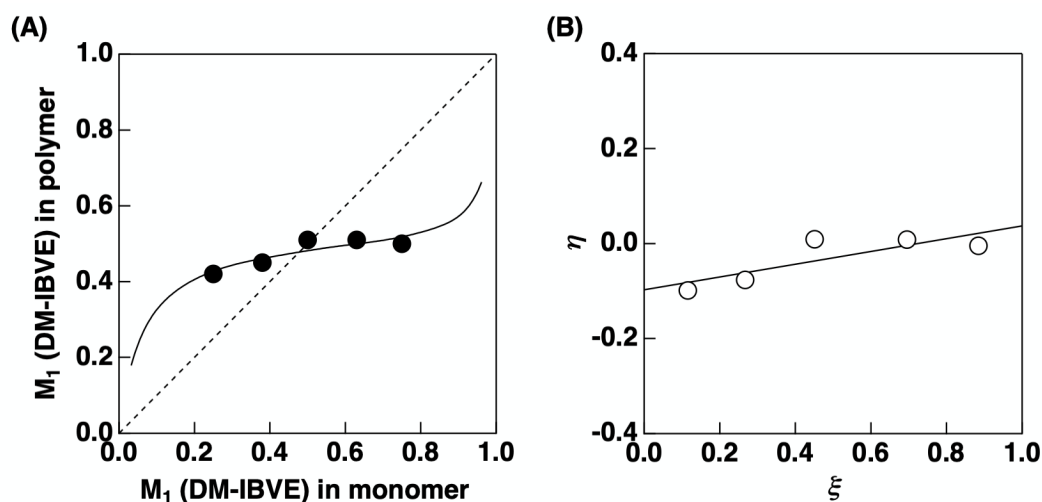


Figure S5. (A) Copolymer compositions for the cationic copolymerization of DM-IBVE (M_1) and OPA (M_2). The solid line was drawn using the r values ($r_1 = 0.04$, $r_2 = 0.12$) obtained by the Kelen–Tüdös method. (B) The plots for the determination of the monomer reactivity ratios by the Kelen–Tüdös method [$\eta = (r_1 + r_2/a)x - r_2/a$; the data listed in **Table S3** were used for the calculation.].

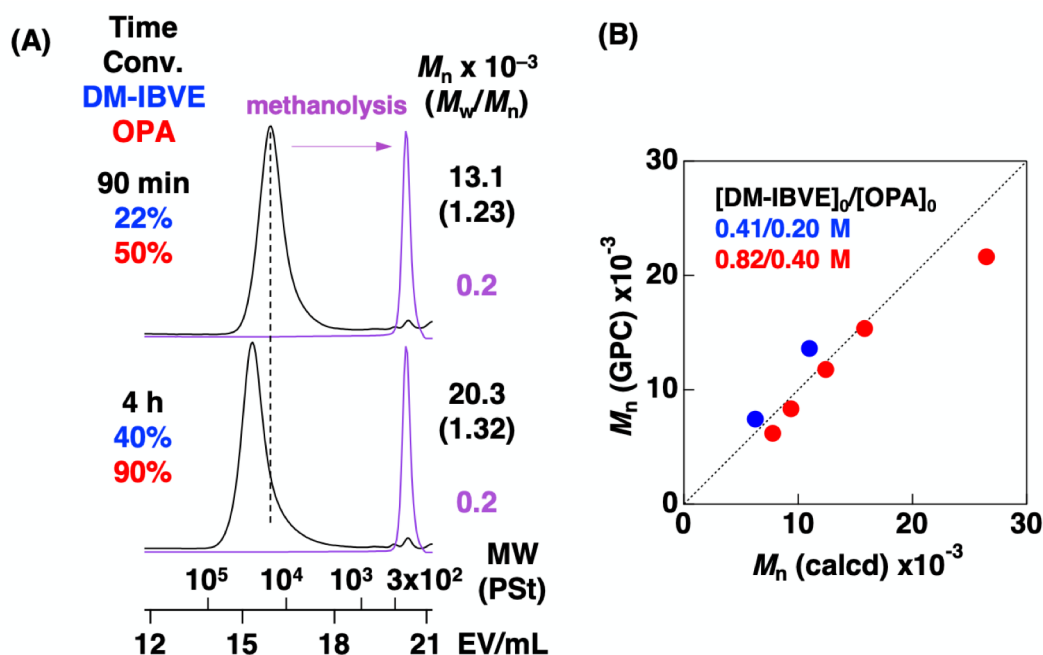


Figure S6. (A) MWD curves of the products obtained by the copolymerization of DM-IBVE and OPA (black: original polymers; purple: products obtained by acid methanolysis, $[\text{DM-IBVE}]_0 = 0.82 \text{ M}$, $[\text{OPA}]_0 = 0.40 \text{ M}$) and (B) M_n plots for the copolymerization of DM-IBVE and OPA ($[\text{EtSO}_3\text{H}]_0 = 4.0 \text{ mM}$, $[\text{GaCl}_3]_0 = 4.0 \text{ mM}$, $[\text{1,4-dioxane}]_0 = 0.50 \text{ M}$, $[\text{DTBP}]_0 = 2.0 \text{ mM}$ in toluene at $-78 \text{ }^\circ\text{C}$).

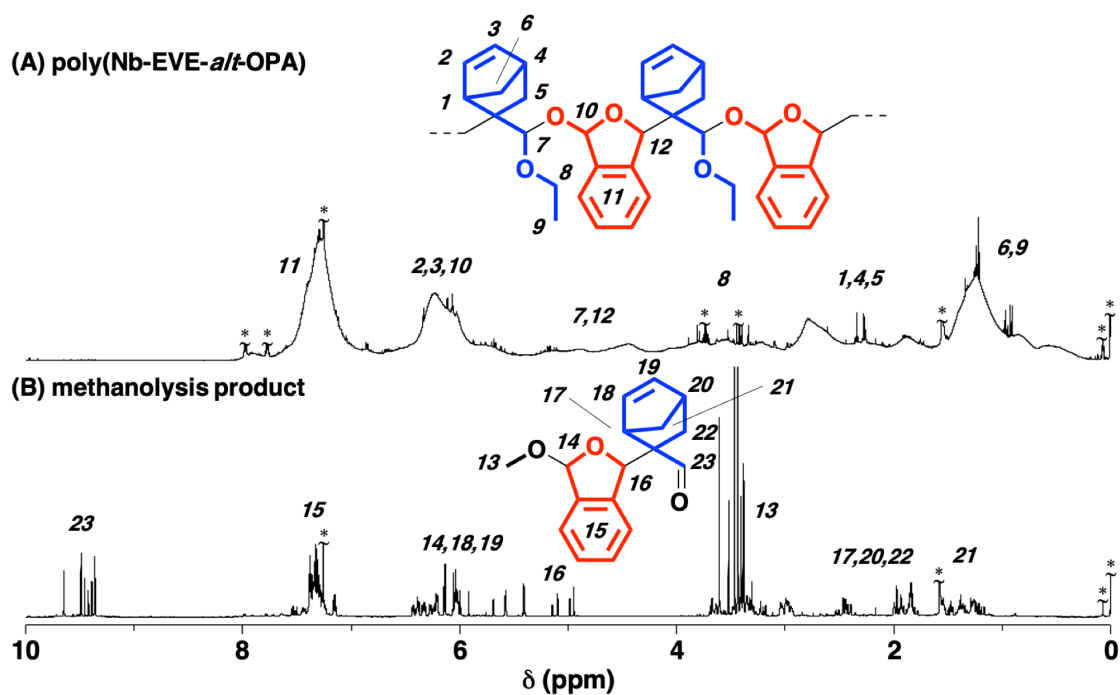


Figure S7. ¹H NMR spectra of (A) poly(Nb-EVE-*alt*-OPA) (entry 12 in **Table 4**) and (B) its methanolysis product recorded in CDCl₃ at 30 °C. Peaks with asterisks are due to TMS, grease, water, methanol, CHCl₃ and residual OPA.

Chapter 5

Summary

In this thesis, the author focused on the cyclic propagating species that exhibit unique reactivity and potentially overcomes the problems and limitations in the copolymerization. In addition, the author aimed to design copolymers that have precisely programmed molecular weights, monomer sequences, and degradability.

Part I described the exceptional copolymerization behavior of OPA due to the cyclic propagating carbocation derived from OPA. In particular, the difference in copolymerization behavior between OPA and conventional BzA was investigated.

In Chapter 2, the cationic polymerization behavior of OPA in the copolymerization with some vinyl monomers was investigated. OPA exhibited quite different copolymerization behavior compared to BzA derivatives. For example, living copolymerization of OPA and IBVE proceeded to yield copolymers containing OPA homosequences, unlike a BzA-IBVE copolymer in which BzA homosequences are absent due to the nonhomopolymerizability of BzA. Moreover, successful copolymerization of OPA with β,β -dimethyl vinyl ether or 1,1-diphenylethylene, which is not copolymerizable with BzA due to the large steric hindrance, proceeded to yield linear copolymers. The exceptional copolymerizability of OPA is most likely due to the small steric hindrance and high reactivity of the OPA-derived carbocation.

Part II described the development of novel copolymerization based on the exceptional copolymerizability of OPA. The copolymerization of OPA with various vinyl monomers including compounds that have never been regarded as a monomer was systematically examined.

In Chapter 3, cationic copolymerization of OPA with various VEs and St derivatives was investigated, particularly focusing on the relationship between the structure and reactivity of vinyl monomers and the copolymerization behavior. In the case of St derivatives, β - or α -substituents or cyclic structures around a vinyl group were the indispensable factors for the efficient crossover reactions. Styrene derivatives with no substituents on the vinyl group did not undergo copolymerization with OPA. In contrast, various VEs other than α -substituted VEs underwent copolymerization with OPA. To realize alternating-like copolymerization, the use of vinyl monomers that have both large steric hindrance and highly reactive β -carbon was effective. In addition, copolymers that are degradable into low-MW compounds were successfully obtained from St derivatives.

In Chapter 4, to expand the range of the bulkiness of polymerizable monomers, various enol ethers were designed from aliphatic aldehydes with alcohols, and subjected to the copolymerization with OPA. Methyl or primary alkyl groups on the β -carbon of enol ethers did not affect the copolymerizability regardless of the number of substitutions. In contrast, freely rotatable secondary or tertiary alkyl group decreased the reactivity of enol ethers to the OPA-derived carbocation. Importantly, some β,β -disubstituted enol ethers underwent

living and alternating copolymerization with OPA under appropriate polymerization conditions. Moreover, very bulky enol ethers that have never been reported to (co)polymerize were found to be copolymerizable with OPA.

In conclusion, this thesis developed the copolymerization that overcomes the problems and limitations in the copolymerization of different types of monomers, particularly in terms of the combination of monomers and the steric hindrance. Moreover, copolymers with precisely programmed molecular weight, monomer sequence, and degradability were obtained. The author hopes that the research conducted in this thesis will be a clue for the development of novel functional materials, such as those that are highly rigid and degradable by mild conditions, from various potential monomers.

List of Publications

1. Keisuke Hayashi, Arihiro Kanazawa, and Sadahito Aoshima
“Exceptional Copolymerizability of *o*-Phthalaldehyde in Cationic Copolymerization with Vinyl Monomers”
Polym. Chem. **2019**, *10*, 3712–3717.
(Corresponding to Chapter 2)

2. Keisuke Hayashi, Arihiro Kanazawa, and Sadahito Aoshima
“Cationic Copolymerization of *o*-Phthalaldehyde and Vinyl Monomers with Various Substituents on the Vinyl Group or in the Pendant: Effects of the Structure and Reactivity of Vinyl Monomers on Copolymerization Behavior”
to be submitted.
(Corresponding to Chapter 3)

3. Keisuke Hayashi, Arihiro Kanazawa, and Sadahito Aoshima
“Living and Alternating Cationic Copolymerization of *o*-Phthalaldehyde and Various Bulky Enol Ethers: Elucidation of the “Limit” of Polymerizable Monomers”
Macromolecules, in press.
(Corresponding to Chapter 4)